Power curve based wind turbine fault detection : A critical performance comparison and proposition of a multi-turbine approach

Usama Aziz

THÈSE

pour obtenir le grade de

DOCTEUR DE L'UNIVERSITÉ DE GRENOBLE ALPES

Spécialité : Automatique - Productique

Arrêté ministériel : 7 août 2006

Présentée par

Usama AZIZ

Thèse dirigée par **Sylvie CHARBONNIER** et
codirigée par **Christophe BERENGUER**

préparée au sein du **Grenoble Images Parole Signal Automatique (GIPSA-Lab)**
dans **l'École Doctorale d'Électronique, Électrotechnique, Automatique et Traitement du Signal (EEATS**

Power curve based wind turbine fault detection: A critical performance comparison and proposition of a multi-turbine approach

Thèse soutenue publiquement le, **23 septembre 2020**
devant le jury composé de :

Pr, Bruno CASTANIER
Professeur, Université d'Angers, Président du jury
Pr, Antoine, GRALL
Professeur, Université de technologie de Troyes, Rapporteur
Dr, Audine SUBIAS
Maitre de conférences, INSA Toulouse, Rapporteur
Dr, Sylvie, CHARBONNIER
Maitre de conférences, Université Grenoble Alpes, Directrice de thèse
Pr, Christophe, BERENGUER
Professeur, Grenoble-INP, Co-Directeur de thèse

Acknowledgements

First of all, I would like to extend my gratitude to my supervisors Sylvie CHARBONNIER and Christophe BERENGUER for all their help in carrying out the work presented in this thesis. Having accompanied me since my final year graduate project, Sylvie and Christophe have always been an incredible source of knowledge, advice, and encouragement. Their time, effort and support has helped shape me and my research project and for that I am extremely grateful.

During the thesis, I had the privilege of working with a company VALEMO, which provided the data and information, without which this document would not exist. I would like to thank Alexis LEBRANCHU and Frederic PREVOST for their contributions. I would also like to thank the entire VALEMO team for hosting me at their premises and welcoming me to an outstanding working environment.

Additionally, I owe gratitude to my colleagues, peers and fellow researchers at GIPSA Lab, especially Firas MOURAD, for their support in spite of their own ongoing projects.

Most importantly, I owe an incomprehensible debt to my parents for their prayers, to my dear wife Raania KHAN for her support, patience, research acumen and proof reading skills. I also owe my gratitude to the rest of my family and friends for their unshakable faith in me.

Finally, I would like to thank the Almighty, for His countless blessings that led me to complete this dissertation.

List of Tables

List of Figures

Table of Content

1 Introduction

1.1 General Context and Motivation

Global energy demand has expanded at an exponential rate during the twentieth century. The demand so far has largely been met by coal, oil and natural gas. These energy sources continue to dominate the world's primary energy supply today. The burning of fossil fuels produces carbon dioxide (CO_2) and other "green-house gases" (GHGs). These GHGs occur naturally in small amounts in the atmosphere, and are vital for sustaining life. By absorbing and emitting thermal radiation (a phenomenon known as the "greenhouse effect"), the GHGs help sustain a habitable temperature for the planet. It has been estimated that without them, the average surface temperature on Earth would have been as low as -18°C (Schmidt et al., 2010).

However, it is now known that the burning of fossil fuels on such an enormous scale, post industrialization has produced an over-abundance of green-house gases. This has intensified the greenhouse effect resulting in a rapidly warming global climate. The global mean temperature has risen by about 1.2 °C since 1850 (Morice et al., 2012). This change towards a warmer climate has resulted in a severe ecological impact, including variation in seasonal behaviors and effect on migratory patterns of multiple species etc. (Masson-Delmotte et al., 2018). The effects are expected to increase over the coming decades with rampant wildfires, extreme flooding, food insecurity and civil unrest being the expected outcomes.

Concentrated and coordinated efforts have been made to reduce the impact of CO_2 emissions in the atmosphere. As a recent example, 195 countries signed the Paris Climate Agreement in December 2015 under United Nations Framework Convention on Climate Change. The agreement aims to respond to the threats of climate change in this century. The attempt is to keep the global temperature rise below 1.5°C of pre-industrial levels. Europe is exploring how to become carbon neutral by 2050. The strategy is to reduce carbon emissions and increasingly meet the energy demands through renewable energy sources.

In-order to meet the global and regional objectives, the contribution of renewable energy solutions has steadily increased in the overall energy mix. The increase is significant in onshore and offshore wind energy sector where a tenfold increase in the installed capacity has been observed over the last decade. This increase in the number of installed turbines and the evolution of wind energy market naturally motivates an evolution of development, maintenance and operational strategies. In order to bring renewable energy costs down, a multi-faceted approach needs to be deployed. Along with achieving economy of scales in manufacturing, reduction in maintenance and operational costs are also of huge importance.

Energy production of Renewable Energy Systems is inherently variable in nature as they rely on the availability of their respective renewable energy sources. With this inherent variation in the source of renewable energy, advanced and continuous monitoring of the installations becomes even more important. Wind farm operators need efficient and reliable tools to ensure maximum up-time for their assets. These tools must provide useful information on the state of health of the assets and help in maintenance-related decisions. Critical failures in key components may cause important production losses, which is no longer acceptable. Thus the industry has found increased motivation to transition from the legacy scheduled and corrective maintenance interventions towards condition-based and predictive maintenance strategies.

Various condition based fault detection and monitoring strategies have been presented in the literature so as to detect faults and under-performances, as early as possible. Several solutions and strategies have been and are currently being explored to create detection and monitoring tools for faults and underperformances. Condition monitoring for wind turbines from a technological perspective can be classified into two general categories (Tavner, 2012).

• Condition monitoring systems (CMS) based approaches that often require installation of dedicated sensory hardware to generate high resolution data for monitoring critical components.

• Solutions based on the exploitation of readily available, low resolution, Supervisory Control and Data Acquisition (SCADA) system's data.

Due to the relative ease of availability and accessibility, various monitoring and fault detection methods based on SCADA data have been proposed in the literature. The industry is highly motivated to exploit SCADA data throughout the value chain of wind energy projects.

All large utility scale WTs already have a standard supervisory control and data acquisition (SCADA) system installed that is principally used for performance monitoring. Hence, for the scope of this work, we restrict our research to SCADA data based analysis.

SCADA data based condition monitoring approaches can be globally classified into two main categories as a function of the key variable being monitored. Two variables of interest from the health monitoring perspective are temperature and produced power (Lydia et al., 2014). WTs being power generators make the monitoring of produced power a key purpose of health monitoring and asset management strategy. An unwanted and unexpected decrease in the produced power can be associated to a non-optimal operational state, under-performance or a fault making the produced power, a vital parameter for this research.

The performance analysis of fault detection methods presented in the literature is usually done on purely simulated data. The famous Simulink simulation model presented by (Odgaard et al., 2009) and resulting in multiple publications based on the benchmark (Odgaard et al., 2013) etc. all use stochastic noise added to sensor measurements. The measurement noise is modeled as a Gaussian white noise. Faults are modelled as fixed offset gains to sensor measurements or actuations. Simplistic assumption are made about blades and towers while the aerodynamics are described by a static model. The nonlinearities in the aerodynamics of the turbine as well as the switching control structure are ignored. The FDI systems are expected to account for all uncertainties and be robust.

Whenever real data are used, the analysis is performed on limited fault cases affecting turbines located in a single geographical location. The fault or underperformance detection methods proposed reach their limitations very soon as they often fail to explore and validate the robustness of their detection capabilities by not subjecting themselves to comparison with other solutions, for multiple fault cases, under different environmental stimuli and for varying durations of time. Hence, a convergence of solutions is not possible. The difficulty and limitations to perform extensive analysis often come from the lack of access to real data and with sufficient fault cases.

In fact, no single approach has been shown to be comprehensively performant or optimal. Neither the key factors impacting detection performance are comprehensively identified nor analyzed. This is also due to a lack of a realistic benchmark that enables methods to be compared on consistent and realistic data. This creates the motivation to establish a comparison framework

for existing solutions that can help quantify the performance capabilities of existing fault detection solutions and establish their limitations. A controlled, consistent, comprehensive an in-depth analysis is required to realistically compare the performance of proposed methods in close to real life like scenarios.

The objective of this thesis is to addresses this concern: How to create a realistic simulation framework to generate a controlled stream of data for power profiles of desired lengths, so as to be able to compare the detection performance of fault detection methods published in literature. For the contribution to be meaningful, the framework proposed must be able to generate realistic and controlled data streams of desired lengths. It should attempt to make the least amount of assumptions possible and capture the real life dispersion in data staying true to the aerodynamics. It should be capable of modeling and replicating real-life fault scenarios of varying intensities. The ability to test and evaluate the detection performance of multiple fault detection methods, published in literature is critical for pertinent analysis. The framework designed should be capable of performance comparison for varying environmental and operational conditions.

Additional constraints addressed in this work include the industrial requirement of keeping the number of false alarms to an acceptable level and using available and familiar approach in the form of power based methods. The use of SCADA data and produced power as the primary tools of research and analysis ensure that these constraints are efficiently met as well.

The main research objectives (ROs) of the thesis are summarized as follows:

RO1. Investigate different techniques for power based fault detection and determine the gap and limitations. Determine if existing literature provides a coherent framework for comprehensive analysis.

RO2. Design a comprehensive and realistic simulation framework capable of generating realistic data streams capable of achieving objectives {RO3-RO6} and propose a suitable performance evaluation strategy.

RO3. Wind farm are located in different geographical areas. Turbines are submitted to different kind of winds and temperature profiles depending on their geographical location. Determine whether the environmental profile has an impact on the performance of a fault detection method.

RO4. Turbines are constructed by different manufacturers, can be of different models and makes. Determine whether the operational profile has an impact on the performance of a fault detection method.

RO5. Determine whether a fault signature or a fault type has an impact on the performance of a fault detection method.

RO6. Determine whether the choice of the fault detection method has an impact on the detection performance for a particular fault.

RO7. Expand the presented simulation framework to multi-turbine/farm level case and evaluate the performance gains of hybrid mono multi-turbine approaches.

1.2 Novel Contributions

The research work presented in this manuscript has multiple novel contributions. These contributions, presented in detail in the subsequent chapters are briefly listed here to give an overview.

- This work develops a novel simulation framework to enable the generation of controlled and realistic power produced data streams.
- Using the proposed framework, the key phenomena affecting the performance of fault and under-performance detection methods are identified.
- The research validates the developed simulation framework through case studies and a comprehensive and rigorous, comparative performance evaluation of existing fault detection methods is also achieved.
- The contributions also include the expansion of simulation framework to the multi-turbine case and a critical analysis of performance gains achieved by multi-turbine approaches.

1.3 Thesis Layout: Structure

The contents of each chapter of the manuscript are presented here briefly. This serves as a layout to the overall manuscript:

Chapter 1 provides an *introduction* to the area of research and gives a global motivation for this work.

Chapter 2 provides the *context and objectives* of the project. A comprehensive overview of the renewable energy sector, costs, wind turbine technology, maintenance approaches, and condition monitoring systems is presented. Produced power and power curve are introduced as condition monitoring tools. The key objectives are also represented in detail.

Chapter 3 presents the *state of the art* for existing wind turbine fault detection methods. Within this, an investigation into various techniques using produced power for fault detection is presented. Research gap is identified and the limitations of existing solution is presented.

Chapter 4 presents a detailed overview of the *data base* used for this research. Different types of wind farms and of data variables and data processing techniques are presented.

Chapter 5 proposes a novel and *realistic simulation framework* for critical comparison of power based wind turbine condition monitoring approaches techniques using the data presented in Ch. 4.

Chapter 6 presents a rigorous case study using the simulation framework presented in Ch. 5. A test bench is set-up to evaluate and compare the performances of fault detection methods.

Chapter 7 details the numerical experiments, *results* and discusses the findings of Ch. 6. The evaluation of the impact of environmental and operational variations on detection performances is presented. The impact of the choice of method and fault family on the performance is explained.

Chapter 8 provides the *findings* for the extension of proposed simulation framework to fleet level. A multi-turbine simulation framework and possible use cases of the proposed simulation in a multi-turbine analysis strategy are discussed and pertinent results are presented.

Chapter 9 *summarizes* all of the findings and research output in this thesis. It presents the main conclusions drawn from the research. The identified extensions and future research areas are presented.

1.4 Publications: Research Output

The following publications have directly arisen out of work contained within this thesis:

- **IFAC 2017**

U. Aziz, A. Lebranchu, S. Charbonnier, C. Bérenguer, F. Prevost 2017. Fusion of fault and degradation indicators for predictive maintenance assistance of wind turbine fleets using SCADA Monitoring data Preprints of the 20th World Congress of the International Federation of Automatic Control - IFAC WC 2017 - 9-14 July, 2017 - Toulouse, France - IFAC, 2017, pages 8347-8351

- **PHME 2018**

Usama Aziz, Sylvie Charbonnier, Christophe Bérenguer, Alexis Lebranchu, Frédéric Prevost. Simulation of wind turbine faulty production profiles and performance assessment of fault monitoring methods. 4th European Conference of the Prognostics and Health Management Society - PHM Europe 2018, PHM Society, Jul 2018, Utrecht, Netherlands. Paper 378, 8pp. ⟨hal-01887418⟩

- **SYSTOL 2019**

U. Aziz, S. Charbonnier, C. Bérenguer, A. Lebranchu and F. Prevost, "SCADA data based realistic simulation framework to evaluate environmental impact on performance of wind turbine condition monitoring systems," 2019 4th Conference on Control and Fault Tolerant Systems (SysTol), Casablanca, Morocco, 2019, pp. 360-365.

- **Wind Europe Offshore 2019**

Usama Aziz, Sylvie Charbonnier, Christophe Bérenguer, Alexis Lebranchu, Frédéric Prevost. A comparative performance evaluation framework for power based wind turbine fault detection methods. Wind Europe Offshore 2019, Nov 2019, Copenhagen, Denmark.

- **RSER : Renewable and Sustainable Energy Reviews (Under Review)**

2 Context and objectives

2.1 Renewable Energy Sector: A growing industry

Global investment in clean energy has seen a continuous and consistent increase over the years. According to the annual report of US Department of Energy for the year 2017 (Koebrich et al., n.d.), the cumulative global installed capacity of renewable electricity grew by 8.9% in 2017, from 2,016 GW to 2,196 GW **(Fig 2.1)**. Wind energy accounted for 24.5% of the cumulative installed renewable electricity capacity with a contribution of 539 GW in 2017 (Koebrich et al., n.d.), and is forecasted to reach 839 GW by 2023 according to the 2017 report published by International Energy Agency (IEA).

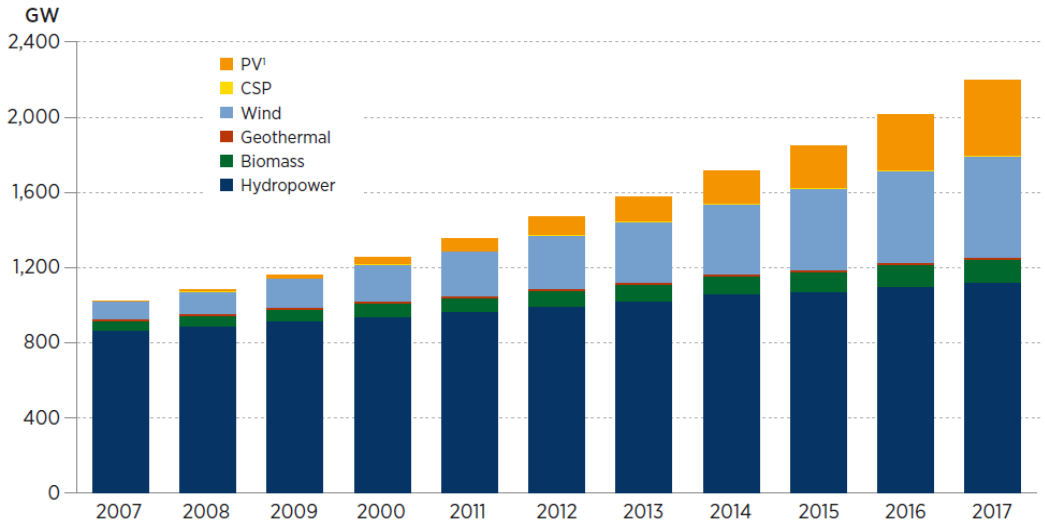

Figure 2.1 Global Renewable Electricity Capacity reprinted with permission from (Source: (Koebrich et al., n.d.)

European Union under its original renewable energy directive (2009/28/EC) also established an overall policy for production of energy from renewable energy sources. Under the directive, EU set a binding target. The EU-28 are bound to meet 20% of the gross final consumption (GFC) through renewable energy sources by 2020. The directive (2009/28/EC)

specifies national renewable energy targets for 2020 for each country in the EU. These targets were set taking into account each country's starting point and overall potential for renewables. These targets ranged from a low of 10% for Malta to a high of 49% for Sweden. France is on track to meet its target of 23% GFC from renewable energy sources (RES). In 2005, the contribution of RES in French energy mix was 9.6%.

Expanding a little further on the situation in France, the total installed capacity in France had reached 13.8 GW as of 31 December 2017. **Table 2.1** presents the evolution of %age contribution of Renewable Energy Sources (RES) in French energy mix from 2005-2020. The overall share of renewable energy sources in gross energy consumption has seen a constant increase over the years. The overall energy consumption can be divided into three major sectors including heating and cooling, electricity and transport. The increase in penetration of renewable energy sources is consistent across all these major sectors and globally.

TABLE 2.1: FRENCH TARGETS AND ESTIMATED TRAJECTORY OF ENERGY FROM RENEWABLE RESOURCES IN THE HEATING AND COOLING, ELECTRICITY AND TRANSPORT SECTORS.

	2005	2008	2010	2011	2012	2013	2014	2015	2016	2017	2018	2019	2020
RES- H&C[1] (%)	13.6%	14.9%	17%	18%	19%	20.5%	22%	24%	25.5%	27.5%	29%	31%	**33%**
RES - E[2] (%)	13.5%	14%	15.5%	16%	17%	18%	19%	20.5%	21.5%	23%	24%	25.5%	**27%**
RES - T[3] (%)	1.2%	5.6%	6.5%	6.9%	7.2%	7.5%	7.6%	7.7%	8.4%	8.8%	9.4%	10%	**10.5%**
Overall RES share (%)	9.6%	11.4%	12.5%	13.5%	14%	15%	16%	17%	18%	19.5%	20.5%	22%	**23%**

In conclusion, just like the global trends, we can see that wind energy in France and in Europe has a strong growth potential. This growth will persist for the next 10 years, to meet the binding 2030 targets of renewable energy mix. In the longer term, offshore and onshore wind energy has the potential to help Europe achieve the aimed status of carbon neutral continent by 2050. This increase in the number of wind turbines and the change in the network will however have a major impact on the operations and maintenance of wind farms, which will have to adapt by developing new reliable, efficient and comprehensive condition monitoring and operational techniques.

2.2 Economics of Wind Energy

2.2.1 Installation costs

As established so far, there is an increase in the number of in-field active renewable energy sources and hence wind assets all over the world. With the multiplication of active wind assets and the production inching closer towards economy of scale, the installation costs have seen a sharp decrease. With rapidly falling renewable power generation costs, policy makers and investors have found increased motivation to confront the economic opportunities, as well as challenges, arising from this scale-up of renewable energy.

In the past 30 years, onshore wind installed costs have declined significantly, according to IRENAs database of onshore wind power project costs from 1983-2016. The estimated global weighted average fall in total installed cost of wind farms between 1983 and 2017 was 70%, as costs fell from USD 4 880 to USD 1 477/kW. This represents a learning curve of 9% for total installed costs for every time installed capacity doubled, worldwide **(Fig 2.2)**.

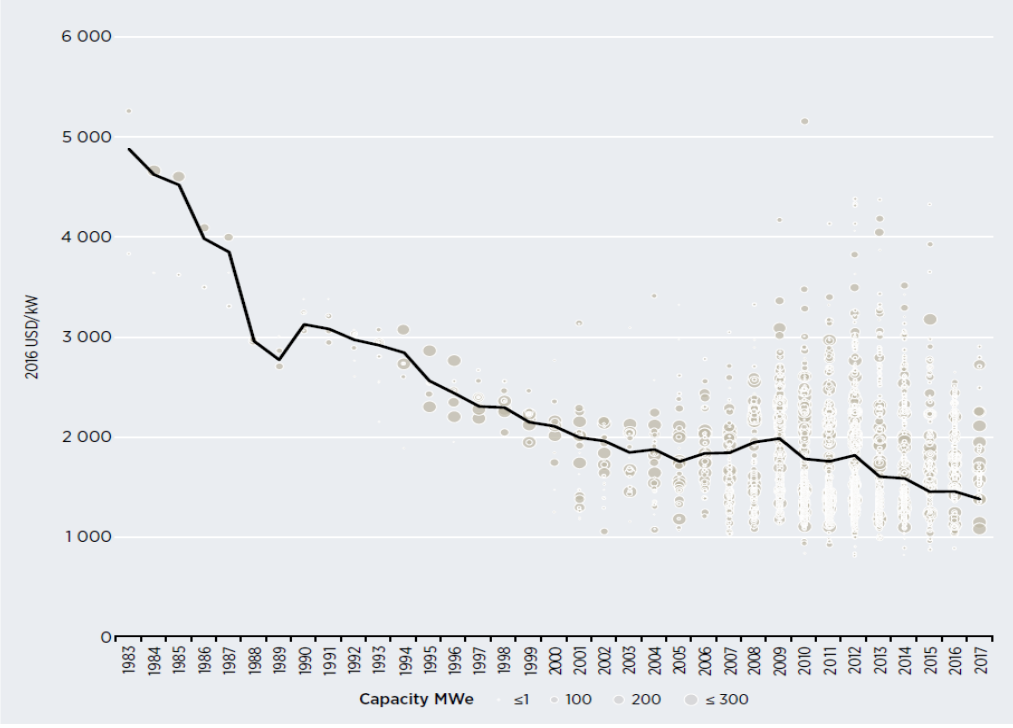

Source: IRENA Renewable Cost Database.

Figure 2.2 Total installed costs of onshore wind projects and global weighted average, 1983-2017 ("Renewable Power Generation Costs in 2017," 2018)

With decreasing installation costs and increasing number of assets to monitor, it becomes necessary to investigate their impact on the profitability of operators.

2.2.2 Maintenance Costs & Profitability

As the installed capacity increases consistently, the operation and maintenance teams for wind farm operators are constantly faced with a challenging task to maintain and increase the availability of existing fleet. According to the report on Renewable Power Generation Costs in 2017 published by International Renewable Agency (IRENA) the operations and maintenance costs, on an average can represent up to 20%-25% of the cost of electricity (COE).

Cost of energy (CoE) is commonly used to evaluate the economic performance of different wind farms. This methodology was adopted in a joint report ("Projected Costs of Generating Electricity," 2005) by the International Energy Agency (IEA), the European Organization for Economic Co-operation and Development (OECD) and US Nuclear Energy Agency (NEA). It compared the cost of different electricity production options. A simplified calculation equation was adopted in the United States to calculate the CoE ($/MWh) for a Wind Turbine system (Walford, 2006):

$$CoE = \frac{ICC * FCR + LRC}{AEP_{NET}} + O\&M \qquad \text{eq. 2.1}$$

$$AEP_{NET} = AEP_{GROSS} * Availability * (1 - Loss)$$

COE	Cost of Energy ($/kWh)
ICC	Initial Capital Cost ($)
FCR	Fixed Charge Rate (%/year)
LRC	Levelled Replacement Cost ($/year)
O&M	Operations and Maintenance Costs ($/kWh)
AEP	Annual Energy Production (kWh/year)

It is important to note in the above Eq. **2.1** that profit margins only come by reducing Maintenance costs i.e. increasing availability which is directly linked to Annual Energy Production. All other costs are constant (construction, logistics etc.) (Walford, 2006). This lays the foundation and motivation for this work i.e. to help develop tools that assist with efficient wind turbine condition monitoring and maintenance.

2.3 Wind Turbine Monitoring

In this section, the foundations of the wind turbine condition monitoring strategies are presented. First, the operation of a wind turbine and its division into sub-groups of components is presented. Then, two classic fault signatures: temperature and power, and their link with the component breakdown is highlighted. The arguments for the variable of choice for the sake of this research, i.e. "power", are also presented hereafter.

2.3.1 Wind Power & Turbine Taxonomy

As a general principle, wind turbines are energy convertors. They convert the kinetic energy of the wind to the mechanical energy and the mechanical energy to electrical energy. The kinetic energy from the wind flow is first felt on the wind turbine blades. This energy is converted into mechanical load as it rotates the WT blades. The blades are directly connected to a low speed shaft that rotates with the rotation of blades which is usually around 10-20 rpm. The rotation speed at this stage is a function of wind speed felt by the blades. The low speed rotating shaft is then connected to a gearbox. The gearbox then drives a high speed shaft which rotates faster by a factor of 100. The high speed shaft is connected to the rotor of a generator that converts this mechanical energy into electrical energy at the output. Usually a transformer is used to regulate the produced power and match it to the grid specifications.

The power in wind P_{wind} is given by Eq. 2.2 as

$$P_{wind} = \frac{1}{2}.\rho.A.v^3 \qquad \text{eq. 2.2}$$

with air density ρ, rotor swept area A and wind speed v.

However, the potential wind power P_{wind} is limited and cannot be completely extracted. The limiting factor is the wind congestion behind the blades and rotor. The extracted kinetic energy from the wind, slows it down the stream, and produces an accumulation of air which further slows down the complete wind system. This theory presented by Albert Betz in 1919 informs the Betz's Law that dictates a limit on the amount of kinetic energy extracted from wind.

Betz's Law identifies the power coefficient c_p and the limit value of 0.593. That means, the maximum possible turbine power which can be extracted by a wind turbine is nearly 60 % of the wind power. In reality however, practical utility-scale wind turbines achieve at peak 75–

80% of the Betz' limit (Burton et al., 2011). **Eq. 2.2** can be re-written with the power coefficient as described by Eq. **2.3**. The power coefficient c_p is determined by the ratio of wind speed before and after the rotor area. (Burton et al., 2011)

$$P_{wind} = \frac{1}{2}.c_p.\rho.A.v^3 \qquad \text{eq. 2.3}$$

Fig 2.3 shows the key components of a 3 blade horizontal axis wind turbine. 3 main structural components can be identified in the figure. These include the tower (label # 9), the nacelle (label # 11) which is the housing mounted on the tower and the hub assembly (label # 1). The hub assembly (label # 1) has the blades attached to it and is connected to the nacelle. These assemblies are further divided into subassemblies that house different components. All the components, sub-assemblies and assemblies constitute the overall system (i.e. Wind Turbine).

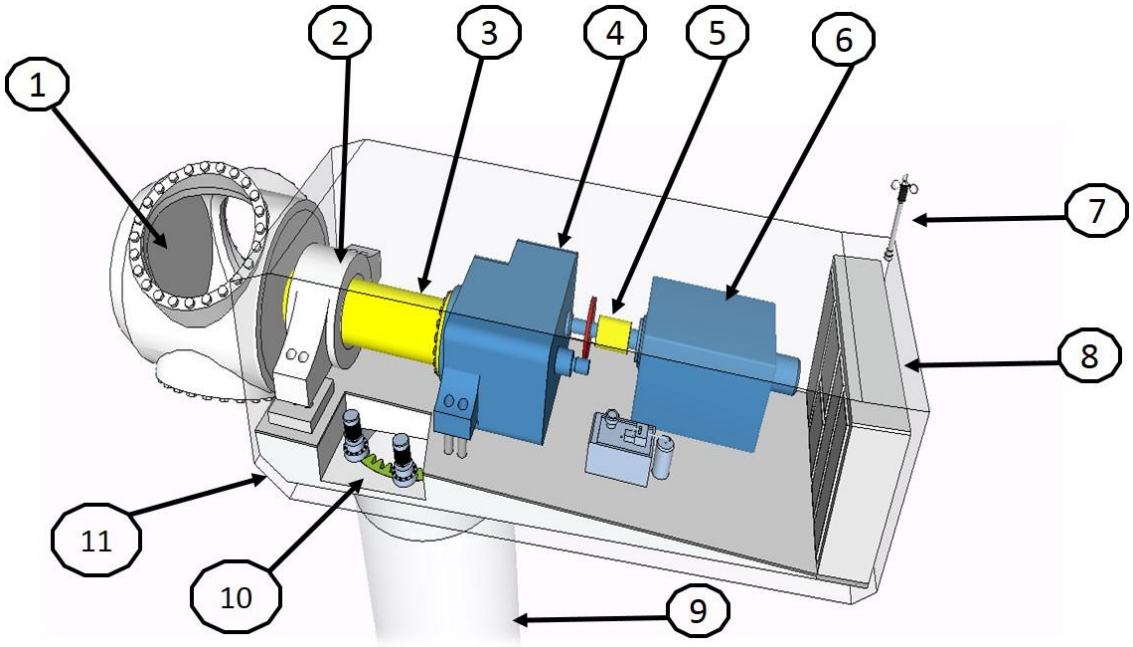

Figure 2.3 Wind Turbine Design (Courtesy: Valemo) Structure of a modern wind turbine, showing major components: (1) Hub or Rotors; (2) main bearing; (3) low speed shaft; (4) gearbox; (5) high speed shaft (6) generator; (7) measuring mast (8) transformer (9) tower (10) yaw motor

From the taxonomical perspective, the choice of division of the overall system (Wind Turbine) into assemblies, subassemblies etc. is based on various aspects. These include the proximity, characteristics and intrinsic behaviors of these components. **Fig 2.4** gives an idea of the component hierarchy to the subassembly level that can be used further to help with the monitoring problem and identify the fault location. This isolation can also be seen from the

maintenance point of view since the type of equipment required for various interventions varies and it is important to identify the component that needs maintenance or replacement.

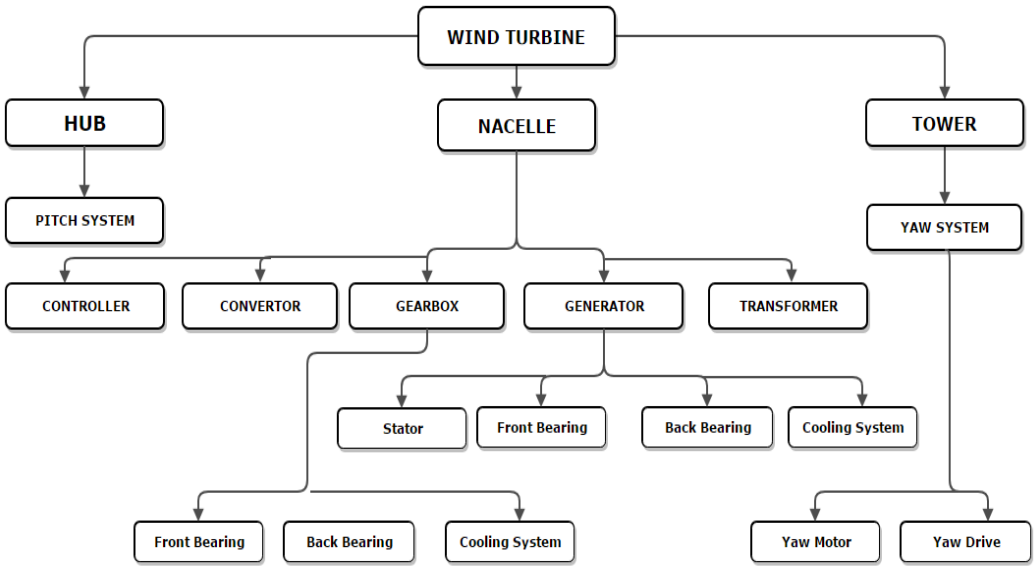

Figure 2.4 Wind Turbine component breakdown

2.3.2 Wind Turbine condition monitoring strategies

As presented in the previous section, once the suitable component level abstraction is agreed upon in the overall maintenance strategy, condition monitoring of these components can be performed. In order to ensure the normal behavior of wind turbines, various strategies have been identified in the literature. (Aziz et al., 2019). Condition monitoring strategies are often based on the primary function of machines under observation.

For power generators like wind turbines, it is of interest to monitor the temperature of key components and/or the power output of the turbine.

Temperature based methods

Parts of the component of the wind turbine are mechanical. For mechanical systems, a fault or failure is often caused by wear. The wear causes friction that increases the temperature. This overheating can then compromise the structural integrity of a mechanical component and cause damage. Thus, for this type of failures, temperature based methods are the most appropriate tools for fault detection and condition monitoring.

Several case studies showing the use of temperature based methods are available in literature related to wind turbine condition monitoring. Some of the key components monitored

using these methods include gear-box, cooling systems, front and back bearings etc. These components are expensive and hence garner the interest of research community towards monitoring these components.

The methods using temperature as a key parameter for condition monitoring systems have to restrict themselves to the faults that are expected to have a temperature signature. However, there is family of faults that may not have a significant temperature signature and hence may be outside the scope of these methods as elaborated in **Table 2.2**.

2.3.3 Power based methods

A wind turbine primary function is to produce power as a consequence of observed wind in accordance to the manufacturer provided specifications. A fault will decrease the ability of the machine to produce power and will cause a production loss. Thus a decrease in the power produced can be an indication that a fault is occurring. Faults and performance degradations are detected by monitoring the power output of the wind turbine in comparison to the normal behavior.

For financial and operational purposes, produced power is the most important indicator and measurement for wind turbine manufacturers, operators and maintenance teams. Since the wind turbine is an energy conversion system that converts wind energy into electrical power, the power produced becomes a natural candidate for key monitoring variable.

Table 2.2 presents some of the key components of a wind turbine system. It also lists the fault signature and identifies if produced power or the component temperature will be more sensitive to the fault occurrence. It also presents the frequency of occurrence of these faults as a %age of the total faults identified in a year. The downtime or the production loss suffered as a consequence of these failures is also presented. This information along with the component replacement costs and the financial consequence of downtime often help devise a condition monitoring and maintenance strategy.

TABLE 2.2: COMPONENT CLASSIFICATION BASED ON FAILURE SIGNATURES, FREQUENCY AND CRITICALITY.

Sr #	Components	Impact: Temperature Rise	Impact: Production Loss	avg. faults/year (Tavner, 2011)	Downtime/ year (Tavner, 2011)
1	Generator Front Bearing	**Yes**	Yes	6%	11%
2	Generator Back Bearing	**Yes**	Yes		
3	Stator Winding	**Yes**	Yes		
4	Generator Cooling System	**Yes**	Yes		
5	Gear Box Front Bearing	**Yes**	Yes	5%	4%
6	Gear Box Back Bearing	**Yes**	Yes		
7	Gear Box Oil/Cooling System	**Yes**	Yes		
8	Pitch Control System	No	**Yes**	16%	20%
9	Misalignment	No	**Yes**		
10	Blade Erosion/Icing	No	**Yes**		
11	Yaw System	No	**Yes**	12%	10%
12	Elec. Convertor	No	**Yes**	12%	13%
13	Slip Ring	No	**Yes**		
14	Transformer	No	**Yes**		
15	Control System	No	**Yes**	14%	9%

As can be seen on this table, many faults cause production loss. It is interesting to note here that many faults with dominant temperature impact (1-7) eventually also cause a production loss. However, faults with impact on production loss (8-15) are of particular interest, hence monitoring power produced is a strategy favored in the literature. For this work, the condition monitoring and fault detection for control system faults (down-rating, acoustic curtailment), yaw system (misalignment) and blade erosion/ icing are of interest. To do so, the power curve, a very familiar tool in the industry, is also one of the many modern condition monitoring strategies available.

2.4 The Power Curve

2.4.1 Definition of the power curve

The measured wind – produced power relationship is often expressed as a curve that is representative of the operation of the wind turbine as a whole. The simplest data curves

represent the electrical power generated at a given moment in relation to the measured wind speed. This curve is plotted as a function of available data and the most common resolution is 10 minutes average of SCADA data samples. This data curve is often processed (bin averaged) using the method proposed in the standard (IEC 61400-12-1, 2005) for better interpretation.

The power curve as shown in **Fig 2.5** is the simplest link that can be established between the environment and the power generated. The wind speed is placed on the x-axis and the power generated on the y-axis. This representation refers to standard atmosphere with 15 °C, 1013.25 hPa, 0% humidity and a density of 1.225 kg/m^3.This representation makes it possible to see that there are several phases in power generation, a start-up, a ramp-up and a production saturation phase.

Based on the produced power, this relationship can be further divided into different modes of operation shown in terms of Zones I-IV. For wind speeds that are below the cut-in value (Zone I on **Fig. 2.5**), i.e. between 0 and 3 m/s, the wind is too weak to overcome the moment of inertia and friction, no power is produced, since the wind does not have enough energy to move the rotor. At wind speeds above the nominal speed (Zone III), the power reaches its nominal value. At the point of wind speeds greater than 13 m/s, the *full-load range* is reached. Mechanisms such as pitch angle attenuation for active control turbines are used in order to maintain power at its nominal value. At extreme wind speeds, the Wind Turbine is stopped in order to ensure the structural integrity of the Wind Turbine (Zone IV). It is only between the cut-in speed and the nominal speed that a cubic relationship between wind speed (v) and produced power (P) is observed (Zone II) (Cambron et al., 2016). The part between 3 and 13 m/s is called the *partial load range*. By reaching the stable revolutions per minute (RPM), the turbine starts to inject electrical power into the grid. With rising wind speeds, the pitch angle is decreased and the produced power increases.

Figure 2.5 Example of an ideal fault free power curve (also referred to as constructor power curve

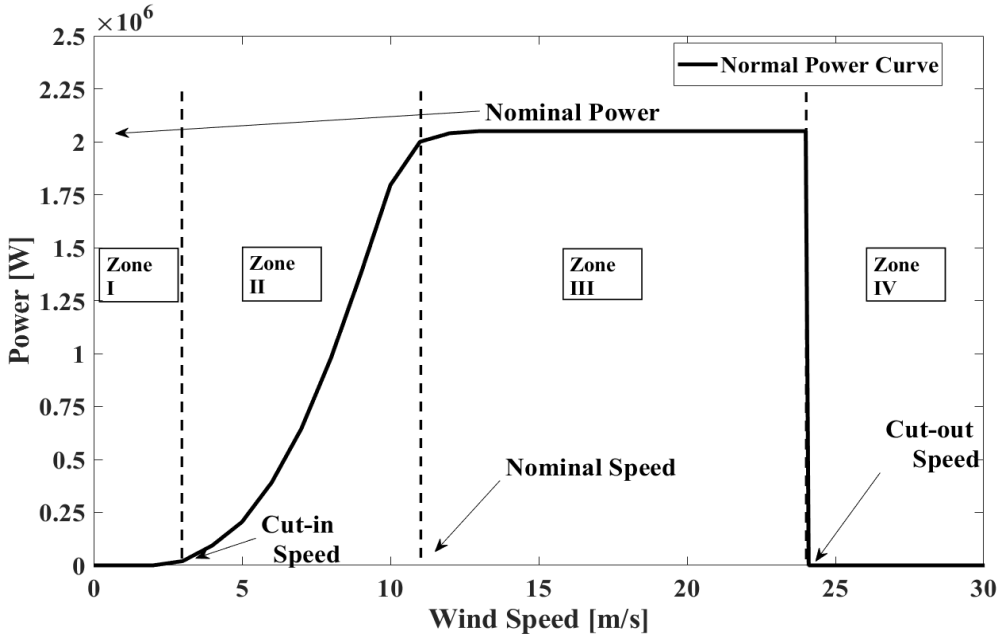

This relationship (power curve) is often used to verify if the machine is able to fulfil its primary function: to produce power efficiently. The wind turbine operators and their maintenance teams try to ensure the maximum possible power production for maximum profitability. The produced power and power curve hence become an important utility for condition monitoring.

Based on the manufacturer, model and operational characteristics of a wind turbine, the wind turbine manufacturers provide the characteristic curve for the "wind to power" conversion capability of their respective machines. The manufacturer power curve is calculated at the beginning of life for a machine. The manufacturer often assures ±5 % production performance for its machine under guarantee. This curve is the most familiar and commonly used tool to monitor wind turbines by the operators and is considered an industry wide standard.

Fig 2.6 shows visual inspection of SCADA data based power curve being performed for detection of wind turbine problems. SCADA data are recorded every 10 minutes. In its basic form, the power curve is a brute visual tool for inspection and condition monitoring. Annual produced power data when plotted against the observed wind speed can be used to observe the production behavior and monitor the performance.

Figure 2.6 Analyzing SCADA data to detect wind turbine problems [Sources: GL Garrad Hassan, Tavner]

The measured production capability of a wind turbine is often monitored in reference to its expected production capacity. The produced power or power curves as monitoring tools make it possible to evaluate the overall production operation of the turbine. It also provides an indication of the expected theoretical performance between the mechanical power provided by the wind (measured indirectly by the wind speed) and the electrical power delivered by the machine as output.

This curve makes it possible to detect the presence of incipient failures. In fact, if a fault appears, the production efficiency of the machine decreases. This reduction generates performance losses related to the severity of the defect. Any abnormal decrease in the produced power can be termed as under performance and is associated to be caused by a fault. Based on this principle, several attempts to use the produced power and the power curve for condition monitoring of wind turbines have been made in literature. The following section elaborates such scenarios further and gives some more examples of frequently observed deviations from the reference power curves.

2.4.2 Failures as seen on the Power Curve

The British standard on maintenance and maintenance terminology defines a failure as *"termination of the ability of an item to perform a required function"* (BS EN 13306:2010, 2010). In the case of a wind turbine, its primary function is to produce power in accordance to the manufacturer provided specifications. It is important to note that "failure" is an event while a "fault" is a state. A fault is defined as "*state of an item characterized by inability to perform a required function, excluding the inability during preventive maintenance or other planned actions, or due to lack of external resources*". (BS EN 13306:2010, 2010)

A failure or loss in performance is identified when the produced power deviates from the normal power curve. Several faults, failures, change in configurations can change and have an impact on the power production capabilities of a wind turbine. It is important to note that since the power curve is an overall performance indicator of the production capability, multiple causes have the potential to impact it. For the sake of this research, all such phenomena that have the ability to deviate the power curve from its normal or constructor provided reference will be grouped and termed as "faults".

This assumption and classification allows for the inclusion of mistaken configurations, altered control strategy to reduce the acoustic signature etc. to be considered as faults since they can have a significant impact on the production capacity. Some other faults include but may not be limited to down-rating, pitch control malfunction, icing on turbine blades, erosion, and wind speed under reading, dirt or bugs on blades and so on etc. (Park et al., 2014). All these faults have a particular signature and they impact the power production curve in a specific way. **Fig 2.7** shows some of the fault cases and their peculiar signatures on the power cure. It is important to note that any abnormal behavior can result in an unplanned stoppage which translates into financial loss for the operator.

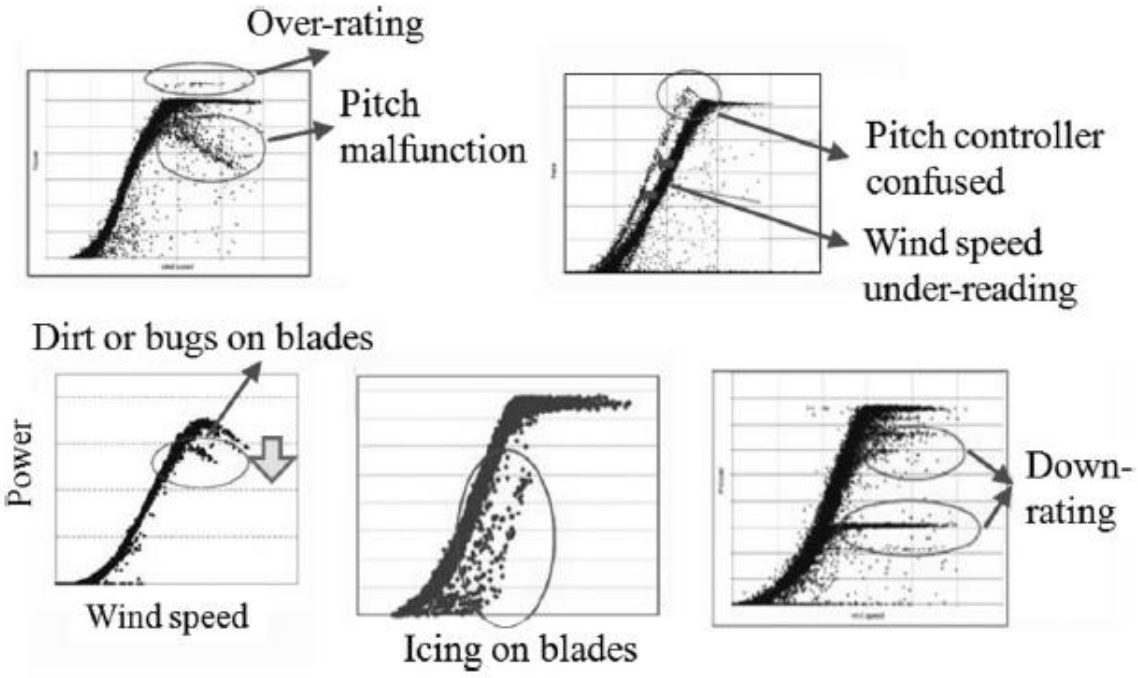

Figure 2.7 Types of Power Curves that appear in different fault cases, reprinted from (Park et al., 2014)

2.4.3 Power Curve Data Dispersion

As shown in the **Fig 2.5** above, theoretically, a wind turbine should produce a fixed amount of power for a given wind speed but practically, when the power curve is built using SCADA data recorded every 10 minutes, high dispersion of data is observed around this curve. This results in several values of produced power being measured for any given wind speed. This phenomenon is visible in **Fig 2.8** below where a scatter plot of 10-min wind speed & power for a WT over 3-years period is presented. The mean power curve is also plotted to give an idea of data dispersion around the mean.

The difficulty in using the unprocessed power curve for condition monitoring is this data dispersion. If the standard deviation of power as a function of wind speed is plotted this concern becomes even clearer. Thus, for a given wind measurement, in normal operation, the power measurement observes a range of acceptable values which increases with the power and can reach up to plus or minus 200 kW compared to the theoretical value. This means a possibility that any production loss of up to 200kW can go un-noticed. Such production loss for an extended duration of time amounts to a significant financial loss for the operators.

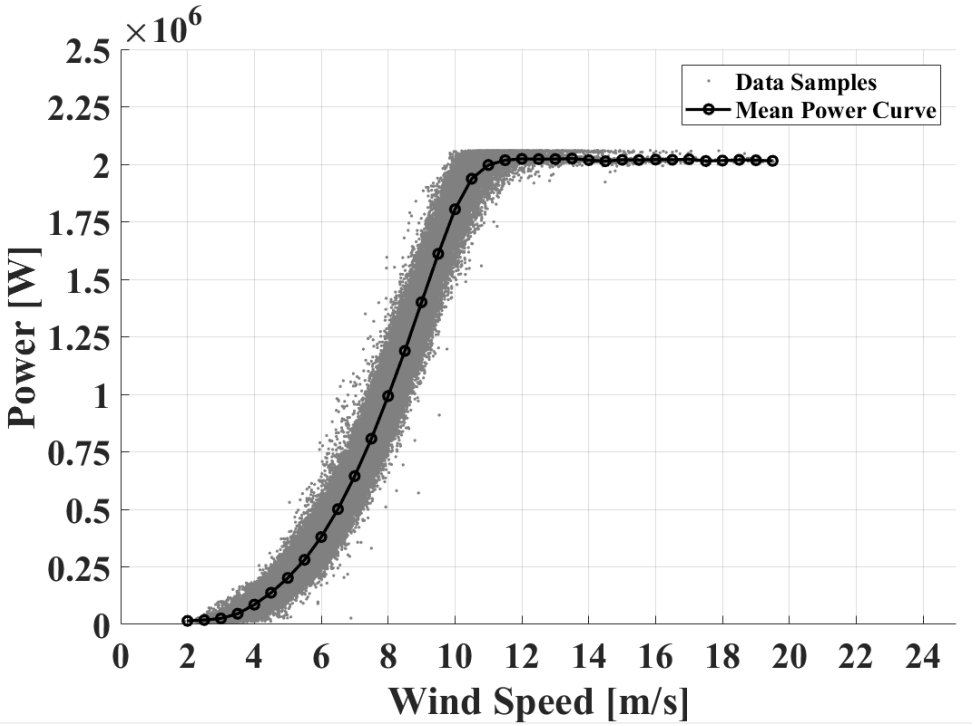

Figure 2.8 Scatter plot of 10-min wind speed & power for a WT over 3-years period along with mean power curve

This dispersion of data can be associated to various characteristics including.

1. Environmental Factors
2. Operational Characteristics

The dispersion is caused by environmental factors such as the nature of the wind (turbulent, laminar), the density of the air or the angle of inclination of the blades that affect the amount of mechanical energy transmitted to the turbine. It is to be noted that the dispersion is significantly less in the beginning (Zone I) and end (Zone IV) of the power curve as labelled in **Fig 2.5**. If the dispersion is not reduced, only the faults with signature higher than the normal dispersion will be detectable. For any condition monitoring system to work efficiently, it is important to reduce the data dispersion.

2.4.4 Power curve for fault detection: summary, objectives and challenges

Since the power curves and power related data is very familiar for the wind turbine operators, methods using power curves become promising candidates for a fault detection and condition monitoring system. These fault detection methods can find use in independent performance monitoring systems or as a part of a global solution alongside other approaches to provide a wholesome monitoring solution. A comprehensive mechanism to compare the

available methods is however necessary as it can help evaluate respective performances and identify limitations.

So far we have seen a comprehensive overview of the renewable energy sector, the costs associated, existing wind turbine technology, current maintenance approaches and available condition monitoring systems. Produced power and power curve are introduced as potential condition monitoring tools since any faults and underperformances are shown to have a signature on the normal power curves. This makes produced power and power curves a familiar, useful and potentially effective tool for condition monitoring.

The use of power curves for condition monitoring is however not without challenges. Data dispersion around power curves add to the difficulty of detection. The appropriate handling of this dispersion and the variations caused by other operational and environmental conditions become key aspects when considering power curves as monitoring tools. This makes both fault detection and dispersion reduction capabilities the parameters of interest as decreased data dispersion could mean increased detection performance.

One of the key objectives of this research is thus to evaluate the power based fault detection methods on their ability to address such operational and environmental variations. This includes but is not limited to, the exploration the available solutions, identifying their limitations and propose a comparative benchmarking technique to quantify the best practices. A comprehensive literature review and state of the art analysis for various fault detection and condition monitoring systems using power is performed in the next chapters. Such investigation helps determine if existing literature provides a coherent framework for a comprehensive analysis.

3 Power Based Condition Monitoring

As established in detail in the previous chapter, produced power and power curves are potentially pertinent tools for fault detection and condition monitoring. A rigorous and in-depth literature analysis of state of the art is required to investigated various solutions proposed and strategies employed in this domain. This chapter explores, evaluates and presents a concise analysis of power based fault detection methods and performs critical analysis. It is useful to recall here that the scope of this research has been restricted to SCADA data based approaches. Hence the literature review excludes de facto all the methods using high frequency CMS data. The SCADA data based research domain can be divided into various families of approaches explained below.

3.1 Model Comparison based Methods

The main principal of this family of methods is the comparison of two power curves. One power curve is first built offline on reference data under normal conditions. The second power curve is built online during an observation period. Fault detection indicators are created by comparing these two power curves. The type of comparison techniques include difference of areas under the curves and other distances between the reference curve and curve under observation. **Fig 3.1** presents an overview of model comparison based approach.

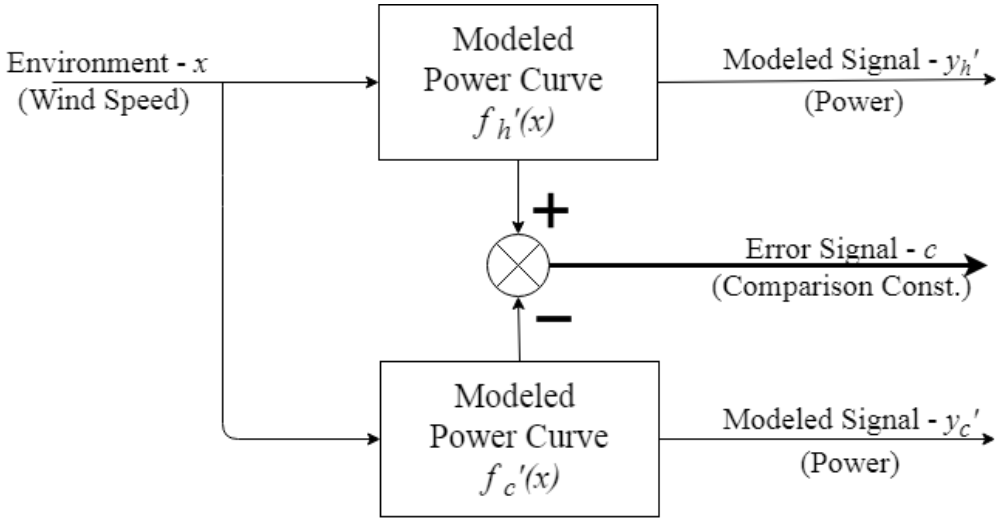

Figure 3.1 Model Comparison based method overview: x is the on-line input, f_h'(x) is the historic modelled curve, f_c'(x) is the current modelled curve, and 'c' is the comparison constant or error signal

In the context of wind turbine fault detection, the function $f(x)$ is the wind turbine power production process/relationship, characterized by the power curve. The process has environmental influences (e.g. wind speed) labelled (x) as input. This relationship can be modelled by a number of modelling techniques and as a consequence, two modelled power curves $f_h'(x)$ & $f_c'(x)$ are possible based on the historic or current data (**Fig. 3.1**). The difference between the historic and current modelled power curves can be labelled as error $\boldsymbol{c}$ or also commonly referred to as the model comparison constant.

The idea behind these methods is the fact that any fault in the wind turbine system will have an impact on the production capacity of the wind turbine. This will express itself as a change in the wind-power input output relation that is visible as the power curve. By comparing the normal behavior and the changed curves, faults can potentially be detected. However, it is important to remember the limitations of operational variation and data dispersion while using power curves as condition monitoring tools and taking note of how different solutions presented in literature approach and address this problem.

Several ways are proposed in literature to compare the power curves. They include i) learning models on two sets of data and comparing the models, ii) reducing the curve data to representative points and comparing these representative points or iii) translating the data into a different coordinate system (PCA) and comparing. Each approach holds its benefits and drawbacks and tries to address or avoid the operational and dispersion limitations. The authors attempt to remove the need of handling the operational factors and data dispersions by choosing one of the strategies listed above.

3.1.1 (Yang et al., 2013)

The method proposed by **(Yang et al., 2013)** uses the relationship curves between wind turbine variables for condition monitoring. Models learnt on fault free data and online data are compared to create condition monitoring indicator.

The hypothesis here is that based on the subassembly or component being looked at, any fault will have an impact on the corresponding relationship between key variables. The authors in (Yang et al., 2013) identify the potential correlations of SCADA variables with relevant sub-assembly for condition monitoring purposes.

As explained in section 2.4.3 the operational and environmental dispersion need to be handled for better condition monitoring. (Yang et al., 2013) proposes a data pre-processing technique to reduce the dispersion of SCADA data. Inspired by (IEC 61400-12-1, 2005) standard's "Method of Bining" the raw SCADA data is pre-processed. The IEC standard looks at the wind speed-power relationship (power curve) and proposes the sorting of measured power data into wind bins. All values in a particular wind bin are then averaged and a representative mean value is assigned corresponding to each a bin.

(Yang et al., 2013) use 4th degree polynomial equation of form shown below Eq. (3.1) to model the relationship between variables under observation.

$$\widehat{y_i} = a_o + a_1 x_i + a_2 x_i^2 + \cdots a_k x_i^k \qquad \text{eq. 3.1}$$

The model curve constructed from the data measured over the observed period is then compared to that of the reference period. Any abnormal difference between the two makes it possible to highlight a loss of production related to a defect. The proposed method to evaluate the deviation between the curves is a criteria 'c' explained in Eq. (3.2). The loss of production or inception and progression of a fault is evaluated by looking at the value of this criteria 'c'. An increase in value of this criteria means an increased distance from the normal curve and hence the variation in the value of 'c' comments on the occurrence and progression of a fault.

The value of the condition monitoring criteria 'c' is calculated as

$$c = \frac{\int_{x_{min}}^{x_{max}} \left| \sum_{j=0}^{k} (a_j - b_j) x^j \right| dx}{x_{max} - x_{min}} \qquad \text{eq. 3.2}$$

Where a_j and b_j represent the coefficients of the models derived respectively from the present and historic data; $x_{max.}$ and x_{min} are respectively the maximum and minimum values of x when x is the input variable.

The criteria *'c'* is developed to show the evolution of historic to present data. As a fault develops, the indicator is expected to evolve. **Fig 3.2** shows power output vs. generator speed for various modes of operation. The metric, 'c' is shown where c= 0 represents normal condition and as the fault develops, the value of 'c' changes serving as an indicator.

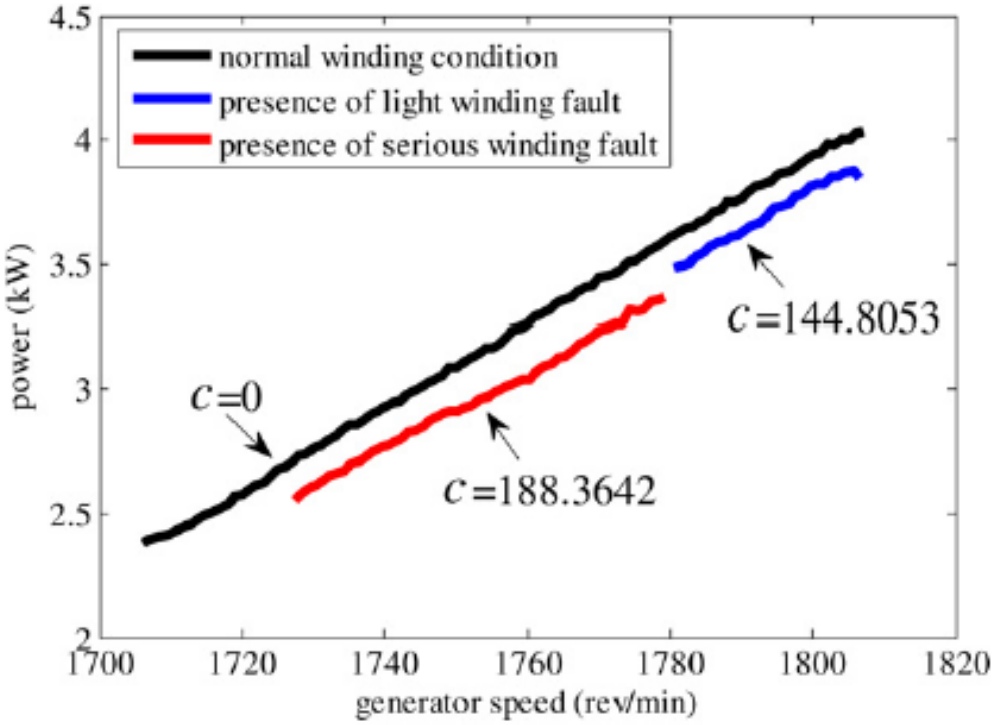

Figure 3.2 Generator speed vs power for various values of fault indicator 'c' showing development of winding fault, reprinted from (Yang et al., 2013)

The validation of the proposed approach is done on a specially designed test rig and on two real case studies. Two types of faults tested using the test rig include electrical asymmetry of the rotor and progressively increasing gear teeth damage to the leading edge of high speed pinion. For the real case study validation examples, the blade failure of a two blade wind turbine and the generator failure of a 3 blade 750 kW wind turbine are considered. In case of all fault cases the curves show an increased deviation from the normal reference and hence an increased value of the criteria 'c'.

It is important to note here that despite the fact that validation is done for the proposed method on a test rig and on real case scenarios, many important questions remain unanswered.

When using the wind speed-power relationship curve for blade failure, the method restricts itself to the linear region of the power curve. This is the data from the cut-in wind speed to the rated wind speed, right before the pitch control system of a wind turbine kicks in. This is done to remove the inclusion of non-linearity, simplify the relationship curves and ease the modelling. This comes at a cost of ignoring any failures in the pitch control system that have shown to cause a significant loss of production.

Another consideration when using the proposed approach for online condition monitoring problem is the inherent need for sufficient data. (Yang et al., 2013) fail to comment on the need of an appropriate duration of analysis window. The criteria 'c' proposed cannot be calculated until sufficient data is available to build a curve comparable to the normal curve. Also the analysis of the condition monitoring criteria is graphical and left to interpretation by the operator. No automatic detection method for fault detection using the criteria 'c' is proposed.

3.1.2 (de Andrade Vieira & Sanz-Bobi, 2015)

The authors in **(de Andrade Vieira & Sanz-Bobi, 2015)** use the power curve to build a performance indicator for the wind turbine condition monitoring. A power curve model is first learnt on the offline data and then compared to a complete model learnt on data under observation. The normal curve is built on 1 year of SCADA data made available to the authors. The condition indicator is then used to perform anomaly detection based on the selected warning and alarm thresholds. Validation is done on 5 turbines in a farm using the power degradation indicator calculated.

The scientific principal employed here is that a fault or failure will cause a decrease in power production capacity of the wind turbine. Consequently, the wind turbine will produce less power for the same amount of wind energy received. This will cause a shift in the power-curve that can then be detected by comparing the modelled power curves for fault and fault free data periods.

(de Andrade Vieira & Sanz-Bobi, 2015) propose a power curve modeling technique to reduce the dimensionality of SCADA data. A piecewise linear regression model based on piecewise polynomials is used to model power curve. The method is called Linear Hinges Model where a few points are selected to represent the power curve. **Fig. 3.3** presents the definition of Linear Hinges Model. One year of historic data is used as a reference to learn the

reference model and is compared to the new data collected from the wind turbine under observation.

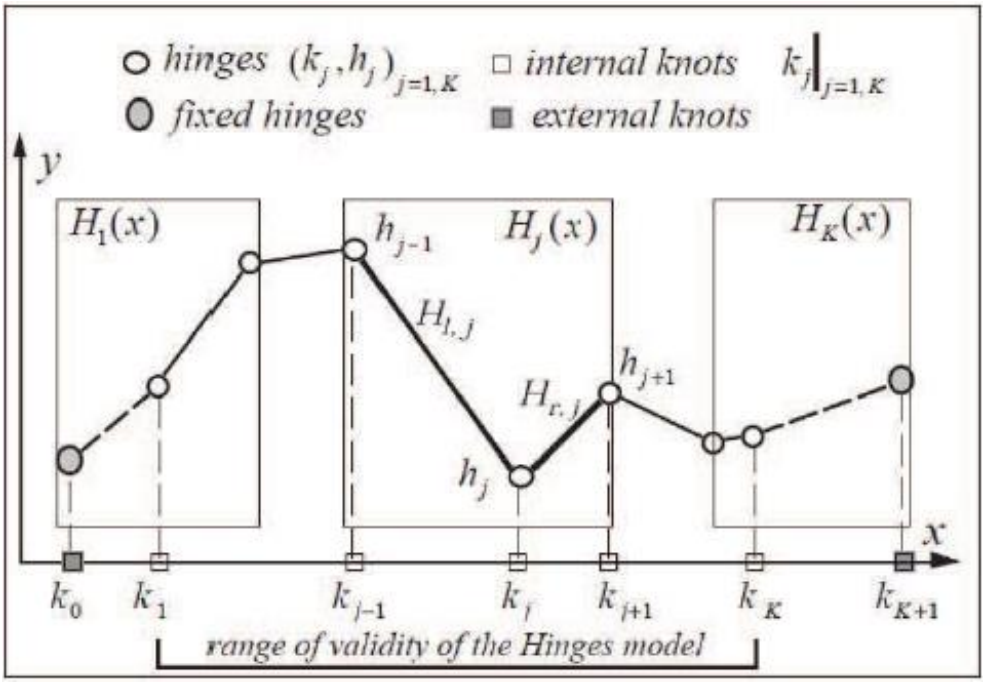

Figure 3.3 Linear Hinges Model definition, reprinted from (de Andrade Vieira & Sanz-Bobi, 2015)

(de Andrade Vieira & Sanz-Bobi, 2015) show that due to the nature of wind, certain wind speed samples occur more than the others. For robust analysis, this variation in wind distribution needs to be considered. For achieving that, the power curve is divided into different segments. A weight is assigned to each segment based on the wind distribution of that segment.

The choice of number of different sections is a function of the operational states of the wind turbines. An indicator PI is calculated by calculating the difference of areas under the curves of reference and online data. The indicator is then weighted according to the wind distribution in each section. The global performance indicator is the finally defined as the weighted average shown in Eq. (3.3) below.

$$HCI\_PC = \sum_{I=1}^{n} (WD_i^T . PI_i) \qquad \text{eq. 3.3}$$

Where WD is the weight and PI is the performance indicator for region i calculated using the Eq. (3.4).

$$PI_i = \frac{S_i^T - S_i^R}{S_i^R} \qquad \text{eq. 3.4}$$

where S_i^T and S_i^R are current and reference areas of respective region i

The validation for the proposed approach is done by looking at the evolution of the difference percentage of the calculated performance indicator form the reference over time. 2% and 5% deviation from the reference indicators are selected as the thresholds for warning and alarm respectively.

Although (de Andrade Vieira & Sanz-Bobi, 2015) propose an approach to reduce the data required for analysis, the need to have sufficient data to create a complete power curve still remains. The idea of short and long term analysis is proposed to address this concern.

The method proposes an anomaly detection approach but the fault detection and isolation capabilities are not shown. A proposed idea is to look at the slope of a decreasing performance indicator but the quantification of the same is lacking. Another fundamental assumption in the approach is a significant production loss observed by the machine. The quantification of the %age thresholds in terms of actual production loss can be important when working with this method.

3.1.3 (Jia et al., 2016a)

The authors of (Jia et al., 2016b) propose the use of principle component analysis (PCA) to extract the model for wind turbine power curve. Similar to the other model comparison based methods, the performance degradation is quantified by evaluating the deviation between normal and degraded condition based representative curves.

The basic theory behind PCA is simple. First, PCA finds mutually orthogonal directions where variation of data is maximized. Then, the original data is projected into these coordinates and the selected vectors that carry most of the variation in the data are chosen as principal components (PC). The detailed procedures of applying PCA are: 1) obtain the covariance matrix of the normalized data; 2) calculate the eigenvectors and eigenvalues of the covariance matrix; 3) determine the number of PCs to keep; and 4) project the original data into PC space. **Fig 3.4** presents the transformation of power curve into PC space.

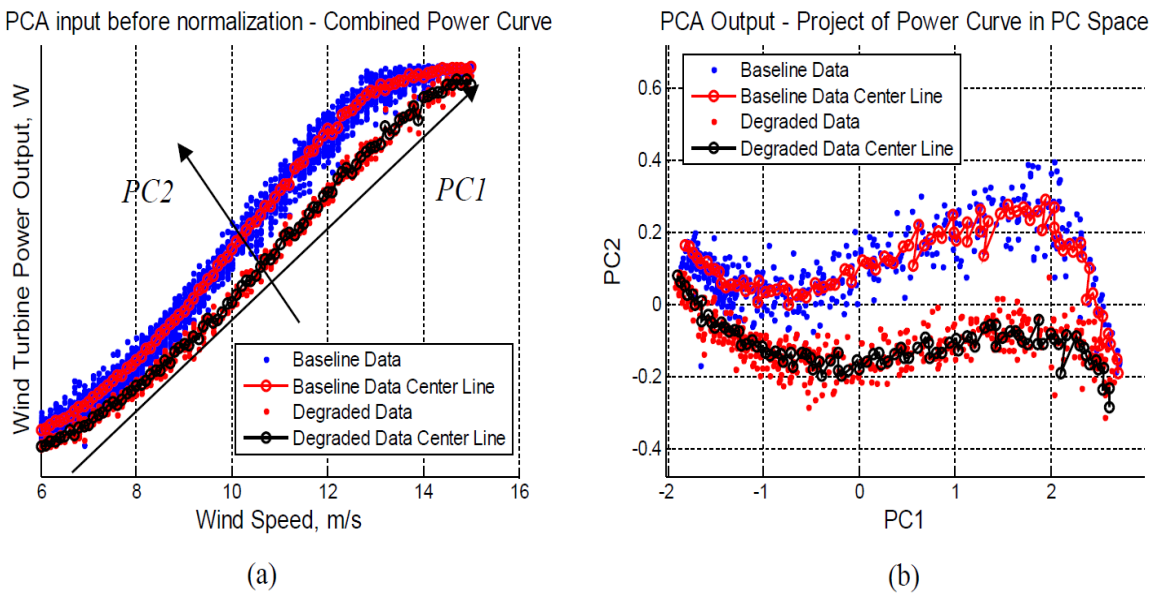

Figure 3.4 Application of PCA in the proposed algorithm: (a) combined power curve before data normalization; (b) combined power curve in the PC space reprinted from (Jia et al., 2016b)

Using the deviation of baseline and degraded data in PC space, a confidence or health value is calculated every day and 1 week (1000 samples) data prior to the evaluation is considered as input. For the reference data set, 3 week data after the first known maintenance intervention is selected by the authors. The assumption for the choice of this data is the normal condition of the turbine right after maintenance. The daily progression of the performance indicator calculated using the algorithm proposed by (Jia et al., 2016b) is used for performance evaluation.

Three other modelling techniques including Gaussian mixture model (GMM) with an L2 distance metric; (2) Self-organizing map (SOM) with Minimum quantization error (MQE) distance metric; and (3) Neural network (NN) with analysis of residues are also implemented and compared with the proposed technique. The proposed technique is shown to generate the least number of false alarms when a threshold of 3 standard deviations is selected.

It is important to note here that the fault data selected by the authors for the validation is statistically significant and very restrictive as a test case. The method proposed restricts its implementation to the linear region of the power curve. This risks is ignoring the faults and failures caused by the control system faults that only activates in the nonlinear region. The method proposes a way to monitor performance degradation but fault identification and isolation still remains a problem.

Due to the inherent nature of the data requirement in order to build the complete power curve 1 week (1000 samples) for analysis and calculation of indicator as used by authors can be case specific and not too relevant to other cases.

3.1.4 Conclusion on Model Comparison based Methods

The type of methods that use a comparison of models approach all share the basic requirement of sufficient data to build a model. Methods falling in this category have the advantage of working with simpler implementations. But the restriction and limitations on the detection capabilities are evident. This family of approaches have been validated on faults having visibly high impact signatures and fault isolation remains a problem. Due to the simplicity of modelling approaches employed, power curves are often filtered to extract only the linear region. This results in filtering out the regime of data where pitch control system is active hence omitting the possible faults related to the pitch control systems.

As concluded above, this type of methods have an inherent drawback when it comes to timely online monitoring. The literature is silent on the quantitative evaluation of the wait times before first results. These methods need enough data to build the complete power curves before comparison. Another drawback is the lack of fault isolation and identification capability. The advantage is the simplicity of condition monitoring indicators.

3.2 Residual based methods

The main principle of this group of methods is to build residuals for condition monitoring of wind turbines. Residual building is a classical approach in model-based fault diagnosis. Fault detection and diagnosis systems use this strategy for a variety of applications in a plethora of scientific knowledge domains. (Isermann, 2006). The same approach is actively used in the wind turbine fault detection problem as well.

First, a way to model expected power from the normal conditions is developed on offline data. Residuals are then calculated by looking at the difference of measured and expected values. **Fig 3.5** gives an overview of such normal behavior models. Fault detection indicators are created on the basis of the calculated residuals. Ideally, under normal conditions, the residual i.e. the difference between predicted and measured values is minimal. Control limits or thresholds are used to detect the deviation of residuals from normal behavior.

In the context of wind turbine fault detection, the function $\boldsymbol{f(x)}$ is the wind turbine power production process, characterized by the power curve. The process has environmental influences (e.g. wind speed) labelled $\boldsymbol{x}$ as input and as a consequently the produced power $\boldsymbol{y}$ as the actual/measured system output **(Fig. 3.5)**. If the same process is modelled; through any of the mathematical process modelling techniques, the output $\boldsymbol{y'}$ becomes the modelled system output. The difference between the measured and modelled outputs can be labelled as error $\boldsymbol{e}$ or also commonly referred to as the residual.

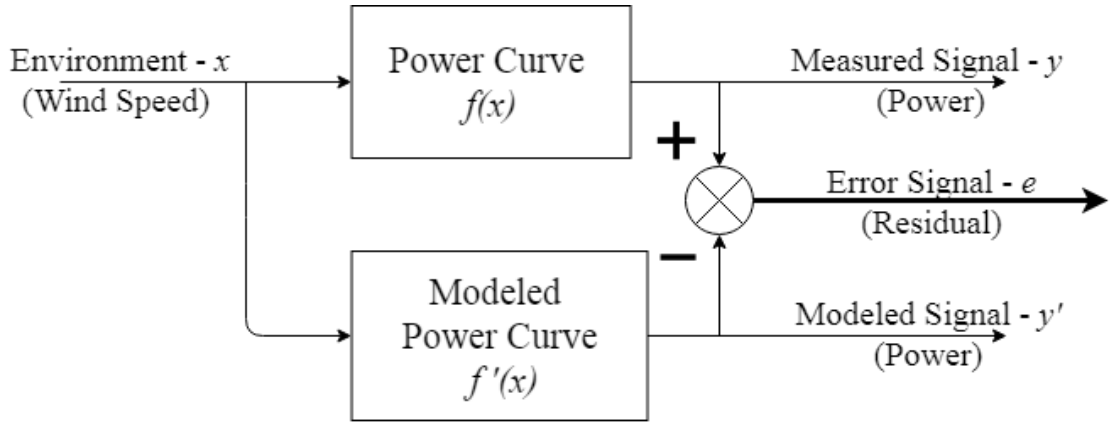

Figure 3.5 Residual based method overview: x is the on-line input, y is the actual system output, y' is the modelled system output, and 'e' is the residual or error signal

The idea behind the residual based condition monitoring is that any deviation in the residuals from nominal values can hint a change in system. If a significant deviation from the normal is detected through control charts or thresholds, a fault can be associated. The strength of residual building approaches is the superior online monitoring capabilities. Once the offline prediction model is learnt, the modelling of expected output power can be done in real time and condition monitoring is possible. Moreover, the historic residuals can also be used to look at the evolution of overall behavior of the system over time.

However, wind turbine systems are greatly affected by the environmental and operational variations. The impact is clearly visible in built residuals, even under the normal conditions (e.g. visible seasonal variations). Considerable data scatter/dispersion is observed by looking at the scatter plots of residuals that make it hard for learning suitable threshold and control limit values for condition monitoring. Hence, for residual based condition monitoring, it becomes even more important to take into account environmental and operational variations.

Residuals based condition monitoring approaches have been used in several ways. Based on the literature review, two clearly distinguishable ways of building the residuals for condition monitoring emerge. The categories are termed here as the explicit methods and the implicit methods.

3.2.1 Explicit Methods

The explicit methods exploit the graphical relationship curves between produced power and other operational variables of interest. The most common relationship used is the power curve but produced power versus other operational variables like generator's shaft speed and pitch control angle etc. are also used. This family of approaches is labelled explicit as the explicit nature of wind power relationship is preserved and the data dispersion, noise etc. are handled separately. The classification principal of this family is better represented as the eq. A

$$\widehat{\boldsymbol{P}} = \boldsymbol{f}(\boldsymbol{WS}) + \varepsilon(\boldsymbol{T}, \boldsymbol{\rho}, \boldsymbol{RS} \dots) \qquad \text{eq. A}$$

$\widehat{\boldsymbol{P}}$ is the power modeled as a function of, most commonly wind speed $\boldsymbol{WS}$, or otherwise operational variables and the data dispersion ε. As visible from the eq. A, it is imperative to note here that dispersion for this approach is considered separate of the modelled power curve. The dispersion is reduced by making corrections for temperature $\boldsymbol{T}$, air density $\boldsymbol{\rho}$, or using rotational speed $\boldsymbol{RS}$ etc. This is in contrast to the second family of residual building solutions presented later.

The expected normal behavior curves are either learnt on the data or drawn from technical specifications. The residuals are then built by calculating the difference between the measured data and reference curves. One of the more persistent approach to build a reference curve is the 'method of binning' inspired by (IEC 61400-12-1, 2005) standard. Other means of developing the reference curves include the constructor provided curves (power curves and operational curves).

Several ways of handling operational and environmental dispersions are proposed by this family of methods. (Cambron et al., 2016) propose multi-stage normalization to address the dispersion while (Uluyol et al., 2011) show the operational variations by looking at power residual as a function of measured wind speed. (Bi et al., 2017a) propose moving away from the power curve due to the dominant dispersion and propose using other operational relationship curves that are less affected by dispersion. (Park et al., 2014) take a more graphical

approach to address the operational variations of using power curves. They propose envelopes around the power curve to serve as thresholds.

3.2.1.1 (Cambron et al., 2016)

(Cambron et al., 2016) propose a method to detect underperformance in wind turbine generator by using power curves and control charts. The reference power curve is modeled using the (IEC 61400-12-1, 2005) proposed method of binning and a residual is calculated as the difference of the reference and observed power data.

The residual is then monitored using exponentially weighted moving average (EWMA) and generally weighted moving average (GWMA) control charts to identify when the process goes out of bound, i.e. statistically away from the fault free reference. The aim is to detect small changes in production of wind turbine using its power curve (wind vs. power). The authors choose to work on the quasi-linear region of power curve where the cubic relationship between wind speed and produced power holds.

The dispersion around power curve depends on various atmospheric conditions including air density, turbulence intensity etc. So, it is desirable to correct for these conditions such that the power curve becomes independent of these conditions or that the dependence reduces. (IEC 61400-12-1, 2005) presents an air density correction to density reference of ρ_0 = 1.225 kg m^{-3}. A correction due to turbulence was also done i.e. normalization of power curve raw data to a pre-defined target Turbulence Intensity was added as suggested by (Axel Albers, n.d.). Nacelle wind speed data was used instead of meteorological mast to reduce data dispersion. The main objective was to bring all measurements to same operational conditions.

The operational variations are handled by working with data sorted within bins as proposed by (IEC 61400-12-1, 2005) standard. The standard looks at the wind speed-power relationship (power curve) and proposes the sorting of measured power data into wind bins of 0.5 ms^{-1} resolution. In order to agglomerate each 0.5 ms^{-1} bin's normality on a single control chart, further transformation of measured power values is proposed. The aim is to ensure that the distribution of power within a bin is normal as the data distribution amongst different bins can vary. All data points for power in respective wind bins are translated along a linearized segment on the intermediate values of each bin.

After density correction, turbulence adjustment and Power value transformation, the bin specific residual between measured and expected power is calculated as Eq. (3.5).

$$R_{i,i+1} = P_{i,i+1} - P_{trans} \qquad \text{eq. 3.5}$$

where $P_{i,i+1}$ is the average of the power curve in the Bin i and $i + 1$. The calculated residuals are then reset to a normal distribution. **Fig 3.6** presents an overview of the methodology implied by the authors.

The validation of the proposed approach is done by looking at two simulated underperformance scenarios and also by evaluating the underperformance on one case of real SCADA data. Two underperformance scenarios evaluated are ramp and a step shift applied to simulated stream of data. (Cambron et al., 2016) try to express the underperformance in terms of production loss. The key criteria for performance evaluation of such methods is the ability to quantify the smallest detectable shift in the power curve and the time needed to detect such a change.

The authors make an effort to compensate for environmental and operational variations but the proposed technique lacks validation on different types of faults, under different operational and environmental conditions. The fault scenarios simulated, are the introduction of a ramp shift to emulate gradual and progressive faults like blade erosion and a step shift in the entire power curve. The step shift is aimed to replicate a sudden change in components but the authors fail to associate a real example scenario to have this kind of an impact.

The approach proposed by (Cambron et al., 2016) looks to filter out the nonlinear region of the power curve. The argument for that is the fact that in the nonlinear region, the control system of the wind turbine interferes with the operational conditions and also that the linear region of the power curve is where the most energy is produced. However, this restricts the capabilities of the proposed approaches as it neglects a possible family of faults associated to the wind turbine control system.

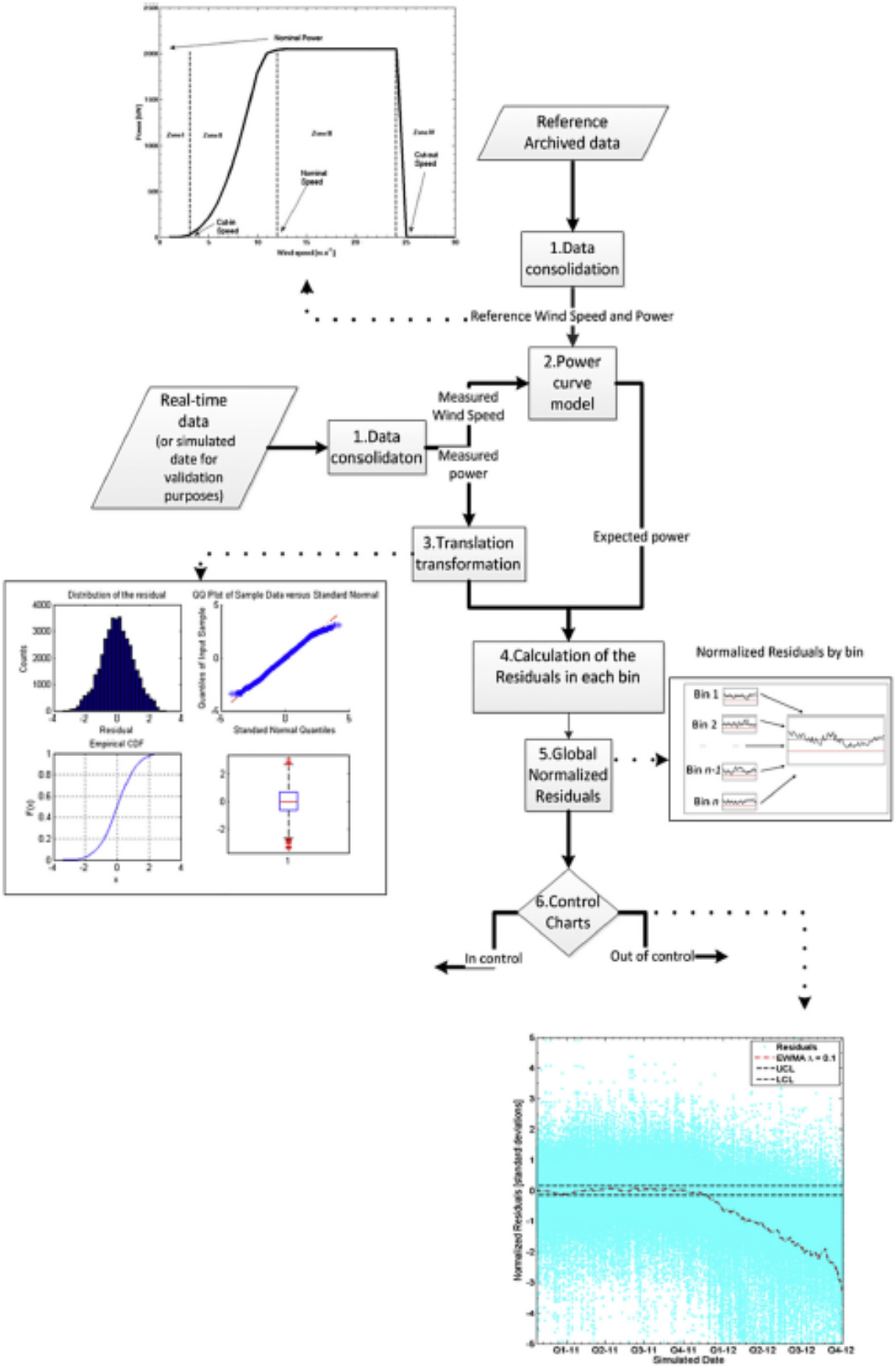

Figure 3.6 Step by step methodology reprinted from (Cambron et al., 2016)

3.2.1.2 (Uluyol et al., 2011)

(Uluyol et al., 2011) propose the use of explicit power curves for wind turbine condition monitoring. The anomaly and change detection is performed by calculating statistical indicators like mean, skewness and kurtosis on generated residuals, where a residual is generated as the difference of reference and observed power curve values. The inherent operational and environmental variation in the power curve data are expressed by working with power residuals as function of wind speed instead of looking at the evolution in time.

The constructor provided power curve is used as reference where available and polynomial fitting is used as an alternative in case of unavailability of constructor reference. The actual power curve usually deviates from the nominal power curve. This is due to a number of site specific factors like complex wind regimes, complex or benign terrain and due to different meteorological conditions like wind direction, wind shear, turbulence intensity etc.

The authors propose to first quantify the variations on the baseline or reference data in order to better address and account for these variations. **Fig 3.7** presents a graphical manifestation is the scatter plot of power residual as a function of wind speed. The data dispersion of power residuals is lower for low and very high wind speeds while the maximum dispersion is observed in between. This region is also the linear region of power curve and is the most common region of operation for a wind turbine.

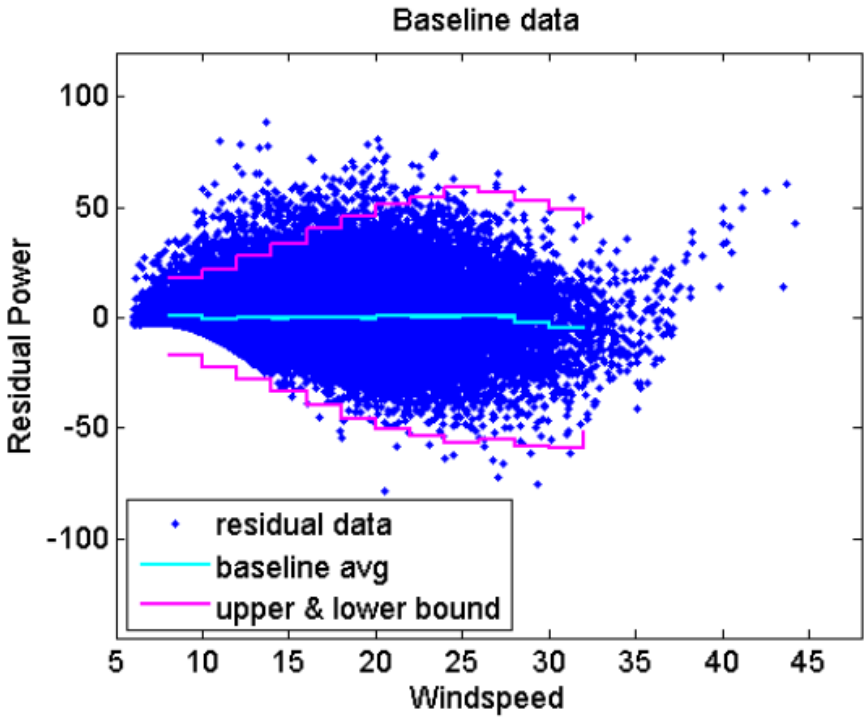

Figure 3.7 Power Residual as a function of wind speed

(Uluyol et al., 2011) propose the calculation of statistical indicators for data in each wind speed bin to better account for the operational variation and dispersion. Three statistics are proposed to serve as the overall condition indicators namely mean, skewness and kurtosis, calculated for data in each wind bin. The resolution of a wind bin is not mentioned by authors but (IEC 61400-12-1, 2005) standard proposes 0.5 ms^{-1} as a suitable wind bin resolution.

Monthly, seasonal and quarterly evolution of statistical condition indicators are presented by authors. Validation is done on two cases from SCADA data of different operators. The first test case (10 min SCADA data) shows an improvement of condition indicator. This is observed when looking at mean values of data in a bin for mid-range wind speed values (linear region). This is probably due to the fact that the turbine is seldom in the low or high speed operational modes. The analysis here was done by looking at the seasonal evolution (winter, spring, summer, and fall) and comparing between two years 2008 and 2009. However, the authors were unable to associate this improvement to any maintenance action due to a lack of maintenance logs.

The second data set (1 min SCADA data) contained a gearbox fault identified during a semi-annual maintenance action by the operator. The nature of the fault and timestamp logs of maintenance logs were available. The condition indicators used were kurtosis and skewness of

the data in each wind bin and the evolution of indicator was looked at for quarterly and monthly periods. The increase in deviation for both indicators close to the fault was shown in the quarterly and monthly analysis periods. 20 days prior to the maintenances, a significant increase in the indicator values for high speed bin was shown. A proposition was made that the impact of a fault may be more significant under certain operational modes or in certain wind bins.

(Uluyol et al., 2011) are aware of the realistic operational and environmental dispersion when using power curves and propose to evaluate power residuals as a function of wind speed instead of time to better address the same. The variations caused by seasonality are also shown. However any clear identification or association to a particular fault scenario is lacking. The validation scenarios used are very specific and cannot be associated to the clear detection capability of the method proposed. A proof of generalization is also missing as it is unclear how the approach will perform for different machines and faults.

3.2.1.3 (Bi et al., 2017a)

(Bi et al., 2017a) perform condition monitoring of wind turbines by calculating the distance of measured data from reference operational curves. The authors look at various operational curves for wind turbine including the most common wind speed vs power curves. Other operational relationships shown include wind speed vs pitch angle, wind speed vs generator speed, generator speed vs power and generator speed vs pitch angle curves respectively. The last two curves are selected for condition monitoring due to the least amount of operational variation and dispersion. Anomalies are detected by raising an alarm when the Euclidean distance of the observed data from the reference curve crosses a statistical limit.

The authors have 4 days of high resolution data (1 second SCADA data) at their disposal. In-depth operational insight into the wind turbines is used to identify and label the operational modes of a pitch controlled machine. This domain knowledge and technical specifications are used to construct the reference curves. The specification based reference curves, if available, remove the need to learn normal behavior models on data. Fault detection is done by putting statistical limits on the Euclidian distance of data for each section of the curve depending on the operational state of the machine. **Fig 3.8** shows the generator speed vs produce power curve. Different operational modes are marked and distances calculated in each mode are used as indicators.

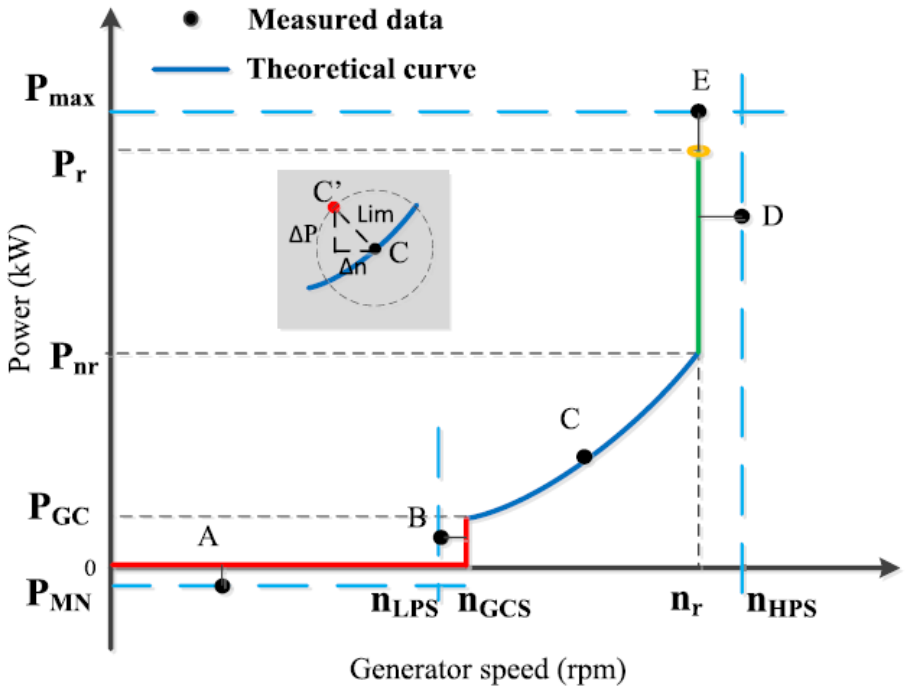

Figure 3.8 Generator speed vs power curve with operational modes, reprinted from (Bi et al., 2017)

As explained earlier, the indicator for anomaly detection and alarm generation for condition monitoring using the Generator Speed vs *Power* curve is the Euclidian distance calculated as presented in Eq. (3.6).

$$D_1 = \left\{\sqrt{(n_i - n)^2 + (P_i - P)^2}, (n, P) \in C_1\right\}_{min} \qquad \text{eq. 3.6}$$

Where C_1 is the set of points on the reference curve; n is generator speed and P is the Power Output. Similarly, the distance on the Generator Speed vs *Pitch angle* is calculated as the distance between i^{th} normalized data and its neared point on the curve given by Eq. (3.7).

$$D_2 = \{|1 - n_i|, |\beta_i|\}_{min} \qquad \text{eq. 3.7}$$

The validation is done by comparing the alarm generation capability of the proposed method with that of Artificial Neural Network (ANN) and Adaptive neuro-fuzzy inference system (ANIFS). The fault scenarios compared are slip ring pollution of Doubly Fed Induction Generator (DFIG) type wind turbine, two instances of pitch controller malfunction for DFIG turbine. The second type of wind turbines looked at were with the Permanent Magnet Synchronous Generators (PMSG). In order to comment on the false alarms generated by the proposed approach in comparison to the other two techniques, three normal operation behavior scenarios, (1 for DFIG and 2 for PMSG) wind turbines are also presented. The proposed

method was shown to detect polluted slip ring fault 20 h earlier and the pitch controller malfunction 13h earlier than the AI approaches.

Additional domain knowledge and technical specifications are required to implement the proposed approach. The correlation curves showing the relationships amongst different operational variables are still familiar for the operators. But the approach presented is highly dependent on the availability of technical specifications. The reference curves are also highly machine specific and can change drastically based on the manufacturer and the model.

However, if the technical specifications for the reference curves are not available, normal behavior model learning techniques can be applied to learn reference curves. The efficiency and applicability of the proposed approach on the industry standard (10 minutes SCADA data) is not shown.

3.2.1.4 (Park et al., 2014)

The authors in (Park et al., 2014) take a novel and graphical approach to wind turbine condition monitoring. A graphical envelop with a lower and upper bound is learnt on the power curve and warnings or alarms are generated based on the distance of each data point from the reference. SCADA systems come installed with alarm generation systems where alarms are generated by the turbine's controller. The aim is to propose a more meaningful alarm generation technique.

The proposed algorithm uses an approach inspired by the (IEC 61400-12-1, 2005) standard's "method of binning". First the power curve data is sorted into bins and a mean is calculated for data in each wind bin. A B-Spline model is learnt on these mean values of power curves to serve as the reference. The learnt reference model is then shifted left right and up down to find the optimum bounds of the given power curve data. Warning and Alarm limits around the power curve data are selected, effectively making the distance from the reference power curve a residual with two layer upper and lower control limits in the form of Warning and Alarm envelops around power curves. The envelop serves as a variable threshold and can be considered as a means to consider operational variation of the graphical power curve. **Fig 3.9** shows envelop around mean power curve along with labeled warning and alarm limits.

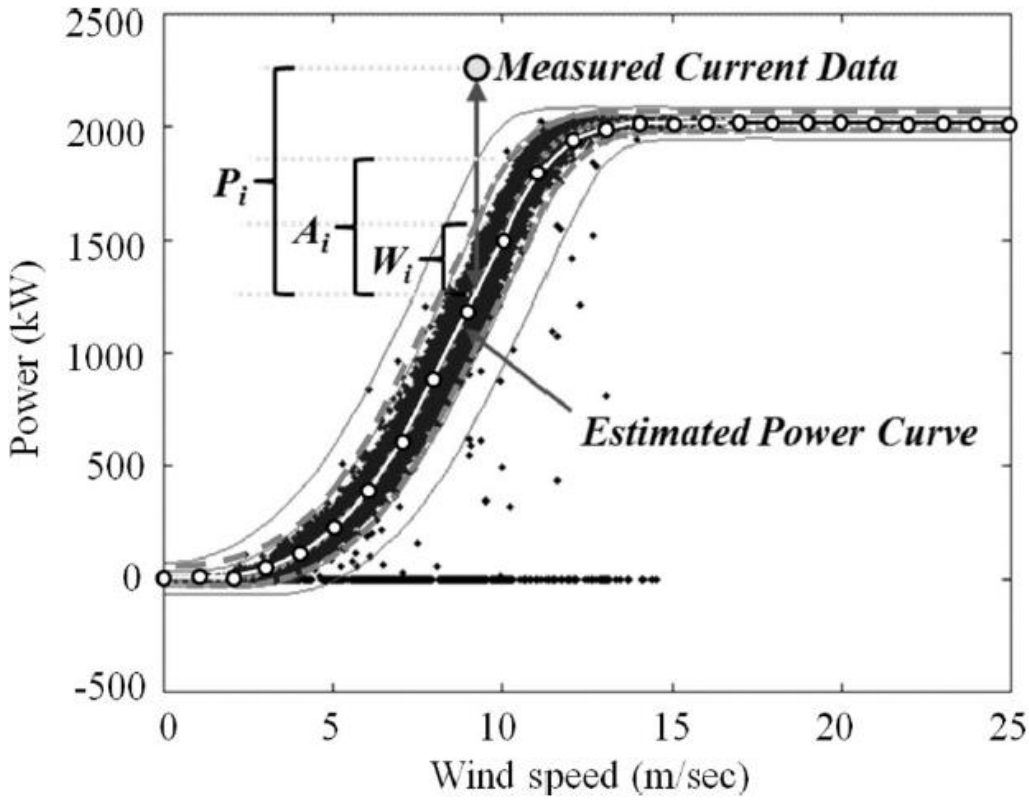

Figure 3.9 Power curve with real data, warning and alarm limits, reprinted from (Park et al., 2014)

For the monitoring phase a three stage fault data queue approach is proposed. The data queue is generic First in First out (FIFO) data structure. Instead of raising a warning or an alarm right away when an observed data point enters the waring or alarm zone or crosses the limits, three parameters are calculated. For each new observation "i", three members of the fault dataset include the residual value or error distance from the reference curve center termed as P_i , the corresponding warning limit value W_i and the corresponding value of the alarm limit A_i .

An alarm or a warning message is generated if the 3 stage fault data queue are saturated or a message has already been raised. Message is disabled when the queue is cleared. The choice of a warning or alarm messages is made based on the following criteria as presented by authors.

a) Using all three fault data sets in the queue, a fault index F is calculated as: $F = P_1 + P_2 + P_3$
b) An alarm is generated if "$F \geq A_1 + A_2 + A_3$"
c) A warning is generated if "$W_1 + W_2 + W_3 \leq F < A_1 + A_2 + A_3$"

The validation of the proposed approach is done on a 22MW wind turbine by showing a 100% fault analysis reliability with less messages generated as compared to the wind turbine's own controller. The proposed approach is a graphical perspective of anomaly detection but the fault isolation is still a problem.

3.2.1.5 Overall Comments on Explicit Methods

The type of methods that work to build residuals by taking explicit curves as a reference are usually computationally cheap. The common power curve is familiar to operators and is often provided by the constructor or can be calculated by (IEC 61400-12-1, 2005) proposed method of binning. If not, the shape is easily learnt by simple curve fitting techniques. Similarly, the reference or normal behavior for other operational curves can be built by using technical specifications or employing other normal behavior modelling techniques. The techniques may include parametric modelling (Linearized Segment, Polynomial curves, probabilistic models etc.) (Lydia et al., 2014).

However, it is important to consider and address the operational and environmental variations of the data when working with these methods.

3.2.2 Implicit Methods

The implicit methods are defined as rather black box approaches where machine learning algorithms are used to model and predict target variable (power). Little attention is given to the domain knowledge integration or conscious dispersion reduction. Normal behavior models are learnt on reference data and used to predict produced power. Residuals are calculated as a difference of predicted and observed power values. This family of approaches is labelled Implicit as the power is modelled with wind speed and other variables so as to address the data dispersion, noise etc. at the modelling stage. The classification principal of this family is better represented as the eq. B

$$\widehat{\boldsymbol{P}} = \boldsymbol{f}(\boldsymbol{WS}, \boldsymbol{T}, \boldsymbol{RS}, \ldots) + \varepsilon \qquad \text{eq. B}$$

$\widehat{\boldsymbol{P}}$ is the power modeled as a function of wind speed $\boldsymbol{WS}$, temperature $\boldsymbol{T}$, air density $\boldsymbol{\rho}$, or using rotational speed $\boldsymbol{RS}$ etc. As visible from the eq. B, it is imperative to note here that dispersion for this approach is considered within the produced power model. The dispersion is reduced by implicitly including temperature $\boldsymbol{T}$, air density $\boldsymbol{\rho}$, or using rotational speed $\boldsymbol{RS}$ etc.

as model inputs. This is in contrast to the explicit family of residual building solutions presented earlier.

The persistent approach is to learn the prediction models using neural network or similar machine learning algorithms. Unlike explicit methods, little or no conscious effort is made to handle operational and environmental impacts of the wind turbine systems. Identification of relevant input variables is one of the only ways shown to consider or address the operational and environmental significance of these variables.

Several ways of selecting the relevant input variables and improving modelling accuracy are proposed by this family of methods. (Pelletier et al., 2016) propose a correlation analysis of different variables to select the best input variables while (Butler et al., 2013) show the environmental variations caused by air density by looking at power curve as a function of measured air density. Hence they propose using both wind speed and air density as inputs to model wind turbine power. To model turbine output power, (Kim et al., 2012) use a number of operational and temperature variables besides wind speed. The reason for the choice of these variables as model input is not commented upon by the authors. (Kusiak et al., 2009a) on the other hand restrict themselves to using just wind speed to model output power but calculate and compare the modelling accuracy of different data mining and evolutionary computation techniques.

3.2.2.1 (Pelletier et al., 2016)

(Pelletier et al., 2016) present a comparison of techniques to model the wind turbine power curve. The approaches shown are modelling techniques and fault detection or condition monitoring is not performed. 2 stage Multi-layer Perceptron (MLP) type neural network is used to model produced power using 6 inputs. The modelling performance is compared with other techniques and it is shown that the proposed approach with the selected input variables outperforms other techniques tested in terms of least mean error (ME) and mean absolute errors (MAE).

For the sake of validation, the authors use 1 year of 10 minutes SCADA data from two wind turbines from different wind farms. Apart from standard SCADA data coming from the turbine controller, the data from meteorological masts at different heights (40m, 50m, 70m and 80m) is also available to the authors. Around 100 different parameters including power, meteorological data, operational data, vibration, temperature components and turbine status

was available but only 6 variables were selected as input. These include wind speed, air density, turbulence intensity, wind shear, wind direction and yaw angle.

Despite having extensive data the authors perform heavy filtration and only consider the sectors that are free from any wind wake effect from other wind turbines in the farms under evaluation. The data ends up being highly filtered and recovery rates for both test turbines under observation are (5.6% and 35.2%) respectively. The high filtration caused by removing data associated to wake effect leaves the wind sectors that are considered valid for calculation to be very limited.

Authors compare the performance of various modelling techniques including MLP-ANN, 5^{th} order polynomial, 9^{th} order polynomial, logistic function and (IEC 61400-12-1, 2005) the proposed method of binning etc. **Fig 3.10** presents a comparison of modelling techniques used. The validation is done by looking at the evolution of the mean error and the mean absolute error.

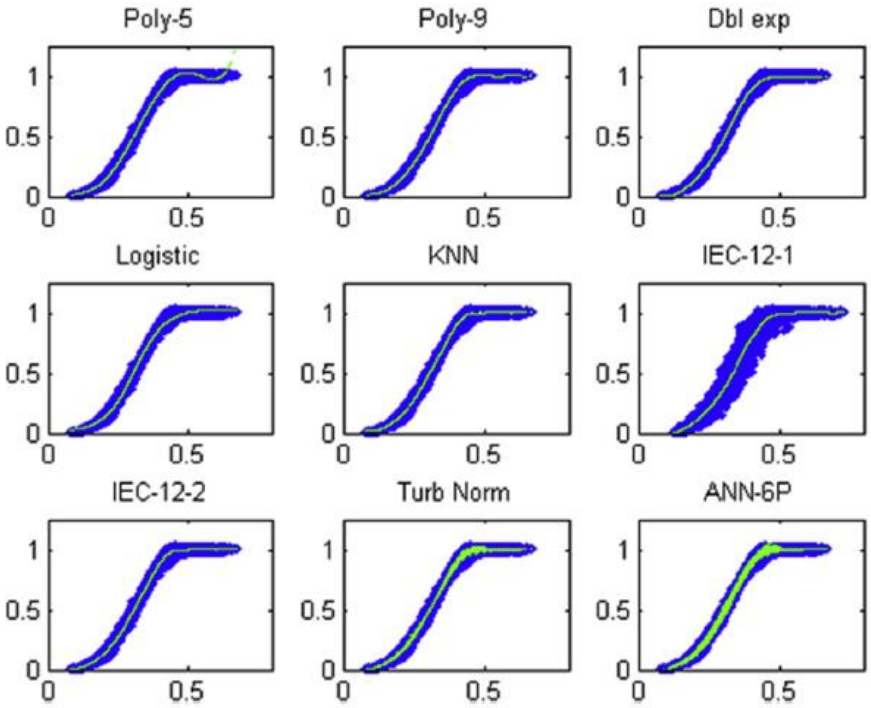

Figure 3.10 Power curve modelling techniques, reprinted from (Pelletier et al., 2016)

No validation is done by using the proposed modelling technique under real fault scenarios.

3.2.2.2 (Butler et al., 2013)

The authors in (Butler et al., 2013) use a Gaussian Process Regression method to model the wind turbine power output. The learnt model is used to predict power output for each timestamp based on two inputs (Wind Speed, Air density). The residual is calculated and cumulative sum of residual is looked at to identify degradation in production or fault.

Visual evidence for considering wind density when modelling wind turbine power output is also shown by the authors. Mathematically, (Farkas, 2011) showed a 16% decrease in root mean squared error when modelling power using both wind speed and air density as compared to only wind speed as model input. **Fig 3.11** shows a scatter plot of power curve data with where color indicates the air density value at each sample time.

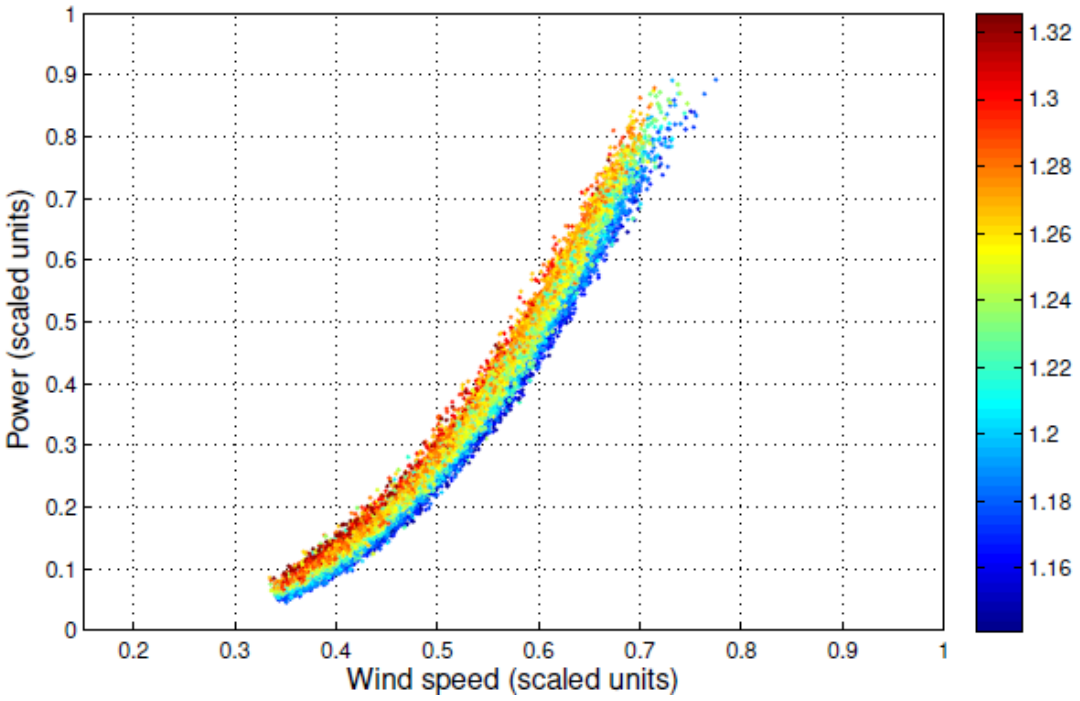

Figure 3.11 Normalized& filtered power curve data, color indicates air density, reprinted from (Butler et al., 2013)

The choice of air density as the model input is an interesting way of reducing the environmental variation but the gain achieved is not quantified by the authors for their example. The validation is done of 24 months of SACDA data. After filtration 60-70% of the data remains as the authors choose to work with the linear region of the power curve. This is to simplify modeling using the Gaussian regression technique but that also filters out the possible pitch control failures.

(Butler et al., 2013) show a degradation trend in the cumulative sum of the residual possibly caused by the main bearing failure but a distinct detection of fault is lacking. The method is not generalized to different faults or turbines from different farms or manufacturers. This limits the performance capabilities of the proposed approach even further.

3.2.2.3 (Kim et al., 2012)

The authors in (Kim et al., 2012) utilizes artificial neural network for training normal behavior of wind turbine system. The considered fault detection scheme, instead of calculating the residual for each time stamp, segments the data to an acceptable time period. For each segment j, the residual (r) are then computed and used in Eq. 3.8 to calculate the health confidence value CV, inspired by (Lapira et al., 2012).

$$CV_j = \frac{Number\ of\ r \geq r_{thresh}}{Number\ of\ samples\ in\ jth\ segment} \qquad \text{eq. 3.8}$$

In order to model the normal behavior, a multilayer neural network with error back propagation and one hidden layer is used. Input variables including wind speed, pitch angle, rotor speed, nacelle temperature, gearbox oil temperature, gearbox bearing temperature and generator's temperature are used to mode produced power. Residuals (r) are calculated as a difference of the measured and modelled power.

As briefly referred to earlier, fault detection is proposed by segment wise (on time axis) indicators. This is done to address erratic behavior of residual. Validation is also done by looking at histogram shift of residual. The authors in (Kim et al., 2012) fail to present an objective way of quantifying the shift in residuals from normal behavior nor a fault detection strategy is proposed. The visual aspect of the presented performance indicator could be of use but the method presented can't be used for fault detection.

3.2.2.4 (Kusiak et al., 2009a, 2009b)

The authors in (Kusiak et al., 2009a) present multiple models for monitoring wind farm power production. They compare a number of different machine-learning methods of modelling the power curve. Authors use wind speed as model input to predict power output and show the use of different modelling techniques for wind turbine condition monitoring problem.

Outliers are removed from the training data, before training data is used to model the power output. The techniques used include a least squares method, maximum likelihood estimation, and a number of non-parametric approaches, including multi-layer perceptron and random forests.

Upper and lower limits of acceptable power output for each wind speed were used to build control charts, as shown in **Fig 3.12**. In this way, any values which resided outside the control charts were highlighted as anomalous. This study did not contain any information on possible reasons for the anomalous values. Models were learnt on the quasi-linear region of power curve and modelling accuracy was compared. No application or validation on fault scenarios was done by the authors and the scope was limited to only the derivation of accurate predictive models.

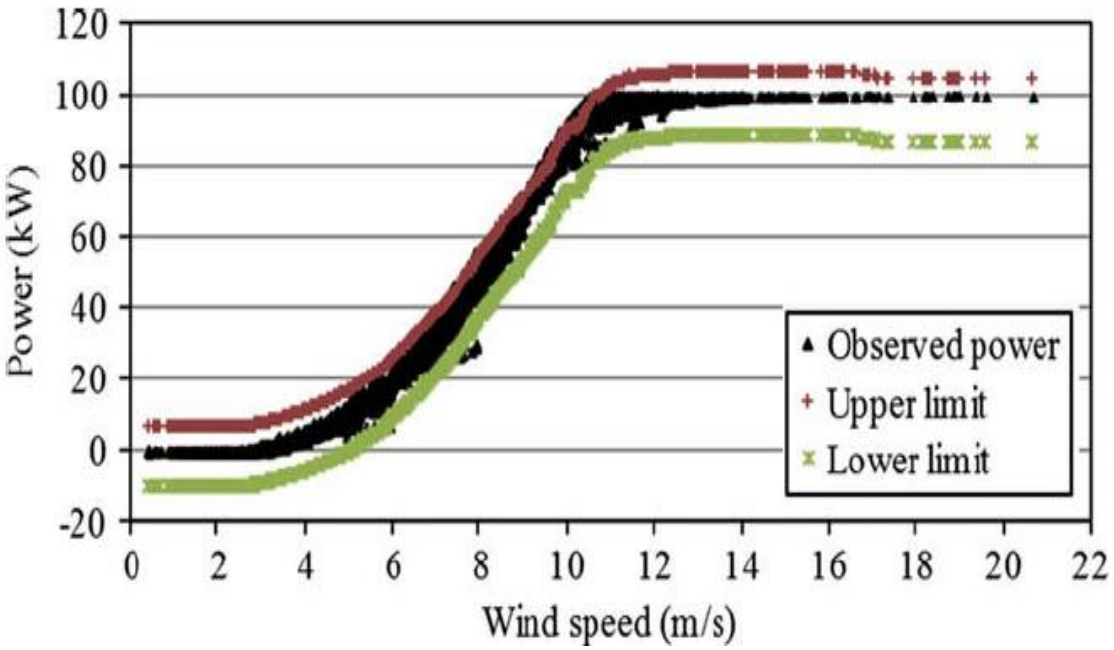

Figure 3.12 Power curve data for 100kW wind turbine, and control chart limits based on modelled values, reprinted from (Kusiak et al. 2009)

3.2.2.5 Overall comments on Implicit Methods

The type of methods that work to build residuals by taking implicit approach are usually computationally expensive. They require sufficient data to train and often require an increased level of expertise. But once the model is learnt, they allow for online monitoring and instantaneous response and hence are more robust. Fault localization is difficult as they model

the overall behavior of the machine. Based on the literature review of power based fault detection approaches, some conclusions can now be drawn.

3.3 Conclusion on Literature Review:

In the scientific domain of wind turbine condition monitoring using SCADA data and more specifically using power based methods, many major problems occur. It is noted that a major concern includes the operational and environmental variations that introduce dispersion and thus make condition monitoring difficult. Data dispersion is also introduced by the 10 minutes averaging of data since 10 minute SCADA data is the industry standard. A lot of variation comes from the geographical locations, field conditions like the terrain and operational characteristics specific to the turbine manufacturer as well.

Several different strategies have been proposed in the literature to address these concerns but no quantitative evaluation has been presented. A comprehensive analysis of what works and to what extent is lacking. Another noticeable gap is the lack of in depth analysis and performance evaluations of the proposed approaches under different scenarios. Wind energy is an ever expanding field and often each operator has multiple wind farms from multiple manufacturers. Different faults may occur during the lifetime of a machine. The faults although critical in terms of production loss are often few, far between and highly variable in their impact on a case to case basis.

To summarize:

Through the extensive literature review, it has been established that power curves and produced power are sensitive to faults and underperformance. The faults have been shown to have a measurable influence on the produced power; the output of a wind turbine. Hence their use for fault detection and identification is validated. However, following issues and gaps are identified

- It is observed that power curves as condition monitoring tools are also sensitive to environmental influences, operational conditions, noise and data resolution etc. in addition to the manipulated input variable (wind). These influences manifest themselves as data dispersion that makes FDI difficult.
- The literature fails to provide an in-depth, generalized and comprehensive proof of concept for using power/power curves for fault detection and identification.

- The proposed solution lack an extensive validation on real data from different turbines or on a realistic simulation framework replicating similar conditional variability.
- The solutions also lack an extensive validation of a method on different possible fault types.
- Globally, very few methods approach the problem from an industrial perspective and take into account the industrial and real life implementation concerns.

This opens a window for improvement and a scientific gap to be filled by the research contribution in in this thesis. A controlled simulation framework is required to analyze the impact of environmental and operational variations. A comprehensive and critical performance comparison for detection capabilities under different fault scenarios is also essential. All these conclusions present an opportunity to develop a comprehensive framework hence providing for the context of this work.

4 Presentation of the VALEMO data

In order to proceed further with the analysis and to develop a realistic simulation framework, a relevant database needs to be created. In this chapter, we present the rich and extensive data made available for this research. Operational and environmental characteristics of data source along with the motivation for each selection is presented. Since extensive SCADA data from all over France is available, a careful selection of representative wind farms is made to keep the scope manageable. Data quality control and pre/post processing strategies are detailed along with real data fault cases that motivate this research.

The data used are sourced from the industrial partners of this project, VALEMO. VALEMO is a subsidiary of the VALOREM group (an independent French renewable energy operator). It specializes in the exploitation, operations and maintenance of renewable energy installations. VALEMO has been working on the O&M of renewable energy systems since 2011 and has a dedicated R&D activity unit enabling it to develop specific software tools for in-house and customer use.

4.1 Nature & description of raw SCADA Data

For this study, data from VALOREM's fleet containing multiple large wind-farms from geographically distant locations and from different equipment manufacturers was made available. For each turbine, the complete history of sensor information and turbine status information, for a period of multiple years, was provided. The SCADA system for each turbine records 10-minute averages of each monitored sensor. In addition, the maximum, minimum, and standard deviation of each of these sensor values, over each 10-minute period, is also recorded by the legacy SCADA system. In addition to the values of the onboard sensors, status information, such as start, stop times and other status alarms, are also recorded by SCADA systems.

SCADA systems installed in wind turbines capture measurements from a number of sensors installed at various locations. (IEC 61400-12-1, 2005) standard recommends a number of SCADA parameters that should be collected. On an average, around 40 such variables are measured by SCADA systems and can vary according to the make and model of a wind turbine. As listed by (Yang et al., 2013) some key variables are however common for all SCADA systems. Wind turbine operators can have direct access to these data through manufacture provided data portals or can store these data locally in data servers for further analysis.

Four major categories of data variables include environmental parameters (e.g. wind speed, wind direction, ambient temperature) electrical characteristics (e.g. active power), component temperatures (e.g. gearbox bearings temp.) and control variables (e.g. pitch angle, rotor speeds). Additional information often includes status codes and alarms. Some of the key variables are listed in **Table 4.1** below for reference.

TABLE 4.1 OVERVIEW OF KEY PARAMETERS OF INTEREST

Environmental Parameters	***Electrical Parameters***	***Component Temperatures***	***Control Variable***
Wind Speed	Active Power	Gearbox Bearing	Pitch Angles
Wind Direction	Reactive power	Gearbox Lubrication Oil	Yaw Angle
Ambient Temperature	Power factor	Gearbox Winding	Rotor Speed (High)
Nacelle Temperature	Generator currents	Generator Winding	Rotor Speed (Low)
	Generator voltages	Generator Bearing	

All the variables mentioned above are of importance but for the sake of this research, we limit our interest to *Anemometer measured wind speed* and *Average Nacelle temperatures* in-order to simulate *Active power*. Traditionally, looking at the Power Curve, one can observe that the "Active Power" referred to here on after as "produced power or power" has a direct relationship with the Anemometer measured wind speed referred to here on after as "measured wind speed or wind speed".

However, research has shown a significant contribution of considering air density in wind power production analysis (Farkas, 2011). This use of air density in addition to the wind speed, is captured by the use of "Average Nacelle temperature" referred to here on after as "temperature". It is important to note that air density is calculated through temperature, atmospheric pressure and air humidity using the CIPM-2007 equation from density of moist air (Picard et al., 2008). Since temperature and density are inversely proportional, increasing temperature decreases air density.

Fig. 4.1 shows the evolution of produced power along with the measured wind speed. The curve relationship of wind to power conversion is respected here as well and data for almost one month duration is presented. Other variables of interest include measured temperature and consequently, calculated air density. **Fig. 4.2** presented the evolution of raw wind temperature SCADA data and calculated air density data. It is of interest to observe both the seasonality in measurements along with the inversely proportional relationship of temperature and density.

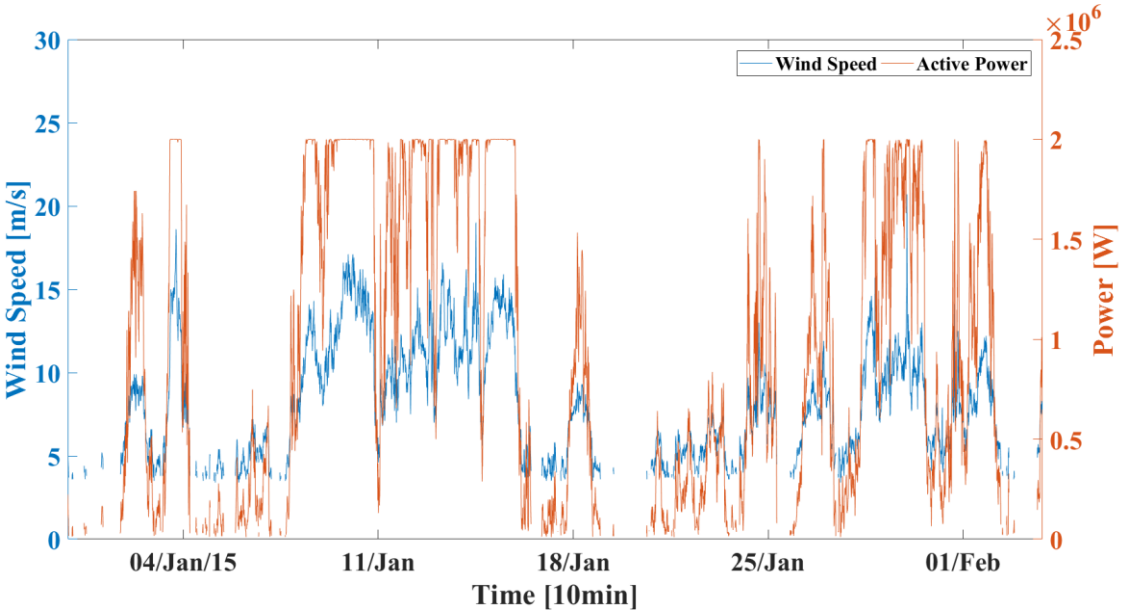

Figure 4.1 Evolution of produced Power [W] as a function of measured wind speed [m/s] (1-month)

The raw data for key parameters identified in Table 4.1 and presented in Fig. 4.1 & 4.2 along with other variables of interest is available for multiple wind farms operated by VALOREM. Since the data is extensive, a careful selection is required based on the key characteristics and variability in order to ensure a representative data set for analysis.

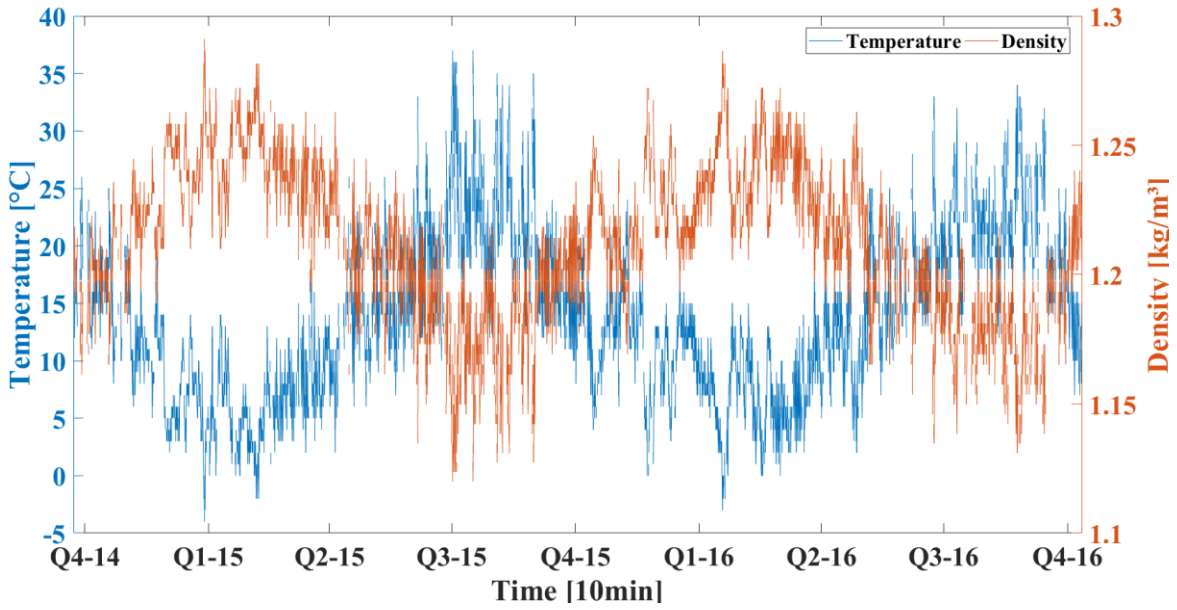

Figure 4.2 Evolution of measured Temperature [°C] and density [kg/m³] (2-years)

4.2 Presentation & description of selected Wind Farms

As briefly explained earlier, VALEMO provides operational and maintenance support to wind farms all over mainland France and is rapidly expanding outside. These wind farms are equipped with wind turbines from many different turbine manufacturers. This provides for an opportunity to have and exhaustive list of options to choose from. **Fig. 4.3** presents some of the fleet operated by VALEMO. As evident from the geographical spread, these wind farms are situated in the east, west, north and the south of France.

Figure 4.3 Geographical Locations of VALEMO's Portfolio – France: 5 selected wind farms (Courtesy: Valemo)

In order to add sufficient variation in the data, 5 wind farms from different geographical locations, with a total of 25 Wind Turbines, manufactured by different OEMs are chosen for this analysis. The data entries from 5 different wind farms enable the capture of environmental and operational variability in our analysis. **Table 4.2** provides a summary of the characteristics of selected wind farms. The selected turbines have different models, variable hub heights, swept area, different rotor diameters and rated powers. The wind farms range from 3 to 6 turbines per farm, implanted in line, grid, L-shape or arc configurations. All the turbines used for this work are vertical axis wind turbines.

TABLE 4.2 DATA BASE SUMMARY

Wind Farms	Wind Farm Characteristics					Wind Turbine Specifications			
	# of WTs	*Farm Location*	*Instal. Year*	*Farm Layout*	*Model*	*Rated Power*	*Hub Height*	*Rotor Dia.*	*Swept Area*
Farm-V	6	Centre-North	2014	Line	SENVION MM92	2.05 MW	68.5/80/100 m	92.5 m	6,720.0 m²
Farm - L	3	Centre-East	2014	Grid	GE 2.5xL/100	2.5 MW	75/85 m	100.0 m	7,854.0 m²
Farm - D	6	Centre-North	2010	L-shape	VESTAS V90	2.0 MW	80/95/105 m	90.0 m	6,362.0 m²
Farm - S	5	South	2009	Line	ECOTECNIA 80	2.0 MW	70/80 m	80.0 m	5,027.0 m²
Farm-C	5	West	2010	Arc	SENVION MM92	2.05 MW	68.5/80/100 m	92.5 m	6,720.0 m²

The geographical location and the farm orientation are important parameters to be considered. Park lay-out of 2 out of the 5 farms is presented for reference. **Fig**. **4.4 a & b** present the farm lay-out of Farm-D and Farm-S. Farm-D **(Fig 4.4a)** contains 6 identical 2MW machines with axis vertical labelled as E1-E6. For Farm-S **(Fig 4.4b)** the southernmost 6 identical wind turbines labelled E6-E11 are available as the remaining turbines are managed by a different operator. The turbines in Farm-S are also 3-blade, vertical axis, and 2 MW wind turbines. This type of power and machine is one of the most common types and although there are larger parks in the world, in France, the farms with less than 10 machines are common.

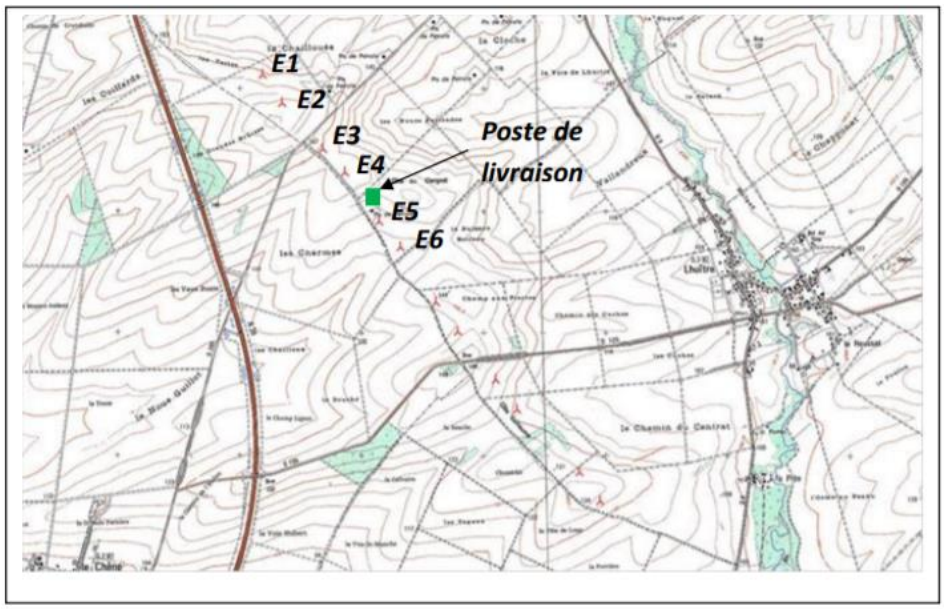

Figure 4.4 a Park lay-out for Farm-D in Center North - France (Courtesy: Valemo)

It is also of interest to note that both parks are organized in a single line due to its size, as shown in **Fig 4.4.** This single line distribution aimed at reducing wake effects. Wake is the influence that one wind turbine can have on another when the wind blows in the direction of their alignment. The wake effect can have an important influence on the performance of the machine. As a general rule, manufacturers of wind farms seek to minimize these effects by placing the farms on areas where a wind direction is predominant and orienting the park according to this direction. This strategy aims to ensure that one wind turbine is rarely in the wake of another.

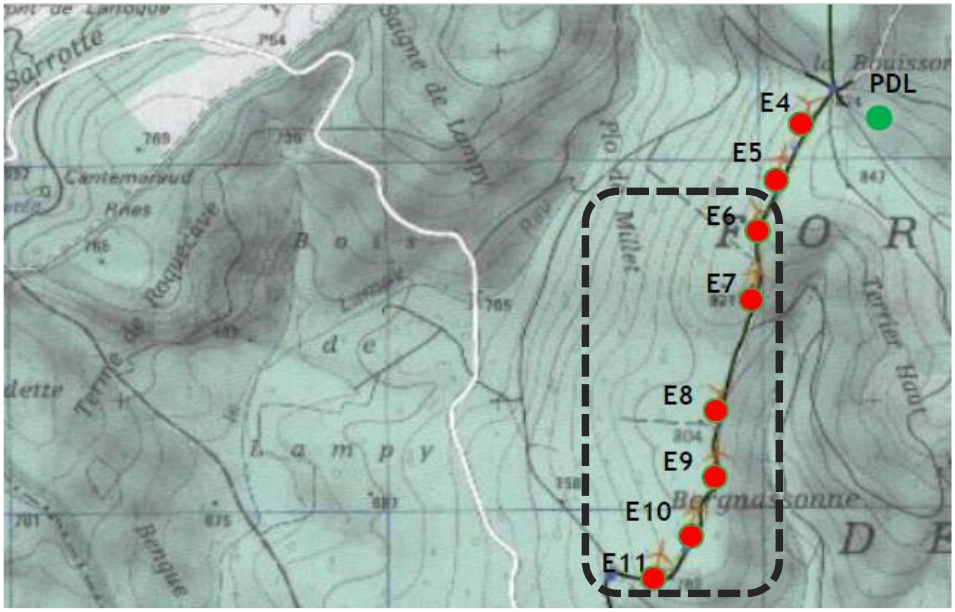

Figure 4.4b Park lay-out for Farm-S in South - France (Courtesy: Valemo)
Note: Valemo only operates Turbines E6-E11

For this research, the choice of the candidate wind farms strives to strike a balance in variability and similarity at the same time for a complete and rigorous analysis. In an attempt to ensure that, two wind farms from the northern France and two wind farms from a unique manufacturer are selected for analysis. **Fig 4.5** presents the power curve data for 1 wind turbine each from Farm V and Farm S. Both turbines being for the same manufacturer and of the same model are expected to have similar operational characteristics. This is in contrast of the power curve for Farm-S which has the same rated power but a different manufacturer and a very different environmental profile.

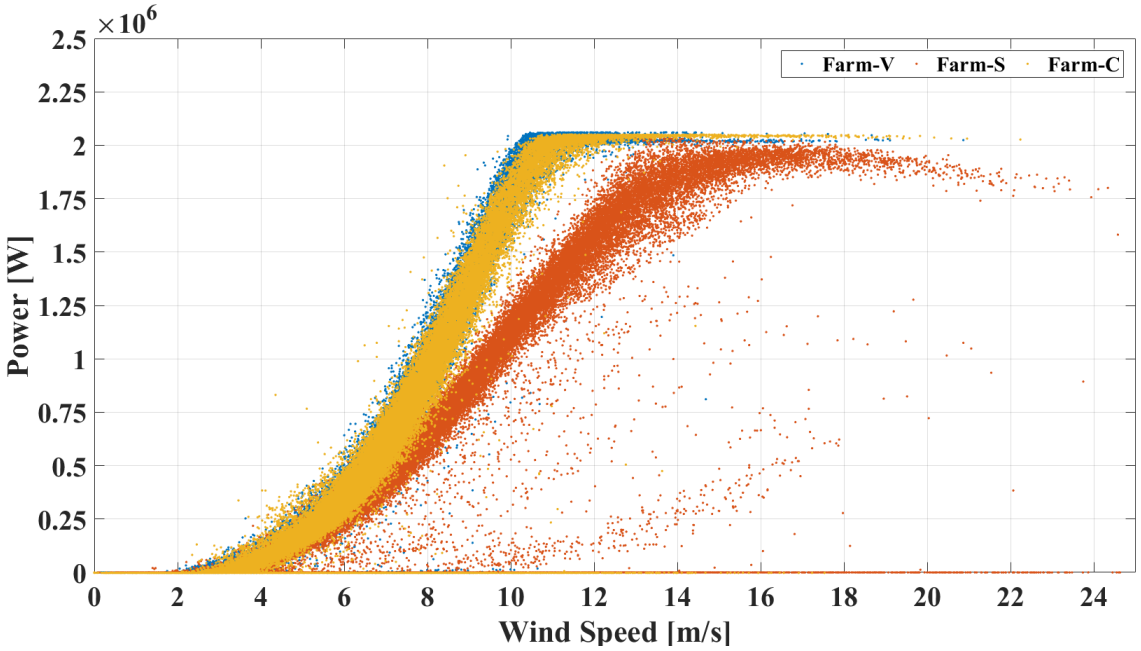

Figure 4.5 On-year Power Curve data for Turbine 1, Farm-V and Turbine 1 Farm C

In addition to the variation in geographical locations, a variation in terrain, farm layout and dominant wind direction, some other key considerations for site selection are environmental parameters. The choice of such a diverse spread of farm locations is also intended to capture a variation in wind and temperature profiles. **Fig 4.6a, b &c** present the mean temperature profile and the normalized wind distribution for 5 wind farms for a 3 year period. The seasonal variation in temperature are clearly visible from the **Fig 4.6 a&b** with temperatures ranging from -5 to 40 °C while the unique wind distribution in **Fig 4.6 c** speaks to the on-site wind variability.

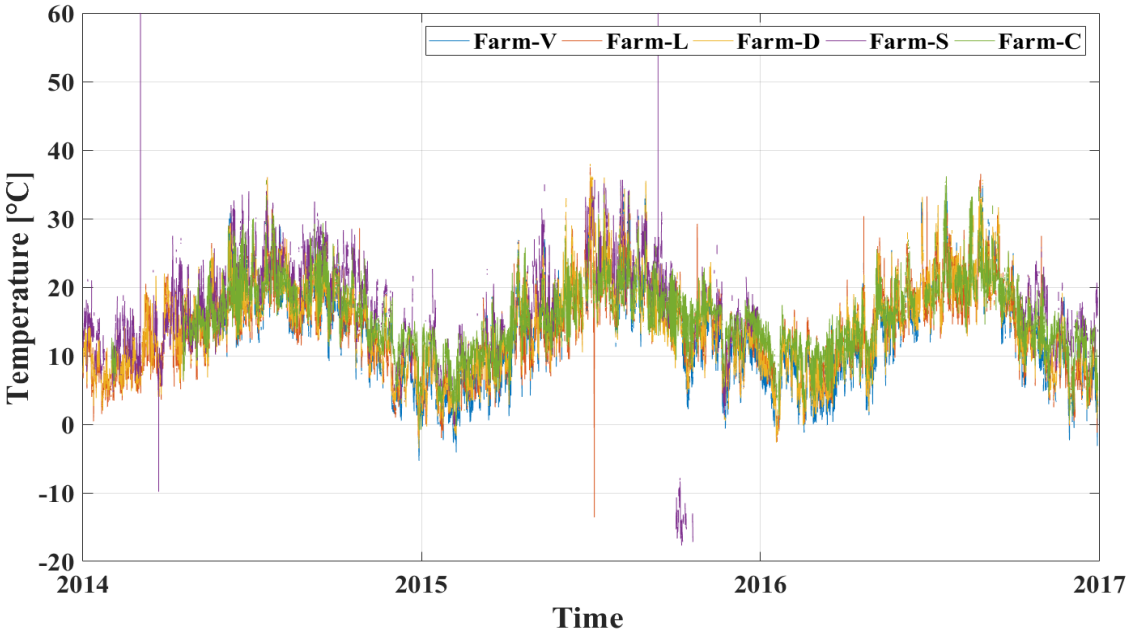

Figure 4.6 a Mean Farm Temperature profile over 3 years for selected wind farms

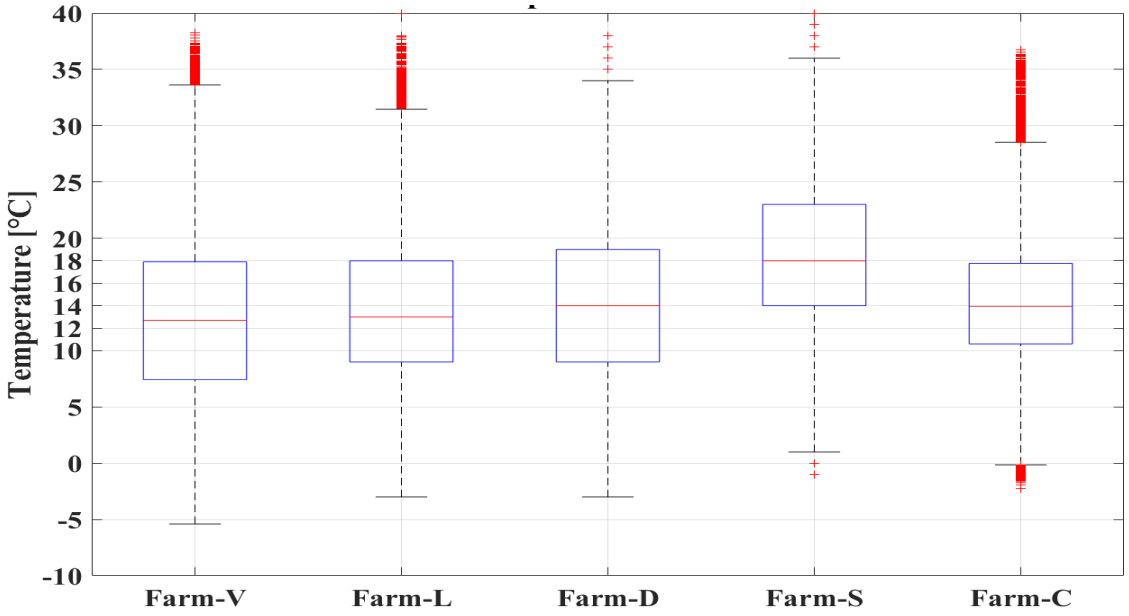

Figure 4.6 b Mean Farm Temperature profile over 3 years for selected wind farms

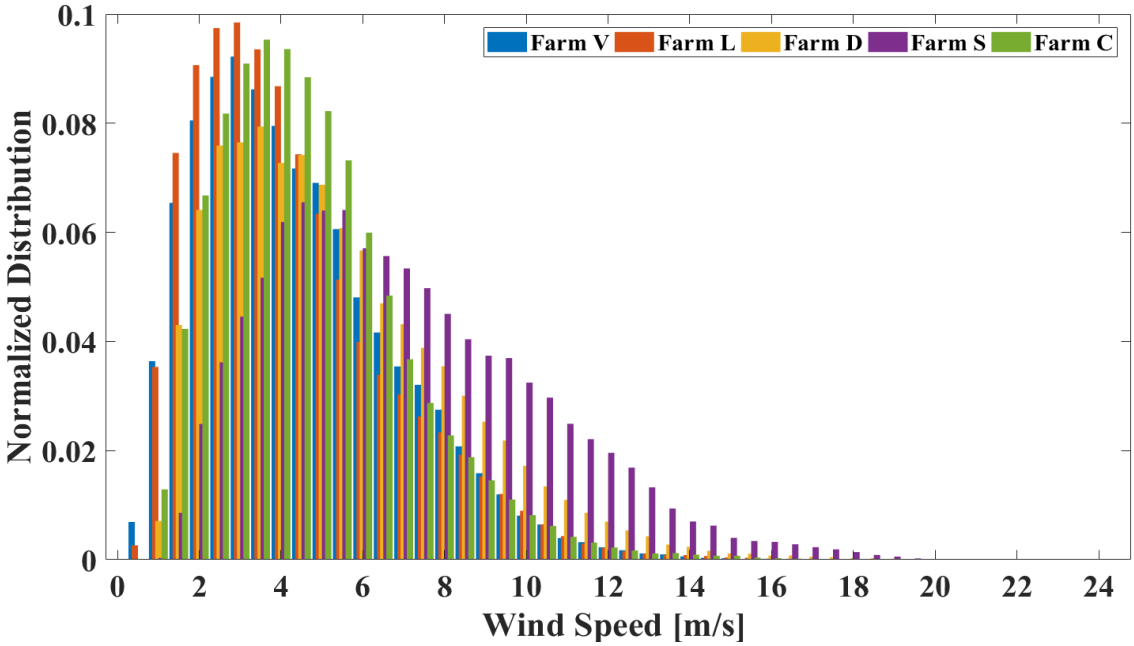

Figure 4.6c: Mean Farm Wind profile over 3 years for selected wind farms

4.3 Presentation of the data pre-processing

It is important to note that SCADA data, although readily available are not easy to use in their raw form and need data pre-processing. In order develop a comprehensive framework, to evaluate the methods proposed in the literature and to validate the eventual framework developed in this thesis, a clean and usable database needs to be prepared. In order to increase the quality, integrity and reliability of data some pre-processing and filtration is performed.

Before we proceed to present the filtration techniques, existing data of interest, available data duration and data resolutions are presented in **Table 4.3** .Of all the SCADA data variables made available, these data of interest are extracted and will be pre-processed for further use in this research. Table also presents the data resolution for each variable selected for analysis.

TABLE 4.3 OVERVIEW OF TIME RANGE AND THE AVAILABLE MEASURING DURATION FOR ALL PARAMETERS

	Wind Farm Characteristics					
	Farm-V	***Farm-L***	***Farm-D***	***Farm-S***	***Farm-C***	***Data Resolution***
Time-stamp	01/2013 to 12/2016	01/2013 to 12/2016	01/2013 to 12/2016	01/2013 to 12/2016	01/2013 to 12/2016	±10 min
Wind Speed	01/2013 to 12/2016	01/2013 to 12/2016	01/2013 to 12/2016	01/2013 to 12/2016	01/2013 to 12/2016	±0.1 m/s
Power	01/2013 to 12/2016	01/2013 to 12/2016	01/2013 to 12/2016	01/2013 to 12/2016	01/2013 to 12/2016	±1 W
Density	01/2013 to 12/2016	01/2013 to 12/2016	01/2013 to 12/2016	01/2013 to 12/2016	01/2013 to 12/2016	±0.01 kg/m3
Temperature	01/2013 to 12/2016	01/2013 to 12/2016	01/2013 to 12/2016	01/2013 to 12/2016	01/2013 to 12/2016	±0.01°C
Rotor Speed	01/2013 to 12/2016	01/2013 to 12/2016	01/2013 to 12/2016	01/2013 to 12/2016	01/2013 to 12/2016	±1 rpm

Since SCADA data are collected through on-board sensors spread all around the wind turbine, certain failures are expected. The inherent sensor tolerance can result in missing values that need to be removed. Once the onboard SCADA system has collected the data, the same data needs to be transferred to a data base, often in the form of data storage sever offsite. This further introduces errors or missing values that need to be pre-processed. Sampling errors though less frequent may also arise and additionally, care needs to be taken with the data synchronization. Different time zones if applicable and the ability to take into account daylight saving if applicable requires careful consideration as well. All these steps and checks are necessary to produce a consistent and reliable database that has and inherent heterogeneity built-in due to the research set-up of multiple wind farms.

We recall here that measured SCADA data are raw and not corrected. Error values, outliers and at times manually influenced a values are still included. It is necessary to pre-process and correct some of the key parameters to get a clear and uninterrupted data set. **Table 4.4** below presents the key variables used for deletion criteria along with reasons for filtration.

TABLE 4.4 CONDITIONS AND FILTER FOR DELETION OF ERROR VALUES

Variable	***Deletion Criteria***	***Reason for Deletion***
Wind Speed	≤ 0 m/s	improbable value/ measurement error
Wind Speed	≥ 30 m/s	
Temperature	≤ -30 °C	
Temperature	≥ 50 °C	
Power	≤10 kW	
Power	≥2.1 MW	
All Variables	Stop Duration	Known Stoppage

In-addition to the processing of capture, storage, sampling and synchronization errors, another, more logical layer of pre-processing is also of interest. For the sake of this research, real data is used to learn the data dispersion around mean power curves for fault free/normal wind turbine operation and to model a reference power curve for fault/abnormal wind turbine operation. It is of interest to filter out un-wanted samples that can't be associated with the normal behavior. Several techniques have been proposed in the literature to ensure the same.(Park et al., 2014) suggest a confidence envelop of 99% around the mean power curve to capture normal behavior and data outside this envelop can be filtered.

For each wind farm used, in addition to the filtration criteria already listed above, known stoppage instances are also available for further data cleansing. The list of known stoppages, initially built automatically through status codes is further compiled by each Farm's operational managers. **Table 4.5** lists some of the stoppage instances for all wind farms where start and stop time of each stoppage are provided. The stoppage can be of varying durations and can be used to filter out relevant data. For this research, information from the maintenance work log, list of machine start and stop duration, extracted from the status codes is also used for filtration where available. All these pre-processing steps provide a high fidelity data set for analysis and capturing real data dispersion.

TABLE 4.5 CONDITIONS AND FILTER FOR MACHINE STOP VALUES (SAMPLE)

	Wind Farm Characteristics	
	Deletion Criteria	***Reason for Deletion***
Farm - V	'04-Jun-2017 11:29:05 to 04-Jun-2017 11:31:25'	
Farm - L		
Farm - D	'27-Dec-2014 12:00:00 to 27-Dec-2014 14:00:00' '29-Dec-2014 10:00:00 to 29-Dec-2014 12:00:00' '07-Jan-2015 12:00:00 to 07-Jan-2015 14:00:00' '07-Jan-2015 23:00:00 to 08-Jan-2015 01:00:00'	
Farm - S		
Farm - C	'07-Mar-2017 15:41:26' '07-Mar-2017 15:57:22' '07-Mar-2017 16:33:25' '07-Mar-2017 21:12:53' '08-Mar-2017 13:59:32' '09-Mar-2017 12:07:07' '09-Mar-2017 13:30:07 '09-Mar-2017 15:04:17'	

Once all filtration mechanisms are put in place, data can now be used for analysis. **Fig 4.7** shows an example of power curve data before and after filtration.

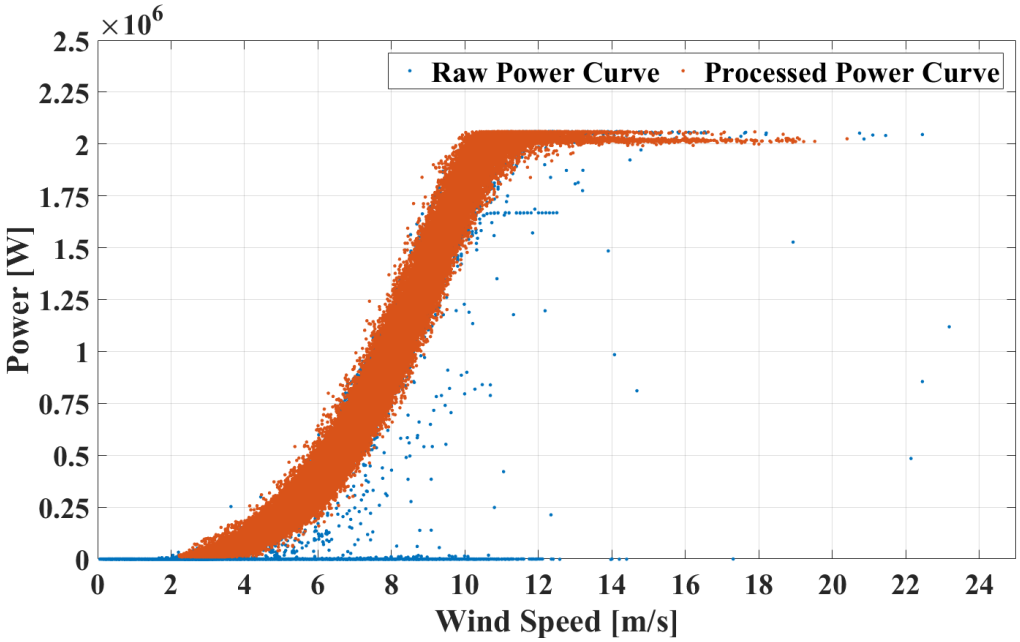

Figure 4.7 On-year Power Curve data for Turbine 1, Farm-V before & after filtration

4.4 Description of Real Fault cases

As briefly alluded to earlier, the real data set made available by VALEMO, after preprocessing, is not only used to learn and capture the data dispersion around mean power curve but also to provide inspiration to model “reference” faulty behaviors. The concept of dispersion reference creation will further be described in detail in the upcoming chapter.

Faults and operational characteristics can alter the normal power curve and cause performance degradation. This is undesirable for wind park operators as most wind parks operate under a contract of 90 or up to 95% production availability sureties. All efforts are thus made to reduce the down-time of a machine. Since the key objective of any strategy is to ensure maximum possible production and minimize downtime, any scenario that causes either of the two is considered a fault in this research. This means, not only the traditional faults like wear, component damage etc. are considered faults but unintentional configurations that cause performance degradation are also classified and treated as faults.

Fig 4.8 presents fault cases down rating and icing on the blades as seen on real data while **Fig 4.9** presents data showing the production loss due to yaw-misalignment of 7°.

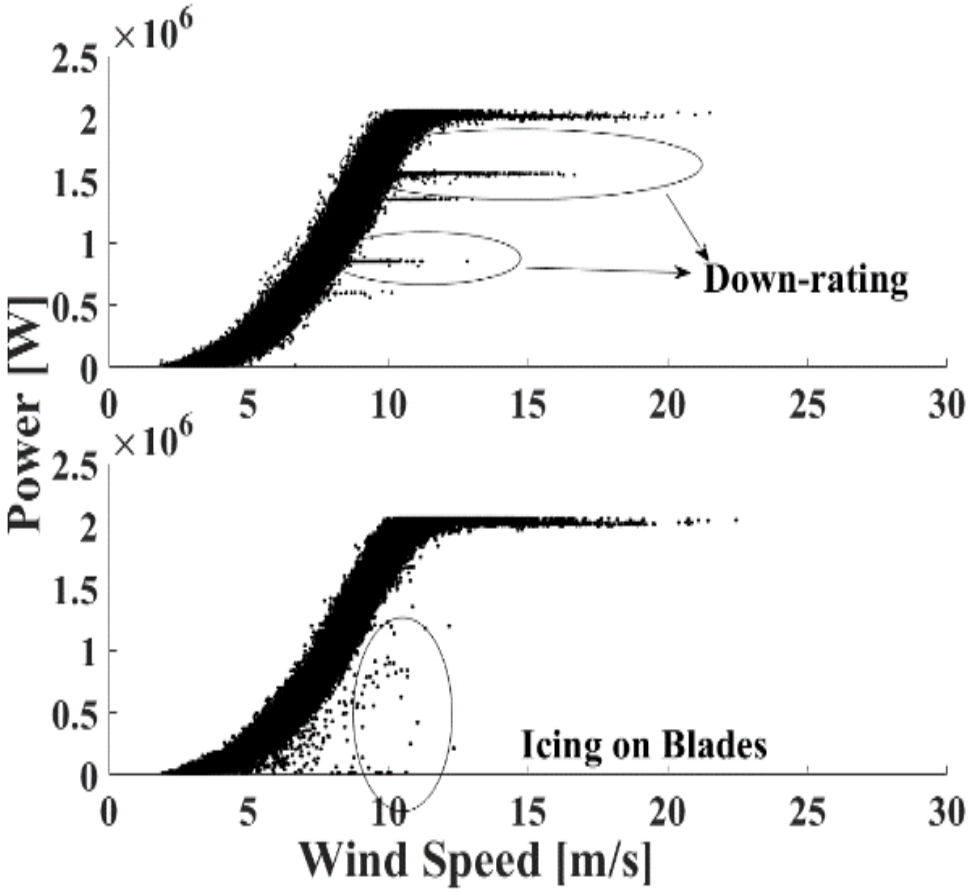

Figure 4.8 Examples of Fault Power Curves for Down-rating & Icing in Real Data

4 different fault scenarios with two of varying intensities are eventually modeled as reference for simulation in this work. These fault scenarios are inspired from real data sets presented here. (Park et al., 2014) present several such scenarios including down-rating, pitch control malfunction, operational misconfigurations, icing on turbine blades, erosion, wind speed measurement faults, dirt or bugs on blades and so on etc. All these fault are highly undesirable as they result in considerable production loss. The faults selected for this research include icing on blades, down-rating, acoustic curtailment and yaw misalignment. These faults are presented in detail here after.

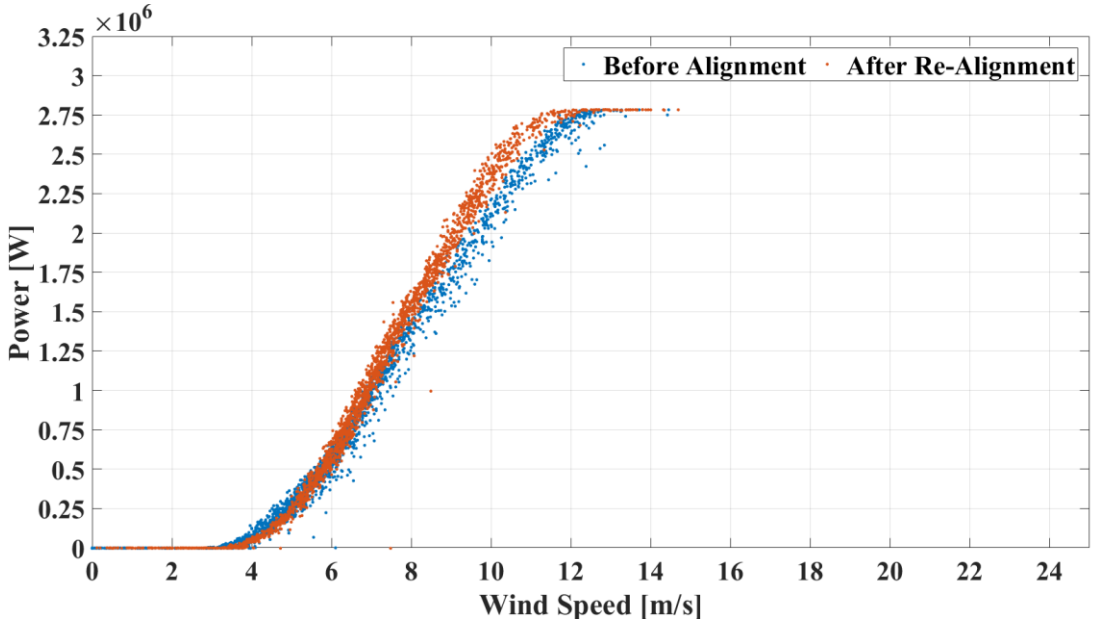

Figure 4.9 Example of Fault Power Curves for Yaw-misalignment 7° with Real Data before and after re-alignment

A complete description of real data sets made available, the pre-processing strategy and the reference fault scenarios to be tested have been presented so far. As referred to earlier, it can be argued whether such operational curtailments and underperformances etc. fall under the strict technical definition of a "fault". Since, the loss of production capacity has significant financial consequences, for the sake of this study, all tested scenarios will be termed as faults. This information can now be used to achieve another of the key objectives of this work; a rigorous and realistic simulation framework. The novel framework developed for this research is presented hereafter in detail.

4.5 Conclusion

It is important to acknowledge that a very rich and extensive data base was made available for this research. The available data provides valuable insight into and informs on a number of key aspects for wind turbine condition monitoring. Some critical and classical faults are identified, impact of environmental variations, operational situations and variation in data dispersion etc. are observed. This warrants/enables an effective use of such a rich knowledge base.

However, the data available, although extensive in size, variability and quality is still not sufficient for a complete and objective analysis of the power based condition monitoring

systems. This lack in the ability to achieve a rigorous performance analysis comes from various factor; most significant being in-sufficient instances of fault signatures on a particular data set. Additional difficulties include the lack of control over the intensity, duration and occurrence of faults visible in the available data set.

Consequently, this research strives to leverage the richness of available data and to overcome the identified shortcomings simultaneously. This is achieved by using real data to develop a simulation framework that provides the control, flexibility and versatility required for an in-depth performance analysis. Such approach allows this research to take the best advantage from the real data on one hand, and from the simulation setup (and its versatility) on the other hand.

This motivates the rationale and basis of developing a realistic simulation tool based on the real data set, complete with a performance analysis and comparison strategy. The real data-based simulation framework is presented in the following chapters.

5 A framework for the simulation of realistic SCADA data

So far, a detailed context of wind turbine condition monitoring using power curves and the available data for this research have been presented. The detailed literature review helped evaluate the state of the art and identify the gaps and short comings in the existing research. Moreover, the detailed presentation of available data set and reference power curves provided the foundational pre-requisites of a novel simulation framework.

A controlled simulation framework is required to analyze the impact of environmental and operational variations on the detection capabilities of different fault detection approaches. The need of a simulation framework also stems from the fact that it is often impossible to find multiple, identical fault signatures on geographically distant and operationally different wind farms. This makes it difficult to isolate the impact of the failures from the impact of operational and environmental factors. Hence a realistically simulated data set is indispensable for a detailed evaluation. It is presented in the following sections.

5.1 Simulation Process

The proposed simulation generation is a two-step process, both of which are inevitable for data simulation. The simulation process steps are as follows

a) First, various realistic and useful reference fault power curve patterns are identified and created. These are inspired from normal behavior constructor power curves and replicate real fault and fault free scenarios.

b) Second, a realistic data dispersion profile is added around the fault curves. This creates a realistic and practical simulation of faulty and fault free data.

5.1.1 Reference Creation

In order to start the simulation process, first the reference power curves for normal and fault behaviors are required. Two choices to establish these reference curves are available. For this study, a manufacturer provided power curve is used as a nominal reference. This power curve depicts the production behavior of a wind turbine in the fault free period. This choice enables the standardized reference across all test cases and was used as a reference to build other fault behavior curves as required. Alternatively, a measured reference power curve can also be learnt from fault free historical data using the "method of bins"(IEC 61400-12-1, 2005). Mean power curve as shown in Fig.5.1 can be represented as $(P_{\omega_i} = f(\omega_i))$ where the averaged produced power P in wind bin 'ω_i' is a function of wind speeds ω in the same bin 'i'. The wind bins ω_i are usually of 0.5 ms^{-1} resolution.

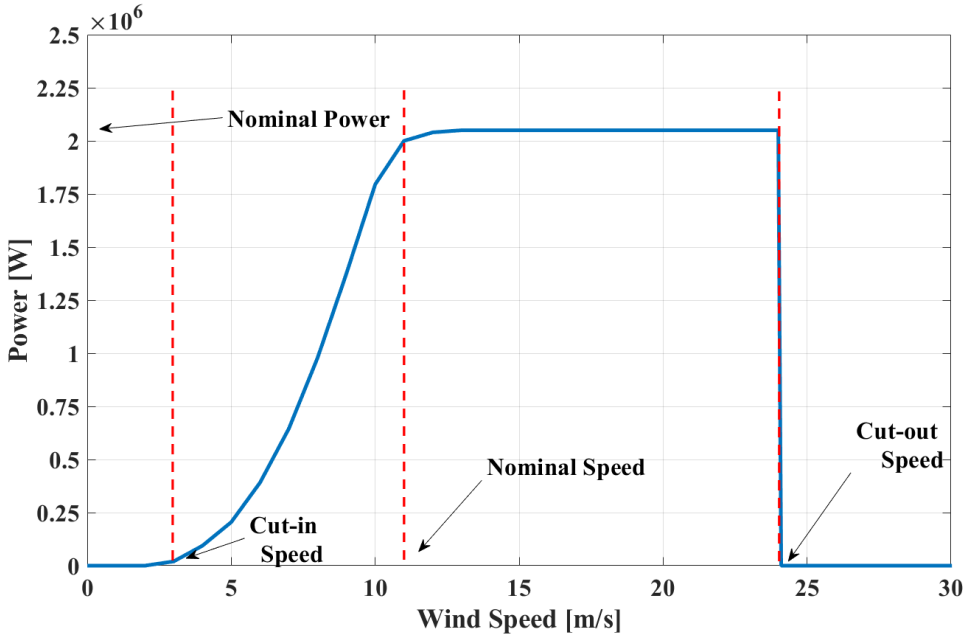

Figure 5.1 Example of an ideal fault free power curve, also referred to as constructor power curve

Based on the literature review (Park et al., 2014), expert knowledge, analysis of real fault scenario data and using the theoretical power curves provided by original equipment manufacturers (OEMs), faulty power curve references can be created. **Fig. 5.1** reminds of the normal behavior fault free power curve also called constructor power curve which is provided by the OEM to represent the production behavior of their wind turbines.

Similar to this normal behavior, the power curves replicating behavior of a WT power curve under "abnormal" scenarios like icing on the blade, operational production curtailment, yaw angle misalignment and production curtailment for noise reduction are presented in detail. These families of faults with varying intensity levels will be used as reference to generate corresponding fault data time series. This will enable the replication and simulation of real turbines behavior experiencing these faults.

5.1.1.1 Icing or Control System fault

The first scenario used to develop a reference curve can be called icing or icing on the blades. During winter season, the snow fall on wind projects in colder climates can change the aerodynamic profile of the blades. Although increasingly, defrost technologies and other solutions have been deployed in such circumstances, a lot of older fleets can still face this problem. This change in the aerodynamics of a wind turbine blade, negatively affects the power production behavior hence resulting in a downward shift of the power curve. This pattern is verified by looking the real fault data and literature (Park et al., 2014).

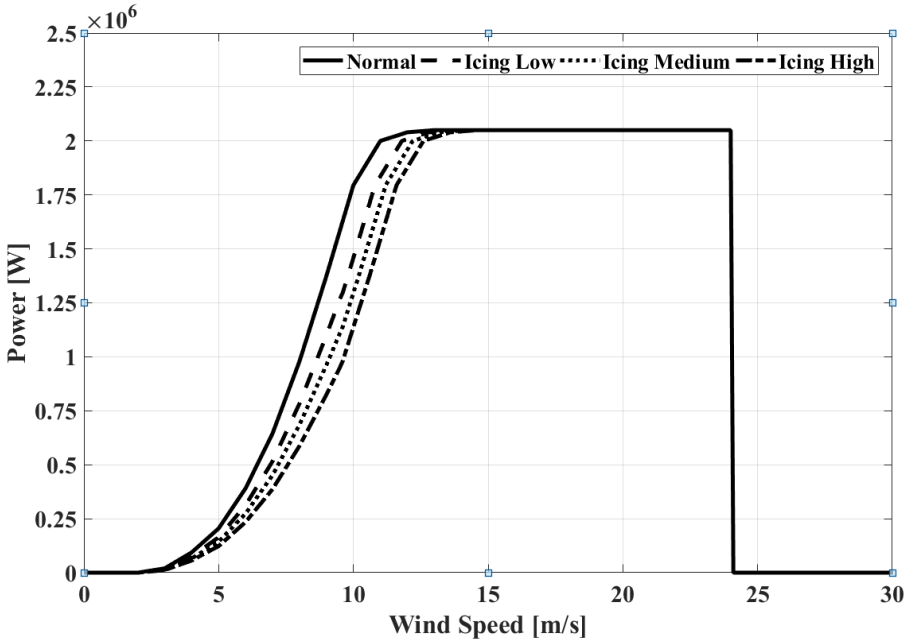

Figure 5.2 Reference Fault Power Curves for Icing with power curves for (a) Normal (b) Low (c) Medium (d) High fault signatures

Fig. 5.2 present three fault intensities for the low, medium and high level of frost on the wind turbine blades. This frost or icing is enough to cause a production loss of 5, 10 and 20% respectively. It is important to note that this family of faults and underperformance have a negative impact on power production for all wind speed values. Hence over time this type of

grave underperformance can accumulate as significant production and hence financial cost. Although the reference power curves generated for this family of fault can resemble that of a control system failure as well, here in this work, icing fault is used as the nomenclature.

5.1.1.2 Down-rating fault

The second family of fault modeled as reference power curve for this work is called down-rating. Down-rating is a scenario where the wind-power production relationship is altered as such that a production curtailment for wind speeds higher than a specific value is put in place. The production capacity of a wind turbine is limited to a fixed value lower than the nominal or rated production capacity of the wind turbine.

The production curtailment or down-rating of a wind turbine stands to achieve various important outcomes. In times of over-production, production curtailment helps with grid and storage capacity compliance. In times of turbulent weather, curtailment could be activated to reduce load on the turbine. Curtailments can also be activated during site visits or prolonged onsite interventions to reduce risks. It is of interest to note that under-normal circumstances, such curtailments are intentional and serve a useful purpose.

However, if the configuration for curtailment are left in place un-necessarily, the production loss becomes significant. Hence this scenario is classified and termed as a fault or underperformance in this work. The reference power curves of this fault for various intensities (15%, 33%,53%) are presented in **Fig 5.3.**

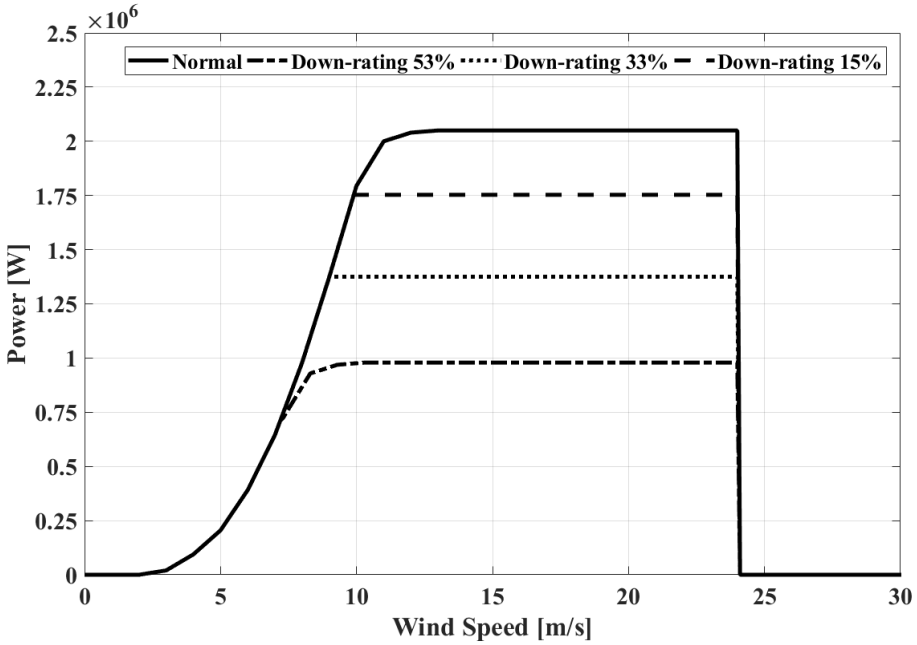

Figure 5.3 Reference Fault Power Curves for Down-rating with power curves for (a) Normal (b) 15% (c) 33% (d) 53% fault signatures

5.1.1.3 Acoustic curtailment fault

Similar to the production curtailment or down-rating fault type presented above, a similar curtailment fault type with a different signature and purpose is presented here. As the name suggests, the acoustic curtailment is to suppress the already feeble acoustic signature of a wind turbine under particular circumstances. A reduction in acoustic signature is desirable during certain hours and for certain wind farm locations. A particular wind direction and wind turbulence regime can also have an impact on the acoustic profile of a wind turbine.

Operators in such scenarios are forced to resort to altering the wind-power relation. **Fig. 5.4** shows a power curve for acoustic curtailment. As observable from the figure, a reduced power production curve for higher wind speed values is a signature of acoustic curtailment. Like down-rating, acoustic curtailment is also a configuration and is put in place by the turbine operator. However, any un-intentional implementation can result in significant production and hence financial loss, such a scenario is highly undesirable. For the scope of this work, acoustic curtailment will be treated as a fault due to associated production and financial cost.

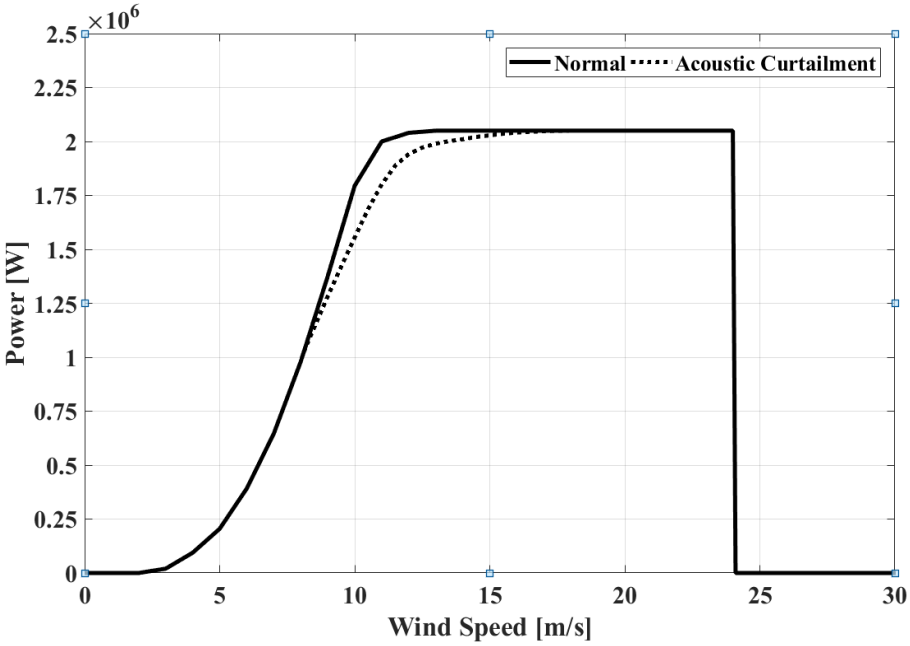

Figure 5.4 Reference Fault Power Curves for Acoustic Curtailment with power curves for (a) Normal (b) fault signature

5.1.1.4 Yaw Misalignment fault

One of the commonly occurring faults with visible impact on the power curve is yaw misalignment. (Tavner, 2012) This fault type can contribute to a significant production loss and down-time. As presented earlier in the section 2.3.1 Wind Power & Turbine Taxonomy **(Sec 2.3.1)** modern wind turbines have a yaw drive between the tower and the nacelle. The purpose of this drive is to adjust and track the wind direction for maximum exposure to the observed wind speed. If in any circumstance, the nacelle and hence the blades are not facing in the direction of maximum incidence of wind, a production loss can occur.

The production loss caused by yaw misalignment is significant enough that it motivates regular audits, dedicated onsite solution and re-alignment campaigns by wind farm operators. **Fig. 5.5** presents a Yaw misalignment of 5° from actual/ nominal yaw angle. The same fault signature can be visibly observed in the real data sets before and after a re-alignment campaign.

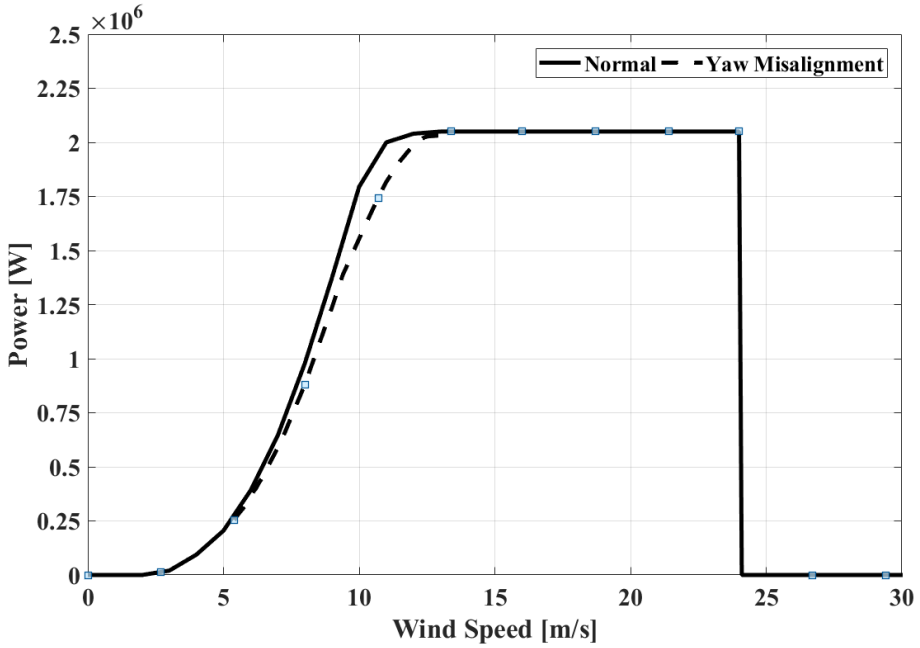

Figure 5.5 Reference Fault Power Curves for Acoustic Curtailment with power curves for (a) Normal (b) fault signature

As briefly alluded to in the overview of simulation process above, realistic fault free and faulty reference fault power curves are required beforehand. The reference power curves are inspired by real fault data in conjunction with the expert knowledge and literature. These fault reference curves are modeled after real fault scenarios. The reference fault curves modelled include down-rating, icing on blades, acoustic curtailment and yaw misalignment.

5.1.2 Dispersion Learning & Reference Matrix Creation

Once the realistic reference curves for fault scenarios are generated, the second stage of the proposed realistic simulation framework is to learn a realistic data dispersion profile. This is to capture the data dispersion of real data set which can then be added to the previously created reference power curves for data simulation. However, first a mechanism needs to be devised for calculating the dispersion, preparing it in a manner that it's addition onto the reference curve results in a realistically simulated data.

In order to achieve a realistic fault simulation, the observed behavior of the real dataset needs to be captured and then replicated. To learn the dispersion profile of real data, 10 minutes SCADA data from real wind turbines, operating in normal conditions during several years is used. Fig. 5.5 shows the power curve data from a 2 MW wind turbine operating under normal

conditions for the years 2014-2016. It also shows the reference mean power curve ($P_{\omega_i}^{ref} = f(\omega_i^{ref})$) calculated using IEC binning method (IEC 61400-12-1, 2005) from the fault free data referenced hereafter as "ref". It is important to note here that all the wind farms and wind turbines presented in **Ch. 4** are eventually used as reference "*ref*" data.

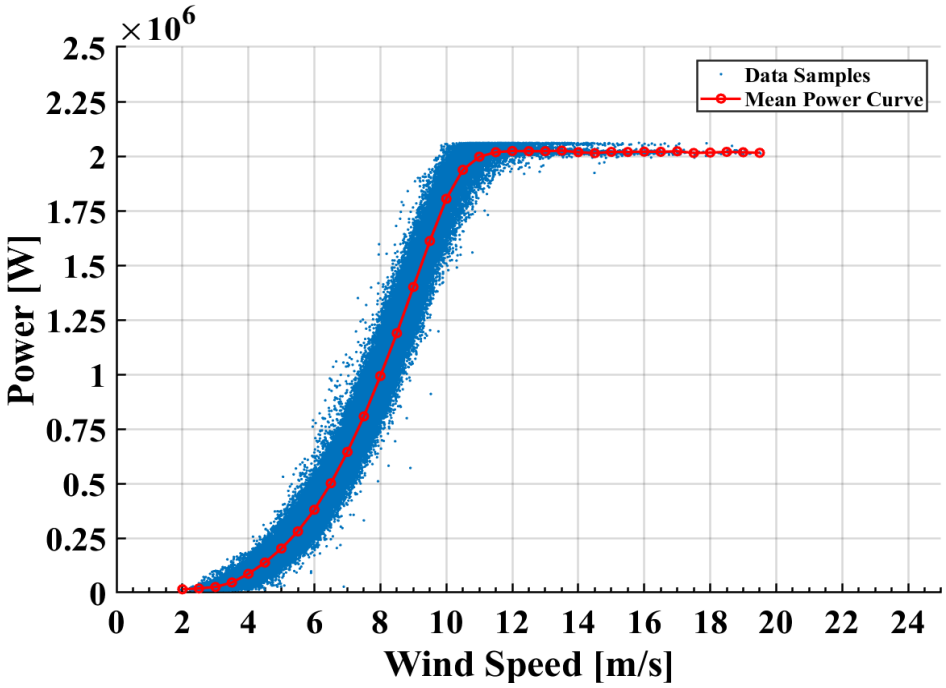

Figure 5.6 Scatter plot of 10-min wind speed & power for a turbine over 3-years period along with mean power curve for dispersion learning

It is important to observe in **Fig. 5.6** that in contrast to the ideal power curve reflected in Fig.5.1, the real data has significant data dispersion around the mean power curve. A significant amount of this data dispersion can be associated to the variation in onsite wind density which is a consequence of the onsite temperature variation (Farkas, 2011). The visual representation of this variation due to density can be seen in **Fig 5.7** in the form of temperature variation. **Fig. 5.7** presents the same data set used to generate **Fig. 5.6** but with color-bar associated to the corresponding onsite temperature values θ. Both **Fig. 5.6 & Fig. 5.7** show data after basic filtering. Outliers corresponding to erroneous samples and known maintenance actions were also removed. Only data where wind turbine is producing power were kept.

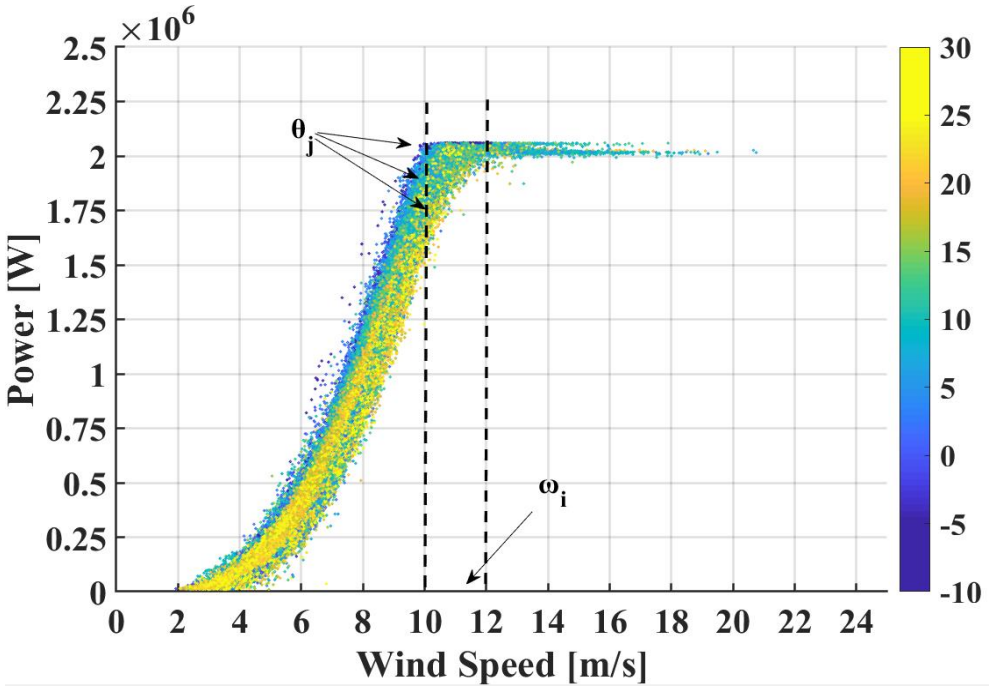

Figure 5.7 Scatter plot of 10-min wind speed & power for a turbine over 3-years with color corresponding temperature value for each sample

The notion of wind bins is not new to power curve analysis, the same concept of binning can be extended to other variables as used in (Bi et al., 2017a). It is of interest to observe that as labelled in **Fig.5.7**, within the same wind speed bin ω_i, multiple values of produced power P at different temperature values θ are present. The values of produced power P have a color bar for temperature values θ. This enables a grouping/binning of produced power values P as a function of both wind speed and temperature 'values' (ω and θ) in their corresponding wind and temperature 'bins' (ω_i and θ_j) respectively. Hence, the produced power values P can be stored into corresponding wind speed bin ω_i & temperature bin θ_j where N_{ij} is the number of samples in a particular cell indexed by (ω_i, θ_j).

In order to better use and visualize this sorting and storage of produced power values, a 2 dimensional reference grid of bins is created. **Fig 5.8** presents this 2-D reference matrix/grid of wind bins i and temperature bins j to be filled with data corresponding to wind speed values ω and temperature values θ. As an example of the varying temperature values, produced power P data, corresponding to the wind bin 10-12 m/s (**Fig.5.7**) will intuitively fall within a varied range of temperature bins as shown and labelled by orange lines in **Fig.5.8**.

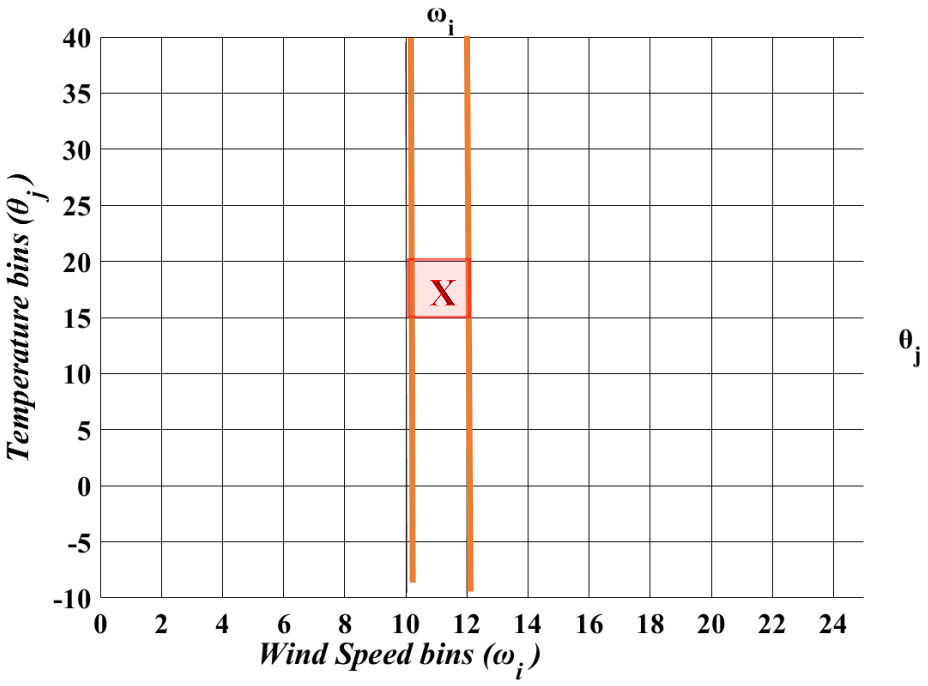

Figure 5.8 2-D reference matrix of wind bins i and temperature bins j to be filled with data corresponding to wind speed values ω and temperature values θ.

The grid presented in **Fig. 5.8** can be elaborated further as a 2D reference of *i* wind bins (ω_i) and *j* temperature bins (θ_j) as shown above. Where one 2D reference bin (marked red in **Fig. 5.8**) is defined by its index, the wind bin ω_i and the temperature bin θ_j that contains a set of N_{ij} power values denoted by $\{P_{\omega_i,\theta_j}(*)\}$. It is of interest to note here that the asterisk '*' suggests that each cell can hold multiple produced power values and that the number of values in each cell is 1) variable and 2) function of the data set in analysis. In programming/coding terminology, this grid can also be imagined as a 2- dimensional data structure of fixed size with cells containing lists of varying lengths, depending on the data samples that fall in each cell of the structure.

This sorting is of interest as it allows for the placement of data dispersion values in these 2-D bins as a function of their respective wind speed and temperature bin ranges. The data dispersion around mean power curve is calculated as the *difference* of mean power curve values ($(P_{\omega_i}^{ref} = f(\omega_i^{ref})$) learnt using IEC method of bins (IEC 61400-12-1, 2005) and the produced power data ($P_{\omega,\theta}$) around this mean power curve. Since, the *difference* between observed and modelled/predicted value is called residual, this work uses the same term for data dispersion calculated as a 'dispersion residual'.

As explained earlier, the produced power data is fragmented in *i* wind bins and *j* temperature bins. For each 2D reference bin defined by the wind bin $\boldsymbol{\omega_i}$ and temperature bin $\boldsymbol{\theta_j}$, the set of dispersion residuals $\{r_{\omega_i,\theta_j}\}$ on power values is calculated using *eq.5.1*.

$$r_{\omega_i,\theta_j}(l) = P_{\omega_i}^{ref} - P_{\omega_i,\theta_j}(l) \qquad \text{eq. 5.1}$$

$$l = 0, \dots, N_{ij}$$

where

N_{ij} is the number of samples within wind speed bin ω_i and temperature bin θ_j;

$r_{\omega_i,\theta_j}(l)$ are the dispersion residuals calculated for wind speed bin ω_i and temperature bin θ_j;

$P_{\omega_i}^{ref}$ is the mean power value in wind speed bin ω_i calculated on reference data;

$P_{\omega_i,\theta_j}(l)$ are the measured power within wind speed bin ω_i and temperature bin θ_j;

As alluded to earlier, the number N_{ij} of dispersion residuals $r_{\omega_i,\theta_j}(l)$ in each wind, temperature bin (ω_i, θ_j) is variable. To get a better idea of the number of samples in each particular wind bin, an image of the residual count per cell is of interest. Fig. 5.6 shows a color image of 2-D reference filled using *eq.5.1* with color bar ranging from 0-500 samples. The scale is determined by the number (N_{ij}) of dispersion residual samples in each cell of 2-D reference matrix. The fault free data dispersion residuals $r_{\omega_i,\theta_j}(l)$ calculated on the reference data set are stored in a residual reference data set R_{ω_i,θ_j} as presented by *eq. 5.2*.

$$R_{\omega_i,\theta_j} = \{r_{\omega_i,\theta_j}(*)\} \qquad \text{eq. 5.2}$$

where

R_{ω_i,θ_j} is the set of dispersion residual sorted in wind speed bin ω_i and temperature bin θ_j as a function of wind speed values ω and temperature values θ;

It is important to note that the resolution of each cell in this 2-D reference (R_{ω_i,θ_j}) can be chosen variably. For the sake of simplicity and visualization, the examples presented in the **Fig. 5.7 & Fig. 5.8** use the resolution of 2 m/s by 5°C. For this work however, the resolution is chosen to be 0.5 m/s by 1 °C and each cell is then populated by *l* dispersion residual $(r_{\omega_i,\theta_j}(l))$ entries. The size of overall empty 2-D reference grid R_{ω_i,θ_j} **(Fig. 5.7)** before population needs to be consistent and representative of the complete range/limits of real data sample values.

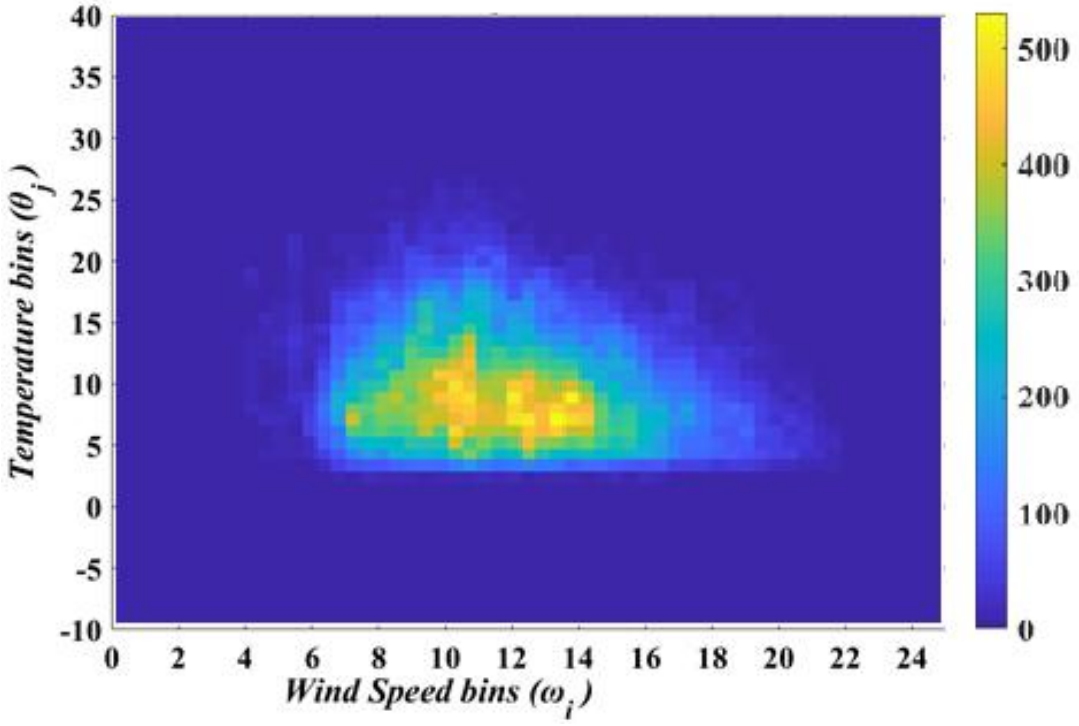

Figure 5.9 Dispersion residuals matrix image with colors scaled for number of dispersion residuals per wind, temperature cell

For this implementation, the range limit for wind speed is chosen as 0 to 25 ms^{-1} (x-axis) and for temperature (y-axis) as -10 to 40°C. The, per bin, resolution of 0.5 m/s by 1 °C for the this reference range (0 to 25 ms^{-1} and -10 to 40°C) makes the size of 2-D reference grid R_{ω_i,θ_j} as 50x50. It is to be noted that the total number of reference bins with *available & non-empty reference data* in the 2-D reference is a function of the data set under consideration and can vary. Different pixel intensities in **Fig. 5.9** further elaborate the varying number of samples in each reference cell. The pixel density in the image comments on the fact that most data lies roughly within the boundaries of 3-22 m/s for wind and 2-25 °C for temperature values.

This 2-D dispersion residual grid filled with variable sized cells of dispersion residuals can now be used as the reference source for using the learnt real dispersion behavior of wind turbines. Also consequential is to state that one such 2-D dispersion residual grid is calculated using each of the wind turbines made available for this research. That brings reference data to a total of 25 wind turbines from 5 geographically and operationally different wind farms with different data dispersion. This provides for a very realistic and extensive source for learning real data dispersion. Hence it becomes possible to simulate multiple realistic data streams of power production profiles of desired length.

5.2 Simulation Generation

5.2.1 Simulation process

Once the reference power cures and realistic data dispersion is learnt, realistic simulation data can now be generated. The realistic simulation generation is a three-step process, two of which have already been presented in detail. To reiterate

- First, various realistic and useful reference fault power curve patterns, replicating multiple faults scenarios are identified and created (Section 4.4 & 5.1.1).
- Second, a realistic dispersion profile is learnt and a dispersion reference matrix is created (Section 5.1.2).
- Finally, reference fault patterns (step 1) and realistic dispersion profile (step 2) can now be used to generate simulated data streams of produced power P. This will be achieved by using a new pair of Wind and Temperature data samples.

To expand further on the third and simulation generation phase, in order to simulate 10 minutes power time series, wind speed and external temperature time series ($U(k), T(k)$) measured on different wind farms are required as the inputs. ($U(k), T(k)$) are times series of wind speeds and temperatures recorded every 10 minutes where *k* is the time index. **(Figs. 5.10a**

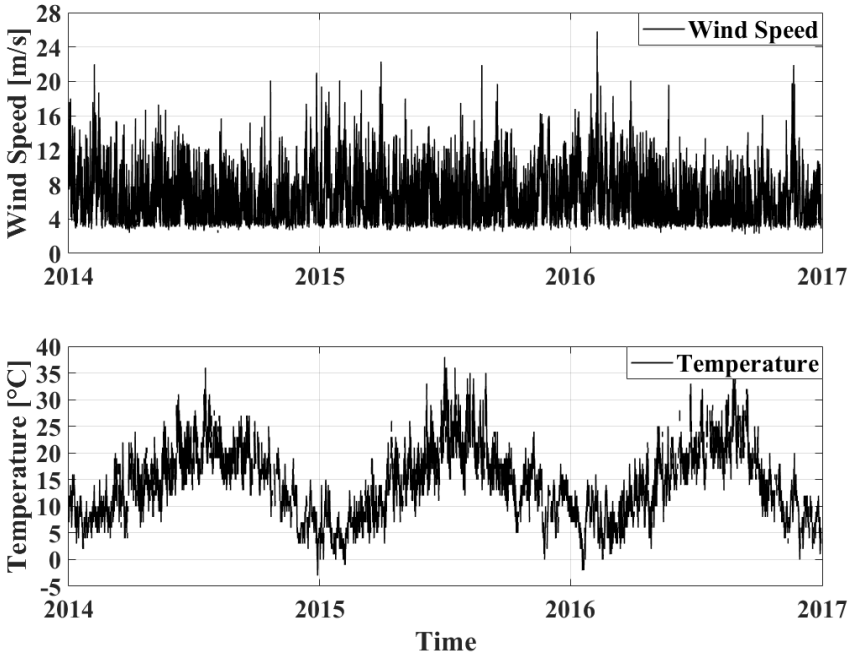

Figure 5.10 Input Profiles (Real data) (a) Wind U(k)(b) Temperature T(k)

&b) show an example of input ($U(k), T(k)$) series across time for 3 years period at 10-min sample. For the consistency of this research and implementation *k = 0,…, 157824 (~3 years for 10-min sampling rate)* for all simulated data streams.

At each time stamp *k*, the values of this "new" pair of environmental parameters (Wind $U(k) \in \omega_i$ & Temperature $T(k) \in \theta_j$) are used to select the corresponding reference power value (from step 1) and the dispersion profile value (from step 2) of the simulation process. The new Wind data sample ($U(k) \in \omega_i$) is used to select corresponding reference power value P_{ω_i} (ref. Section 5.1.1). Whereas both new environmental parameters (Wind $U(k)) \in \omega_i$, Temperature $T(k) \in \theta_j$) are used to identify the corresponding reference wind, temperature bin (ω_i, θ_j) of the 2-D reference dispersion residual set $\mathrm{R}_{\omega_i,\theta_j}$ built earlier (ref. Section 5.1.2).

Once the correct reference bin (ω_i, θ_j) is identified, a dispersion value $\tilde{r}_{\omega_i,\theta_j}(k)$ from the corresponding bin of dispersion residual $\mathrm{R}_{\omega_i,\theta_j}$ is randomly drawn. The value of ($U(k), T(k)$) pair works as a pointer to the corresponding reference wind speed bin ω_i and temperature bin θ_j of the 2-D reference created earlier. Hence, for each ($U(k), T(k)$) pair of 10 minutes data sample, a dispersion residual is randomly drawn from the relevant reference bin. The simulation process needs to be randomized for each new ($U(k), T(k)$) pair of 10 minutes data sample. It is important to note here that once randomly drawn, residual sample $\tilde{r}_{\omega_i,\theta_j}(k)$ is neither removed nor replaced and is available for the next and subsequent withdrawals throughout the simulation process (in a boot-strap like approach).

The randomly selected dispersion $\tilde{r}_{\omega_i,\theta_j}(k)$ value is then added to the corresponding reference power value for the normal P_{ω_i} and faulty $P^q_{\omega_i}$ behaviour modelling. A realistically simulated time series of power data $P_{U(k),T(k)}(k)$ as a function of ($U(k), T(k)$) pair of input data can be generated using *eq. 5.3* for fault free case and *eq. 5.4* for fault scenarios as follows.

$$\ddot{P}_{U(k),T(k)}(k) = P_{\omega_i} + \tilde{r}_{\omega_i,\theta_j}(k) \qquad \text{eq. 5.3}$$

for fault free case

$$\ddot{P}_{U(k),T(k)}(k) = P^{q}_{\omega_i} + \tilde{r}_{\omega_i,\theta_j}(k) \quad \text{eq. 5.4}$$

for fault profiles

$$\left.\begin{matrix} \mathrm{U(k)} \in \omega_i \\ T(k) \in \theta_j \end{matrix}\right\}$$

Where

$P_{U(k),T(k)}(k)$is the simulated power output for new ($U(k), T(k)$) pair;

P_{ω_i} the fault free reference power curve;

$P^{q}_{\omega_i}$ is the fault reference power curve ranging from 1 to q depending on the fault mode selected;

$\tilde{r}_{\omega_i,\theta_j}(k)$is the dispersion residual selected randomly from (l) entries in the reference bin (ω_i, θ_j);

q is the number of fault mode for reference power curves available for simulation (**ref Sec.**);

The simulation framework presented can now be used to generate faulty and fault free power data time series at length. The simulated data is totally controlled and a choice for a realistic data stream can be made on the basis of reference power curve mode selected. The data dispersion used, replicates the dispersion observed in the real world. The three stages of the overall simulation process section of the framework is presented in the **Fig. 5.11**.

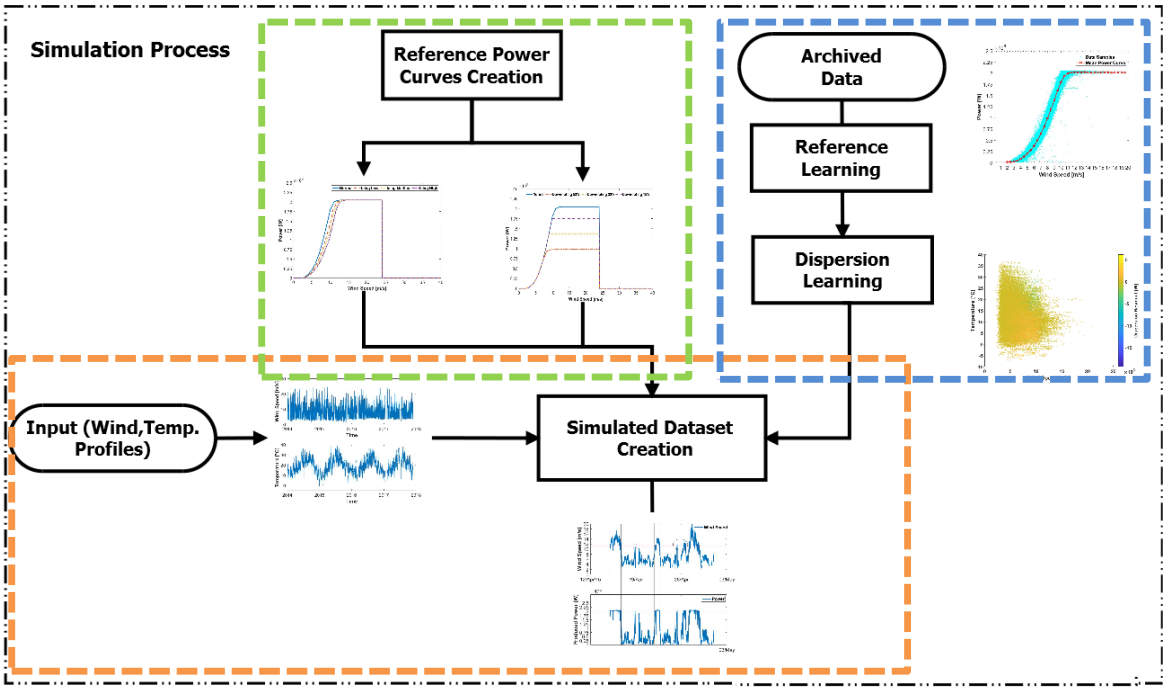

Figure 5.11 Overview of the Simulation Process stage of the overall Framework; Step 1 in green, Step 2 in blue and Step 3 in Orange

5.2.2 Examples of simulated power profiles

An example of a power produced profile generated using the input wind and temperature time series ($U(k), T(k)$) recorded for a 2 MW wind turbine over a period of 3 years (2014-2017) and displayed in **Fig. 5.10a & b** is presented in **Fig. 5.12**. The time series in **Fig. 5.12** is a zoomed version on a 1 week's duration. (19th April 2015- 26th April 2015). In order to validate that the simulated power is a direct and true response to the input wind speed time series used, some key moments are identified in the example. The horizontal red bar in **Fig. 5.12a** corresponds to the "nominal wind speed" above which the produced power reaches the "nominal power" value as marked by the red line in **Fig 5.12b**. The nominal wind speed for the example presented is 11 m/s while the nominal power is 2.05 MW (ref Fig.1). It can be observed that the moment, wind speed values in **Fig. 5.12a** cross the red line (nominal speed of 11 m/s) the simulated power in **Fig. 5.12b** reaches nominal power (2.05 MW).

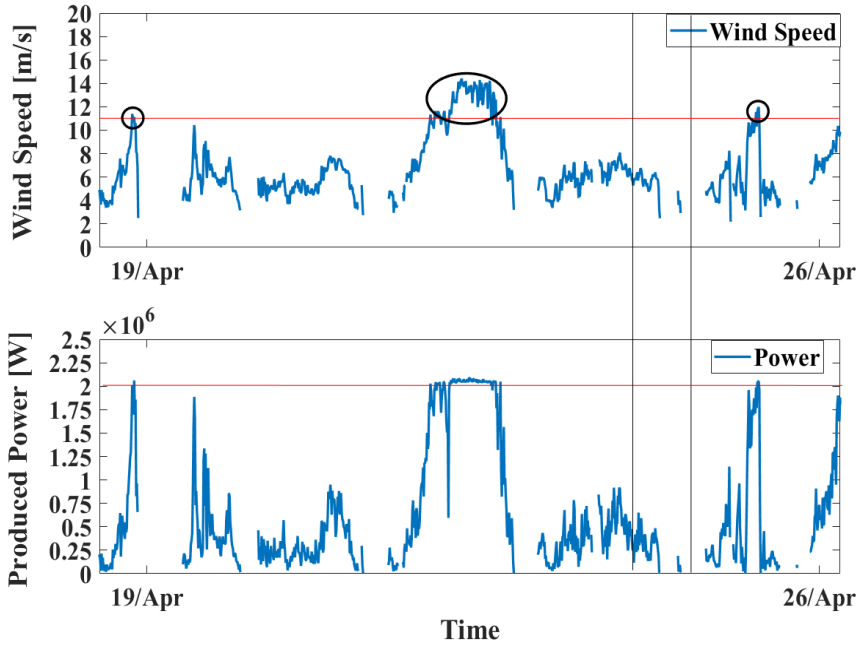

Figure 5.12 (a) Input Real Wind Profile & Nominal Speed draw as red line (b) Output Simulated Power Profile & Nominal Power drawn as red line (1 week)

Fig. 5.13 presents another simulation example with real and simulated data plotted on the same graph for 1 week period along with the measured wind speed overlapped. The simulated power successfully replicates the real data behavior and evolves as a function of measured wind speed. It is important to note that this example is for fault free scenario.

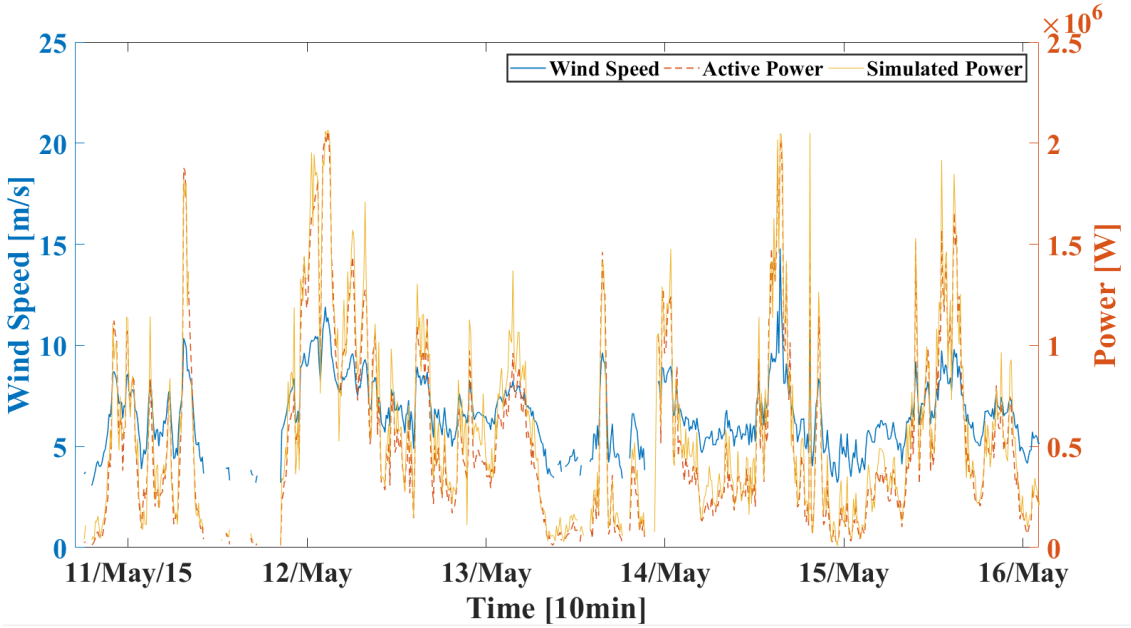

Figure 5.13 Example of evolution of Produced power (a) Input Real Wind Profile draw as solid blue (b) Real Power Profile dotted red line (c) Simulated Power drawn as solid orange line (1 week)

Another example of simulated data under fault condition is presented in **Fig. 5.14.** For visual clarity, the fault case is presented using the fault power curve for fault type Down-rating 15%. This realistic simulation example and data comparison can now serve as a first simulation and can be used to set up an implementation test bench in the following chapters. So far, a detailed description of the novel simulations framework was provided. Real data set examples express the potential and availability of the simulated data streams for further analysis. The realistically simulated extensive data set can now be used for implementation and comparative analysis of existing power based fault detection techniques. The validation test bench, comparative benchmark and eventual results are presented in the following chapters.

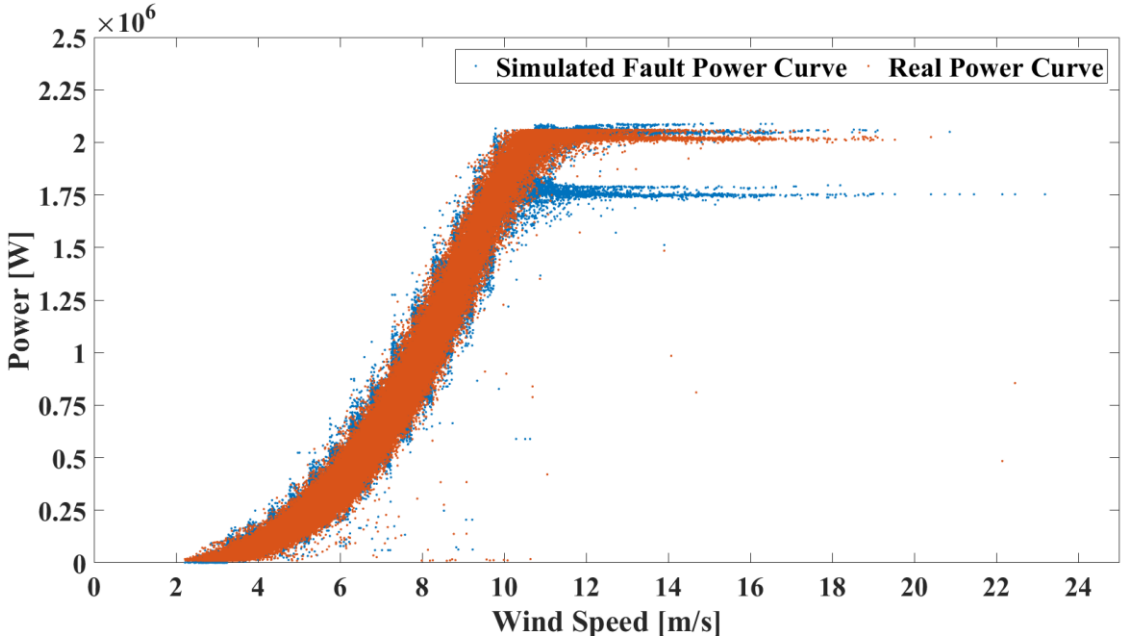

Figure 5.14 Example of Simulated Produced power curve (a) Real Power Curve data (b) simulated fault power curve 15% Down-rating (1 year)

6 Benchmarking of 3 Fault Detection Methods

The simulation framework presented in the previous sections can now be used to set up a test bench to evaluate and compare the performances of 3 fault detection methods. These detection methods are chosen as a representative sample from the plethora of existing methods. These approaches were detailed in the literature review for this work. The simulation framework developed as tool is useful to explore the impact of geographical and operational variations on the detection performance of these methods.

First, the fault detection methods selected for this analysis are presented. Then, the fault detection performance indicators used to evaluate and compare the performances of the methods are detailed. Finally, the performance matrix that can be built for each method and each fault is presented.

6.1 Fault detection methods evaluated

Three representative fault detection approaches proposed in literature are implemented. All methods generate residuals by comparing current 10 minutes SCADA power values to the expected values. The expected power values are predicted by a normal behavior model derived from the power curve. The first method used is a novel residual generation method inspired by the “method of bins” (IEC 61400-12-1, 2005), the second is a more intricate method proposed by (Cambron et al., 2016) and the third one is a Gaussian process regression based on the approach presented by (Butler et al., 2013).

The selection of these 3 fault detection methods considered in the study is based on three different ways of "managing" the data dispersion and variability. Method 1 uses wind only; Method 2 uses wind, density correction and data translation while Method 3 uses wind and air

density for dispersion correction. **Fig 6** presents and overview and the different characteristics of the selected methods. The fault detection methods are presented below in further detail.

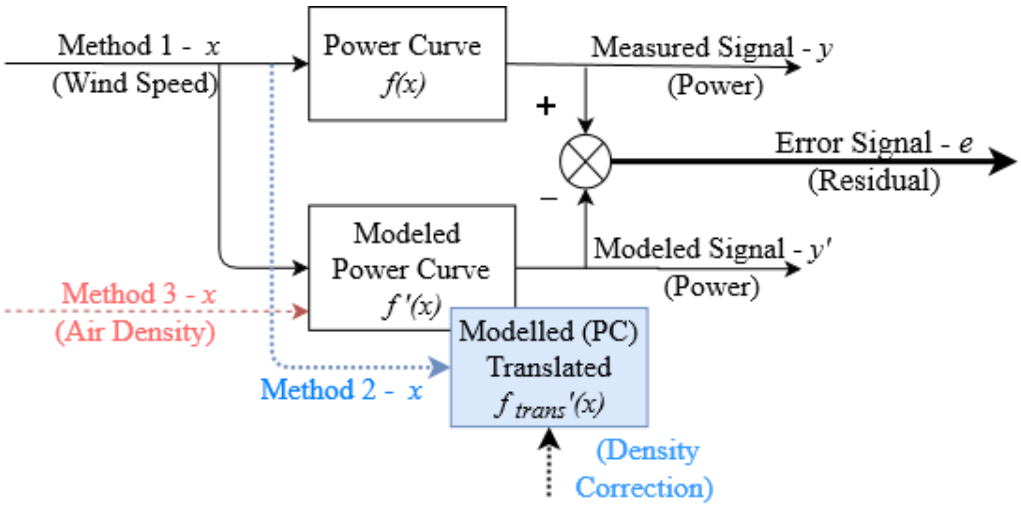

Fig. 6. Overview of 3, residual generation based fault detection methods. Method 1 uses wind only; Method 2 uses wind, density correction and data translation; Method 3 uses wind and Air density

6.1.1 Method 1: International Electro technical Commission (IEC) based approach

Within this technique, the reference power curve is learnt by binning data in wind speed intervals of 0.5ms^{-1} resolution. For each such wind bin of 0.5 m/s resolution, a reference mean value of produced power data samples, as presented by IEC standard (IEC 61400-12-1, 2005) is computed. This in-turn builds a fault free reference power curve. The indicator for fault detection is calculated as the difference between all the produced power samples and the mean power value within each wind bin (Aziz et al., 2018).

Fig. 6.1a shows the example of residuals calculated for a 3 years data stream. The fault scenario presented in this example is 15% down-rating during Year 3 (2016-2017). The faulty period is labelled as the horizontal red bar. **Fig. 6.1**b shows the same residual with one week moving average.

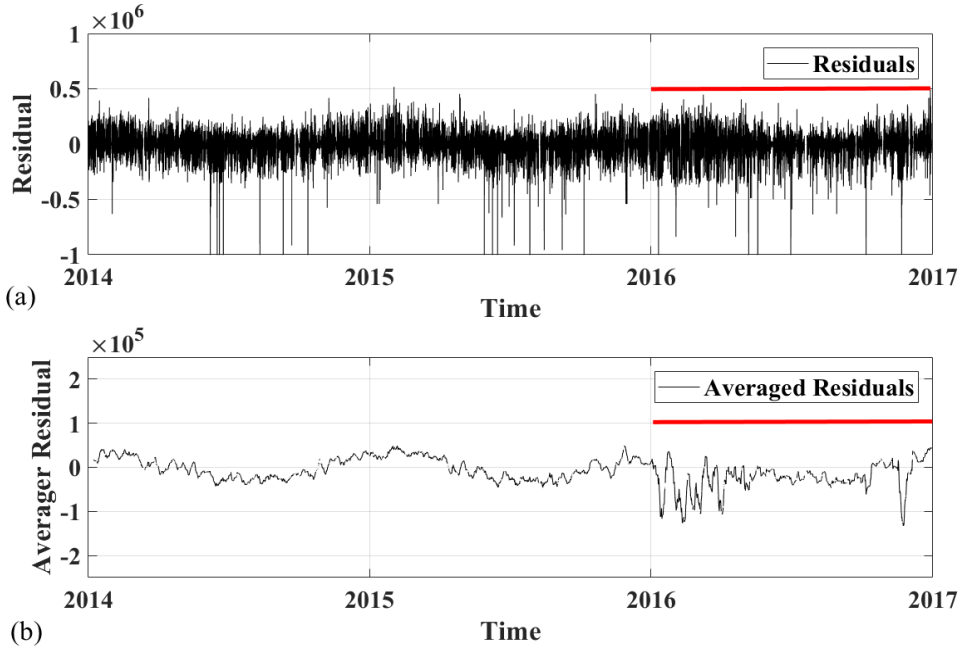

Figure 6.1 Method 1 for: Down-rating15% (a) Unprocessed (b) Moving Averaged & red lines marking fault period (Year 3)

6.1.2 Method 2: IEC inspired nuanced approach

The approach presented in (Cambron et al., 2016) belongs to the set of normal behavior modelling approaches. This technique generates a residual inspired by IEC standard (IEC 61400-12-1, 2005) but taking into account environmental and operational conditions. Similar to Method 1, the data is binned into 0.5 m/s wind intervals and the reference mean is calculated for each wind bin.

However, in line with the recommendation of IEC standard (IEC 61400-12-1, 2005) the data is corrected for onsite density variations and normalized to the reference density of 1.225 kg/m^3. Since the reference mean lies in the center of a wind bin, the residual is only calculated after translating all the data samples within each wind bin towards the bin center(Cambron et al., 2016) .The indicator for fault detection is calculated as the difference between all the produced power samples and the mean power value to two consecutive wind bins.

Fig. 6.2a shows the example of residuals calculated for a 3 years data stream. The fault scenario presented in this example is 15% down-rating during Year 3 (2016-2017). The faulty period is labelled as the horizontal red bar. **Fig. 6.2**b shows the same residual averaged with one week moving window.

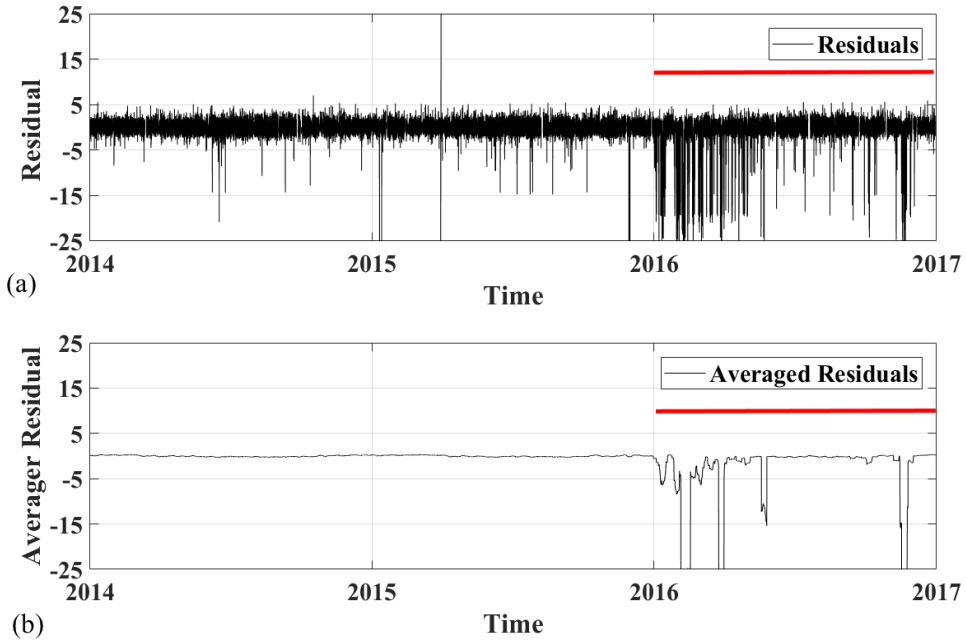

Figure 6.2 Method 2 for: Down-rating15% (a) Unprocessed (b) Moving Averaged & red lines marking fault period (Year 3)

6.1.3 Method 3: Regression based approach

The authors in (Butler et al., 2013) use a Gaussian Process Regression method to model the wind turbine power output. The learnt model is used to predict power output for each timestamp based on two inputs (Wind Speed, Air density). Fault detection residuals are generated as the difference between the simulated power data samples and the predicted reference power data. **Fig. 6.3**a shows the example of residuals calculated from a 3 years data stream with induced fault of 15% down-rating during year 3 (2016) as shown by red lines. **Fig. 6.3**b shows the one week moving average of the same residual.

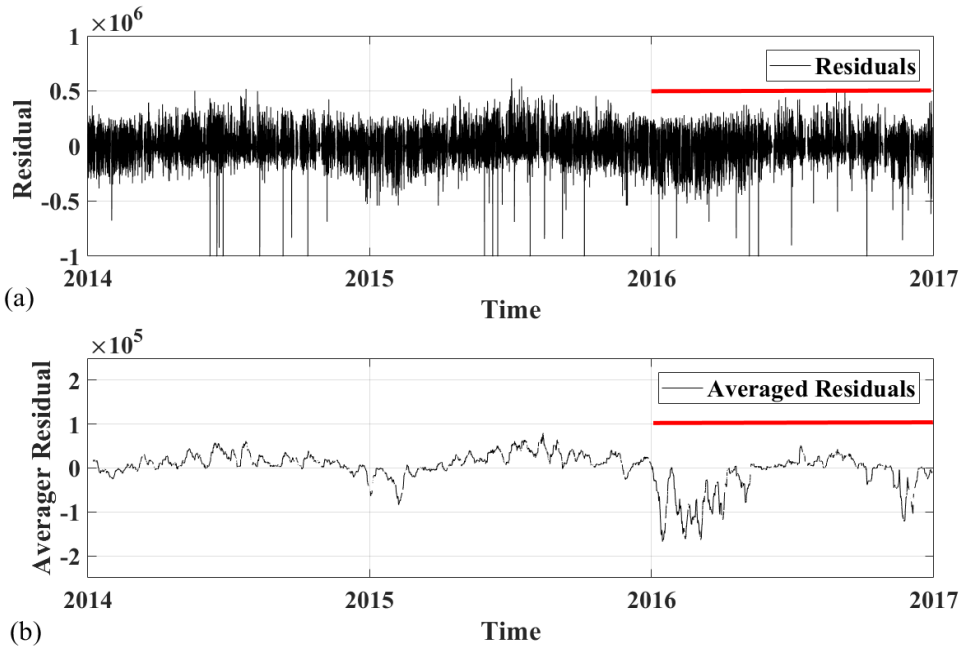

Figure 6.3 Method 3 for: Down-rating15% (a) Unprocessed (b) Moving Averaged & red lines marking fault period (Year 3)

6.2 Performance Evaluation Indicator

Within the overall proposed framework, once the realistically simulated data time series are generated and implementation residuals calculated, performance evaluation metrics are required. Any implementation or analysis is incomplete without a rigorous performance evaluation criteria. As one of the key objectives of this research is to evaluate the detection performance of methods proposed in the literature, an evaluation mechanism becomes critical. This is to evaluate the detection capability of any fault detection method. Wind farm operators need automated monitoring methods that can generate alarms when the WTs experience faults. The detection mechanisms need to be timely, robust and with a minimal amount of false alarms.

The detection of an occurring fault is usually made by deciding on a baseline for what is normal or acceptable and then setting a threshold on the normal behavior. The creation of a detection threshold is a delicate and difficult task since the fault indicators are not perfect and vary even when there is no fault. A compromise must therefore be made between the detection of real defects and the number of false alarms that the system may generate. Despite its significance, very few contributions in the existing literature concentrate on this aspect.

The performance indicator used in this work is the probability of detection (PD) for a given value of probability of false alarms (PFA). This relationship in classical signal theory is called receiver operating characteristic or ROC curve. Several techniques of interpreting and using the ROC curves have been proposed in literature. One of the key control parameters in the industrial context is the number of False Alarms that result in unnecessary onsite interventions. As established earlier in this research, the profit margins for modern turbine operators are dependent on reducing O&M costs. Unnecessary interventions increase O&M costs and reduce margins. This is even more critical for offshore wind farms where per intervention costs are significantly higher.

From and industrial perspective, the number of false alarms must be kept low since they result in impractical and unnecessary interventions. In this research, the detection threshold is set so that PFA is equal to 10%. The performance indicator for the sake of this evaluation is its corresponding PD. This PD indicator for this analysis will be referred to as PD_{10} (Aziz et al., 2019). PD_{10} provides a useful indicator as it represents a relatively descriptive and acceptable tool for this research. Another possible performance indicator could be the minimized distance of each ROC curve from the ideal (0,1). The following section details how the threshold is set for each simulation and how PD is calculated. A brief presentation of our fault detection performance analysis algorithm is as follows:

A three-year long simulation time series of data set is generated: Year 1 and Year 2 are fault free periods. A fault is introduced in Year 3. Let (*Th*) be the detection threshold set on the fault indicator. Whenever the fault indicator is below (*Th*), a fault is detected, as whenever a fault occurs, the residual is negative. This is due to the fact that the power produced is below the power expected under abnormal/faulty circumstances. It is important to note here that these residuals can come from any number of the fault detection methods presented in literature.

Year 1 (*learning period*) of fault free data is reserved to be used for learning fault free behavior by the implemented fault detection solutions.

Year 2 (*validation period, setting of Th*) is used to select the detection threshold *Th* corresponding to the selected 10% false alarm.

PFA is estimated as follows using eq. 6.1:

$$PFA_{EST} = \frac{No.\ of\ data\ samples\ below\ detection\ threshold(Th)}{Total\ No.\ of\ data\ samples\ in\ validation\ period} \quad \text{eq. 6.1}$$

Th is set such as PFA_{EST}=0.1 (10% PFA)

Year 3 (*fault period*) is used to estimate the probability of detection (PD), which is used as the performance indicator for fault detection. It is important to note that only the PD value corresponding to the PFA of 10% is used as an indicator in this analysis using eq. 6.2.

$$PD_{EST} = \frac{No.of\ samples\ below\ threshold\ (Th)}{Total\ No.\ of\ data\ samples\ in\ the\ fault\ period} \quad \text{eq. 6.2}$$

6.3 Performance data analysis

For a given fault detection method and a given fault, the value of PD for PFA equal to 10% can be calculated using several time series data streams generated by the framework. These data streams are generated using real data recorded from wind farms located in distinct geographical locations and wind turbines built by different manufacturers as presented in detail earlier.

Each time series of data can be generated using the dispersion residuals from one turbine of a given wind farm and using the environmental parameters recorded on another wind turbine. It is useful to remember here that two wind turbines are required to generate one data stream. The first wind turbine is used to learn a realistic data dispersion (Step 2 of the simulation process). The second wind turbine furnishes a deal data time series of (Wind, Temperature) to be used as an input to the simulation engine. (Step 3 of the simulation process).

With T the number of wind turbines made available for this research, a total of T by T time series of data can be generated. The T by T number represents all possible combinations where one turbine can be used for either Step 2 (dispersion learning) or Step 3 (simulation input). T by T number of data streams mean that T by T number of fault detection residuals will be built and the same number of PD_{10} (T by T) can be calculated. Once calculated, the performance of a given fault detection method on a specific fault can be evaluated using these T by T performance indicator values.

The performance indicator (PI) values are stored in a tabular form **(Table 6.1)** called Performance Evaluation Matrix (PEM). It is useful to observe that this PEM will have a fixed

size of T by T but can be populated by any PI values. For this work we use PD_{10} as PI. Moreover, one PEM is calculated for one specific fault scenario using one fault detection approach. Using the calculated PEMs, further analysis can be done to compare the performance of different fault detection approaches under different fault scenarios.

TABLE 6.1 PERFORMANCE EVALUATION MATRIX

			Operational Profiles																							
			Farm-V						Farm-L				Farm-D						Farm-S						Farm-C				
			V1	V2	V3	V4	V5	V6	L1	L2	L3	L4	D1	D2	D3	D4	D5	D6	S1	S2	S3	S4	S5	S6	C1	C2	C3	C4	C5
Environmental Profiles	Farm-V	V1																											
		V2																											
		V3																											
		V4																											
		V5																											
		V6																											
	Farm-L	L1																											
		L2																											
		L3																											
		L4																											
	Farm-D	D1																											
		D2																											
		D3																											
		D4																											
		D5																											
		D6																											
	Farm-S	S1																											
		S2																											
		S3																											
		S4																											
		S5																											
		S6																											
	Farm-C	C1																											
		C2																											
		C3																											
		C4																											
		C5																											

Since we are capable of generating multiple simulation scenarios and a combination of (T by T) time series of data, a statistic method can be used to analyze and compare the performance of different methods. A paired-sample t-test is a useful tool to quantify detection superiority of a particular method. The mean value of PD_{10} of two methods can be compared. The null hypothesis that the mean detection performance of two methods is the same can be tested. If the null hypothesis is rejected, that would mean that the mean value of PD_{10} of one fault detection method is significantly higher. This statistical tool can be used to compare and analyze the detection performance of any number of fault detection methods.

6.4 Conclusion & Complete Framework Overview

The simulation and performance evaluation framework developed so far can now be used to achieve the remaining objectives of this work. These include a performance comparison of

existing simulation techniques and evaluation under different fault scenarios, environmental and operational profiles. The detailed overview of the novel simulation framework presented in the previous chapter, complete with the implementation and performance evaluation benchmark is presented in **Fig 6.4**.

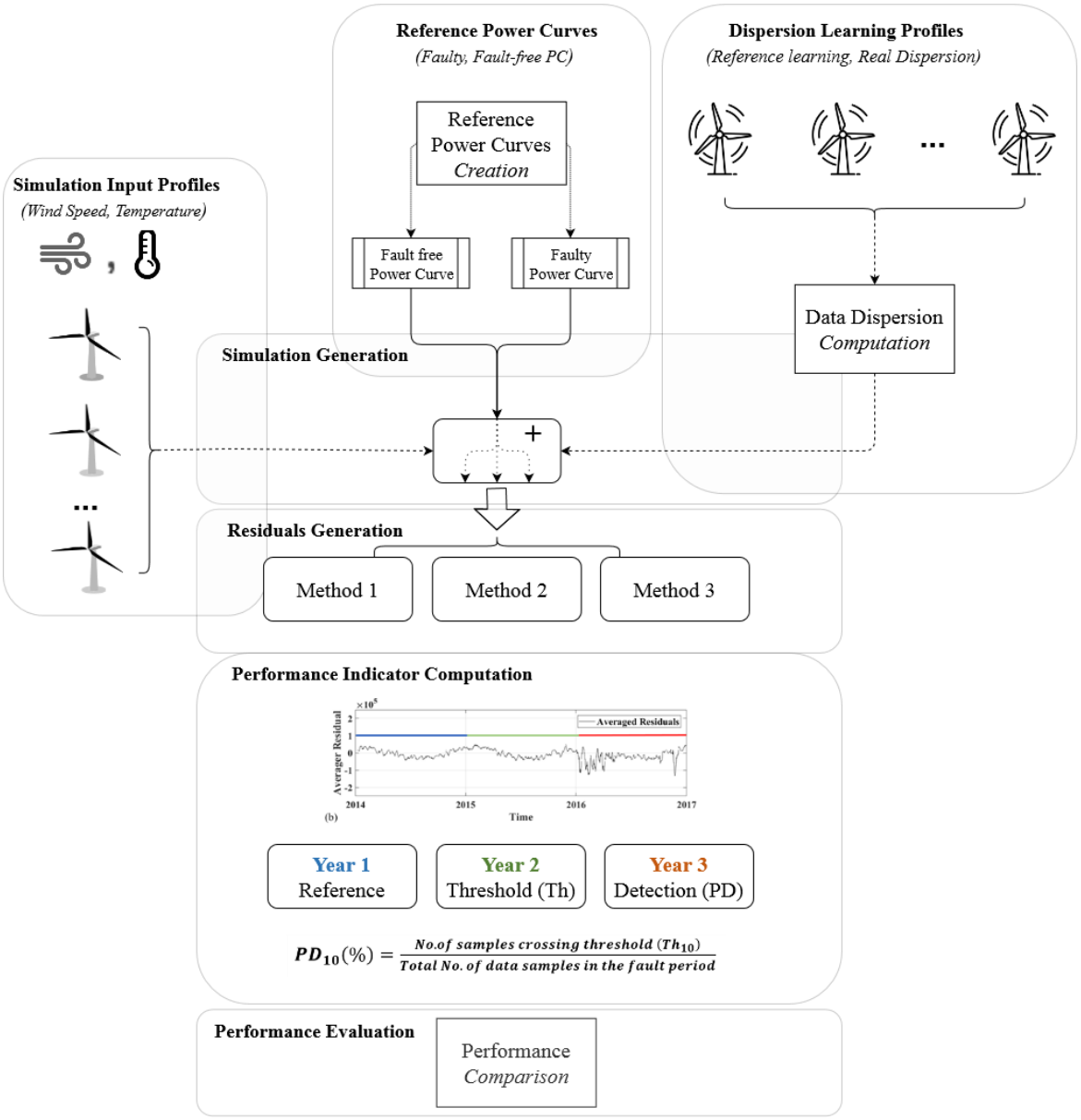

Figure 6.4 Overview of the proposed simulation framework. Input profiles shown to generate simulated power. Residuals are generated and detection performance compared.

The implementation results presented and discussed in detail in the following chapter can be divided into two major analysis families. First, the fault detection performance of all 3 detection methods is evaluated for each family of faults. Second, the wind farm level performance

comparison is used to identify if the detection performance varies from one farm to another. Such analysis is important to develop concrete recommendations to the wind farm operators. The operators need to be confident about all possible performance bottlenecks and limitations of each of the fault detection methods proposed in the literature. This provides a realistic confidence level and use case for each of the fault detection methods under different fault scenarios.

7 Performance Evaluation: numerical experiments, results and discussion

In this section, the simulation framework presented in chapter 5 will now be used to create data streams emulated with data from the data set presented in chapter 4 so as to evaluate the performances of the three fault detection methods presented in section 6.

The results presented and discussed in detail in the following sections are divided into two major analysis families. First, the fault detection performance of all 3 detection methods is evaluated for each family of faults. Second, the wind farm level performance comparison is used to identify if the detection performance varies from one farm to another. Such analysis is important to develop concrete recommendations to the wind farm operators. The operators need to be confident about all possible performance bottlenecks and limitations of each of the fault detection methods proposed in the literature. This provides a realistic confidence level and use case for each of the fault detection methods under different fault scenarios.

Let us recall that, since the data set is made of 5 wind farms composed of 5 wind turbines, a total of 625 (TxT = 25x25) simulation combinations are possible and results in the calculation of 625 performance indicators (PD_{10}) per fault and per method.

7.1 Performance Evaluation per type of Fault

7.1.1 Fault type -Down-rating

To recall, the fault intensities of (1%, 3.5%, 7% & 15% down rating) are selected for performance analysis. In terms of produced power, for a 2.05MW wind turbine, this down-rating translates to a curtailment from the rated maximum of 2.05MW to approx. 2.03MW, 1.97MW, 1.92MW & 1.75 MW respectively. For this fault type, this curtailment is only activated for higher wind speeds. This makes down-rating a critical fault for power production as high wind speed periods are where the operators expect to produce the rated maximum of

each machine. The choice of different fault intensity levels, gives a comprehensive view of the fault detection performance for this particular fault family.

Fig. 7.1 presents the mean value of the performance indicators PD_{10} of each method presented earlier (Method 1, 2 & 3). The bar chart shows mean PD_{10} values and their 95% confidence interval, calculated for different intensities of fault mode "Down-rating". The mean value represented by a single bar, per fault detection method is calculated for the complete performance evaluation matrix PEM (over all the 625 simulations, all environmental profiles and all dispersion profiles). The results show that globally, the increase in fault intensities results in an increase in detection performance for all Methods. This is expected as the increased fault intensity implies that an increased fault signature is going to be visible in the residual.

However, it is interesting to note that the mean value of PD_{10} for Method 2 stays approximately 10% higher than Method 3 and 20% higher than Method 1 for fault intensities 1%, 3.5% and 7%. As the fault intensity increases to 15%, the fault signature becomes relatively easier to detect by all Methods, hence, the detection performance advantage of Method 2 shrinks to approx. 10% compared to Method 1 & 5% compared to Method 3.

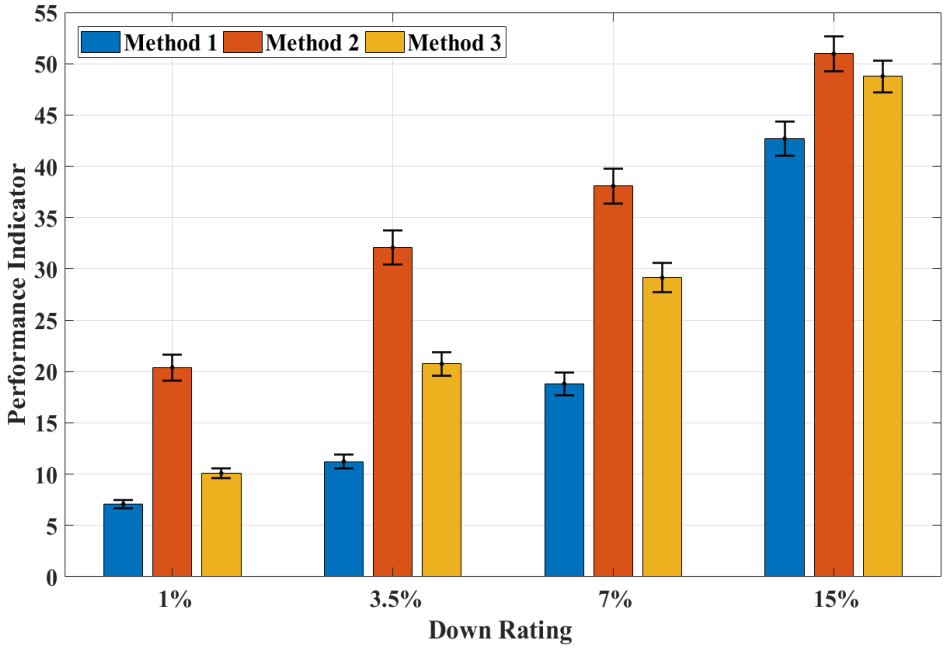

Figure 7.1 Performance Indicators for fault type Down Rating (1%, 3.5%, 7% & 15%) for Methods 1,2&3 with 95% confidence intervals.

It is also important to observe that the overall mean detection performance for fault type down-rating is relatively low. The PD_{10} values in **Fig. 7.1** have the lowest performance indicator value at approx. 7% for Method 1 and fault intensity 1%. The highest value of detection performance is 52% for Method 2 and for fault intensity 15%. We recall here that the subscript "10" of the performance indicator PD_{10} translates to the PD value for the false alarm rate of 0.1 or 10%. For the false alarm rate (PFA) of 10%, the highest mean detection performance (PD_{10}) of 52% is relatively low.

This can be explained by recalling the fault signatures for down-rating. Due to the peculiar nature of this fault (visible only for high winds) the fault signature is not pertinent throughout the fault period (Year 3). This means that even in the supposed fault period (Year 3) the wind turbine is producing normally for periods where wind speeds are lower. Since the performance indicator PD_{10} is calculated over the complete fault period (Year 3), the average detection values for down-rating (visible only for high winds) are lower as compared to a fault that is consistently visible throughout the whole fault period (Year 3).

7.1.2 Fault type –Icing on blades

Similar to the fault scenario presented above, several fault intensities (V-Low, Low, Medium and High Icing) for fault type Icing are selected for analysis. In terms of reduced production capacity, for a 2.05MW wind turbine, these intensities translate to a reduction of approx. 1%, 5%, 10% & 20% of produced power respectively. Unlike down-rating, the inherent nature of this fault type is as such that the production loss is for all wind speeds. The hypothesis here is that the fault type 'icing' changes the aerodynamics of the turbines blades and will affect the production for all wind speeds. It is important to note that although icing is a seasonal phenomenon but for consistency of analysis, in this work, the fault is evaluated for the complete year (Year 3). The choice of different fault intensity levels gives a comprehensive view of the fault detection performance for this particular fault family.

Fig. 7.2 presents the mean value of PD_{10} calculated for different intensities of fault mode "Icing". The mean value is represented by a single bar for each method. The mean value shown is calculated for the complete performance evaluation matrix (over all the 625 simulations, all environmental profiles and all dispersion profiles). The results show that globally, the increase in fault intensities results in an increase in detection performance for all Methods. Just like the

fault type down-rating, this is expected as the increased fault intensity implies that an increased fault signature is visible in the fault detection residual.

It is interesting to note that the mean value of PD_{10} for Method 2 stays ahead of Method 1 and Method 3 for all fault intensities 1%, 5%, 10% and 20%. The advantage of Method 2 in detection performance compared to other Methods is however reduced for fault family "icing" as compared to the previous fault case presented. As the fault intensity increases to 20%, the fault signature becomes prominent and easier to detect and the difference in the detection performances amongst all three approaches (Method 1, 2 & 3) becomes nominal.

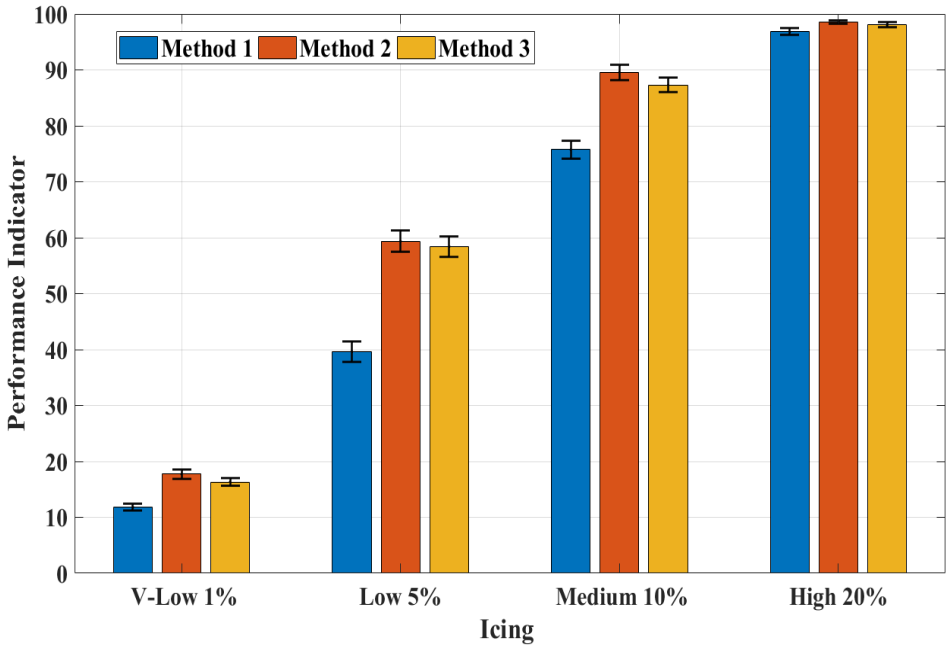

Figure 7.2 Performance Indicators for fault type Icing (V-Low, Low, Medium & High) for Methods 1,2&3 with 95% confidence intervals

Moreover, unlike 'down-rating', the overall mean detection performance for fault type 'icing' is high. The PD_{10} values in **Fig. 7.2** have the highest value at approx. 97% for Method 2 and fault intensity 20%. We recall here again that the subscript "10" of the performance indicator PD_{10} translates to the PD value for the false alarm rate of 0.1 or 10%. For the false alarm rate (PFA) of 10%, the highest mean detection performance (PD_{10}) of 97% is high. On the contrary, the fault signature for 1% icing is virtually undetectable with mean PD_{10} of 18%.

This can be explained by looking at the fault signatures for icing. The production loss for this fault type appears as a downward "step" shift in the fault period. As the fault intensity increases,

the amplitude of step shift increases and the fault becomes easier to detect. Moreover, the fault type icing is visible for all wind speeds and the fault signature is pertinent throughout the fault period (Year 3). Since the performance indicator PD_{10} is calculated over the complete fault period (Year 3), the average detection values for icing (visible for all wind speeds) are higher as compared to a fault that is only visible for high wind speeds (down-rating).

7.1.3 Fault types –Acoustic curtailment & Yaw misalignment

The mean, detection performance results for various fault intensities of fault types down-rating and icing have been presented so far. Two other important faults namely acoustic curtailment and yaw misalignment are added to the analysis and presented in this section.

The acoustic curtailment is a particular operational mode which is often activated at night or specific meteorological circumstances to ensure the compliance with acceptable noise levels. The activation is also a function of wind direction and populated sectors near the wind farms. This type of a fault in reality is occasional and often sporadic but for the sake of this analysis, an active fault throughout the fault period (Year 3) is considered. The fault signature for acoustic curtailment is only visible for high wind speeds. This is due to the fact that noise levels rise for higher wind speeds. It is also important to recall that the acoustic curtailment is a configuration activated by the operator. Since unintentional or faulty activation results in production loss, it is considered a fault.

The results show that for acoustic curtailment, globally the value of PD_{10} for Method 2 is higher than for Method 1 and Method 3. For this fault type, PD_{10} for Method 2 is ~13% superior to Method 1. However, the advantage of Method 2 in detection performance compared to Method 1 is relatively low (3%).

To recall, yaw misalignment is a fault that occurs when the wind turbine fails to align with the direction of maximum wind. The control system of a wind turbine is configured to adjust the yaw angle so that maximum exposure to wind is enabled. Any misalignment results in a sub-optimal power production and is termed a fault. 7-8° misalignment is used as a fault for this analysis but the severity of this fault can vary. Visually, the fault signature of 7-8° misalignment resembles the fault signature of fault type Icing 10% compared to the normal power curve.

For yaw misalignment, the trend of detection performance of Method 2 being superior continues. Globally the value of PD_{10} for Method 2 remains superior to that of Method 1 and

Method 3. For this fault type, PD_{10} for Method 2 is ~11% superior to Method 1. Similar to acoustic curtailment, the advantage of Method 2 in detection performance compared to Method 1 is there but relatively low (3%).

Fig. 7.3 presents these two faults (Acoustic Curtailment & Yaw Misalignment) along with the fault types down-rating and icing. It is important to note that the results for down-rating and icing in **Fig. 7.3** present the mean values across all intensities. For each method the down-rating in Fig. 7.3 is the mean of all values (1%, 3.5%, 7% & 15% down-rating) presented in **Fig. 7.1**. Similarly, the results for icing in Fig. 17 are a global mean of all fault intensities (1%, 5%, 10% & 20% icing) presented in **Fig. 7.2**.

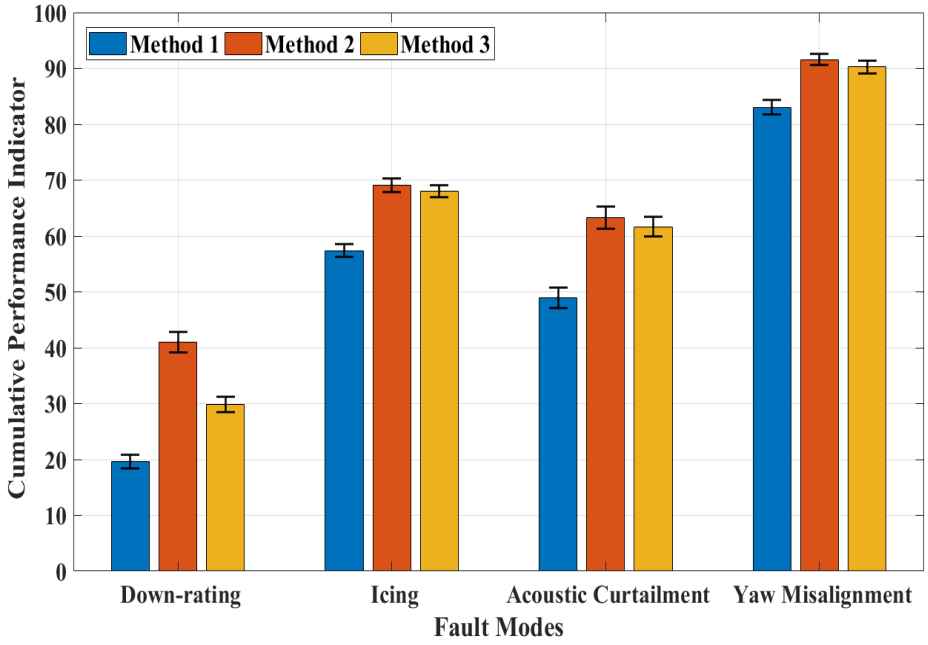

Figure 7.3 Global Performance Indicators for All fault types Down-rating, Icing, Acoustic Curtailment, Yaw Misalignment for Methods 1,2&3 with 95% confidence intervals

7.1.4 Conclusion- Fault Specific Comparison

The aim of the fault specific comparison was to conclude if one Method is globally performant for all fault types and intensities evaluated. As visible from **Fig**.**7.3**, Method 2 performs better that Methods 1 & 3 globally for all cases evaluated. It can be seen from this comparison that Method 1 is the least performant. One of the causes is a lack of mitigation for operational and environmental variations in its implementation. For Method 1, no effort is made to reduce the data dispersion caused by these variations. Method 3 comes in second overall. This

improvement in detection performances can be explained by the use of wind density as an input during the implementation. The consideration of wind density in modelling a wind turbine's output power has been shown to reduce RMSE by 16% (Farkas, 2011). As briefly referred to earlier, Method 2 performs the best out of the 3 methods tested for all fault cases evaluated. Data dispersion due the environmental variation is reduced by introducing the density correction in its implementation. The operational variation is addressed by the data translation within each wind bin (Cambron et al., 2016). Both these consideration enable Method 2 to be the most performant.

However, it is noticeable in **Fig.7.3** that the difference in performance between Method 2 & Method 3 for icing, acoustic curtailment and yaw misalignment is minimal. In order to definitively conclude that Method 2 is the most performant, a statistical analysis is necessary. The results presented in **Fig. 7.3** are validated in **Table 7.1** by using a t-test. The t-test is used to determine whether the PD_{10} means for fault detection methods tested are statistically different one from the other. The hypothesis testing is to statistically validate the performance superiority of Method 2. The statistical analysis is performed for all fault intensities to identify the best method for each fault scenario tested.

In-order to evaluate three fault detection methods (Method 1, 2 & 3) a two-step comparison approach is used. The paired-sample t-test is used to validate three scenarios (Method 2 vs Method 1, Method 2 vs Method 3 & Method 3 vs Method 1). The null hypothesis tested in these scenarios is that no method performs better than the other. The results are presented in Table 7.1. For different fault cases analyzed, the most performant method is represented by green dots, the least by red and intermediate by yellow. These results were reached through the three-step hypothesis testing strategy. The null hypothesis was first tested for Method 2 vs Method 1. The process was then repeated for Method 2 vs Method 3 and finally amongst Methods 3 & Method 1. Based on this analysis, the Table 7.1 was filled with tricolor representation of the most and least performant approaches for all fault scenarios and for all intensities tested.

TABLE 7.1 PERFORMANCE COMPARISON RANKING

	M1	M2	M3
Down-rating 1%	🔴	🟢	🟡
Down-rating 3.5%	🔴	🟢	🟡
Down-rating 7%	🔴	🟢	🟡
Down-rating 15%	🔴	🟢	🟡
Icing V-Low 1%	🔴	🟢	🟡
Icing Low 5%	🔴	🟢	🟡
Icing Medium 10%	🔴	🟢	🟡
Icing High 20%	🔴	🟡	🟢
Yaw Misalignment 7%	🔴	🟢	🟡
Acoustic Curtailment	🔴	🟢	🟡

As visible in Table 7.1, the most efficient method is method 2 with the exception of icing 20% and icing 5% highlighted in the table. This fault type is the easiest to detect so the performance difference between Method 2 & Method 3 is negligible. For this case, the superiority of M2 vs M3 is not significant as reported in Table 7.1a. This difficulty can be associated to the fault family (icing). In all other cases, method 2's mean value is statistically higher than method 3 and method 1 ($p<0.05$). The p values corresponding to the different test are presented in Table 7.1A. It outperforms method 3 and method 1 irrespective of the fault type and the fault intensity. Globally, the second performing method is Method 3, followed by Method 1. This is of course in agreement with **Fig. 7.3** and shows that, though the average PD_{10} for Method 2 and Method 3 are very close for Icing, Acoustic curtailment and Yaw misalignment, the superiority of PD_{10} for Method 2 is nevertheless statistically significant for most cases.

TABLE 7.1A PERFORMANCE COMPARISON RANKING (P-VALUES)

	M2 vs M1	M2 vs M3			M3 vs M1
Down-rating 1%	8,7E-63	4,0E-40		Down-rating 1%	1,8E-24
Down-rating 3.5%	1,8E-127	4,0E-75		Down-rating 3.5%	8,1E-77
Down-rating 7%	5,8E-161	5,6E-70		Down-rating 7%	2,7E-98
Down-rating 15%	1,2E-131	1,8E-31		Down-rating 15%	2,0E-51
Icing V-Low 1%	5,3E-44	8,7E-05		Icing V-Low 1%	4,0E-19
Icing Low 5%	3,4E-83	0,72		Icing Low 5%	7,6E-64
Icing Medium 10%	7,3E-76	0,01		Icing Medium 10%	8,0E-45
Icing High 20%	5,2E-02	0,95		Icing High 20%	3,2E-08
Yaw Misalignment	1,7E-44	5,6E-95		Yaw Misalignment	9,8E-51
Acoustic Curtailment	2,20E-49	0,03		Acoustic Curtailment	4,1E-46

When comparing the performance of method 3 and method 1, the method 3 is always performant and the better performance is always significant as reported in Table 7.1.

7.2 Performance Evaluation- Farm Level

Fault specific detection performance results have been presented in detail so far. However, in the industrial and practical context, any operations and maintenance team has to deal with a variety of machines installed at different geographical locations. These machines are from different manufacturers and are working under different operational circumstances. Hence, any fault detection solution needs to be validated and tested considering these variations.

The performance evaluation matrix (Table 6.1) and the framework proposed in this work, confer the opportunity for such rigorous analysis. The purpose of validating the fault detection methods on multiple wind farms and manufacturers is to identify if the performance remains consistent. Any information about performance variations of the same method for different wind farms is of interest to the wind farm operators.

7.2.1 Environmental Variation Results

As seen in the antecedent chapters, the performance evaluation matrix (PEM) provides the opportunity to observe and evaluate the performance variations caused due to variability in environmental profiles. The rows of PEM represent different environmental profiles (wind, temperature time series ($U(k), T(k)$) from different wind farms. For the sake of this analysis,

the performance indicator PD_{10} for fault type down-rating 15% is calculated and the PEM is populated. The same process is repeated for all 3 methods and the resulting PEMs are appended horizontally. **Fig. 7.4** shows the performance indicator PD_{10} calculated for the three methods of fault detection presented in Sec; 3.2, referred to here as Method 1, Method 2 & Method 3.

The fault type of Down-rating with intensity level of 15% is selected to calculate the performance indicators and to perform a meaningful analysis. The 15% fault intensity level for this type of fault presents a fair opportunity for a comparative analysis. The fault intensity level of 15% was chosen through an iterative analysis of different fault intensities. That iterative comparison is not presented here for brevity. It was determined that 15% intensity presents a borderline case of sufficiently difficult detection problem for all 3 methods. Below this intensity, the fault signature is so low that the detection becomes too difficult and for fault intensities above this value, the fault signatures start becoming relatively easier to detect.

The resulting performance evaluation matrices are concatenated horizontally for side by side comparison. The results are presented in **Fig. 7.4**a as a scaled color image for Methods 1, 2 & 3. This arrangement aims at visually evaluating the impact of environmental variations on the detection performances across all three methods. The image of the PEMs show significantly higher PD_{10} values for Wind Farm – S for Down-rating 15% test case. This shows that the site specific wind and temperature profiles have a direct impact on the performance detection for all Methods.

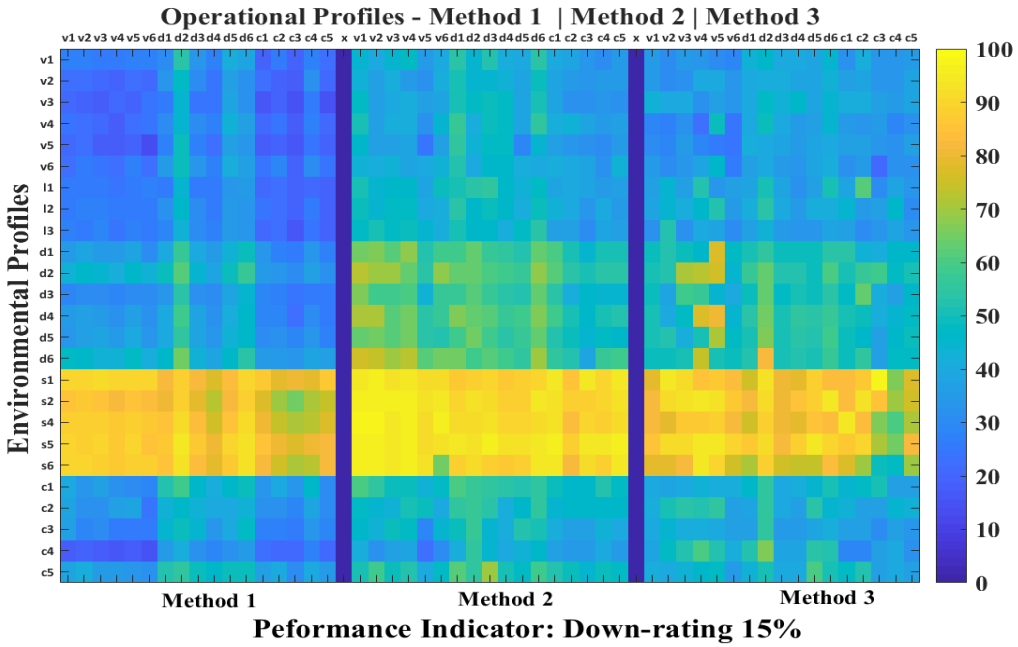

Figure 7.4 a Image of horizontally concatenated performance evaluation matrices, Method 1,2&3 for fault type down-rating of 15%

To quantify this visual observation further, the mean PD_{10} values for each wind farm (for each method) is calculated. The results are presented in a tabular form in **Fig. 7.4**b. When compared to wind farms (V, L, D, C) the mean detection performance for Farm S is on average approx. 52% higher for Method 1, 43% higher for Method 2 and 40% higher for Method 3.

Another important observation when comparing the results of Method 2 to Method 1 & 3 in **Fig. 7.4**a is the visibly lighter shades for Method 2.This suggests that PD_{10} values for Method 2 are globally higher. The same is reinforced by the mean values calculated in **Fig. 7.4**b. Hence, the findings in **Fig. 7.4**b reiterate both the conclusions drawn in **Sec. 7.1.1**.

The findings being,

i) For the fault type down-rating, the detection performances are generally low &

ii) Method 2 is more performant than Method 1 & 3.

Environmental Profiles	Method 1	Method 2	Method 3
Farm V	27 ± 1.4	41 ± 2.1	36 ± 1.5
Farm L	27 ± 1.4	44 ± 2.6	39 ± 2.5
Farm D	38 ± 1.3	58 ± 2.1	52 ± 2.1
Farm S	84 ± 1.2	92 ± 3.2	83 ± 2.1
Farm C	35 ± 1.6	47 ± 1.4	43 ± 1.4

Figure 7.4 b: Farm Average and 95% confidence interval of Performance Indicator, Method 1,2&3 for down-rating of 15%

The impact of environmental variation on detection performance can be explained by looking at the signature of the fault under observation and the distinct environmental profile of Farm-S. Farm-S is located in the south of France where relatively higher wind speeds are experienced as compared to the other 4 locations. **Fig. 7.5a** & **Fig. 7.5b** show the fault family of Down-rating and the onsite wind distribution for all Farms under observation respectively. The distribution of wind for higher wind speeds (from 8 m/s to 16 m/s (**Fig. 7.5b**) is of interest here. As identified by the region between red dotted lines), one can see that there is a significantly higher number of wind speed samples for Farm-S in this high wind region. The same wind region (from 8 m/s to 16 m/s) is displayed in **Fig. 7.5a**.

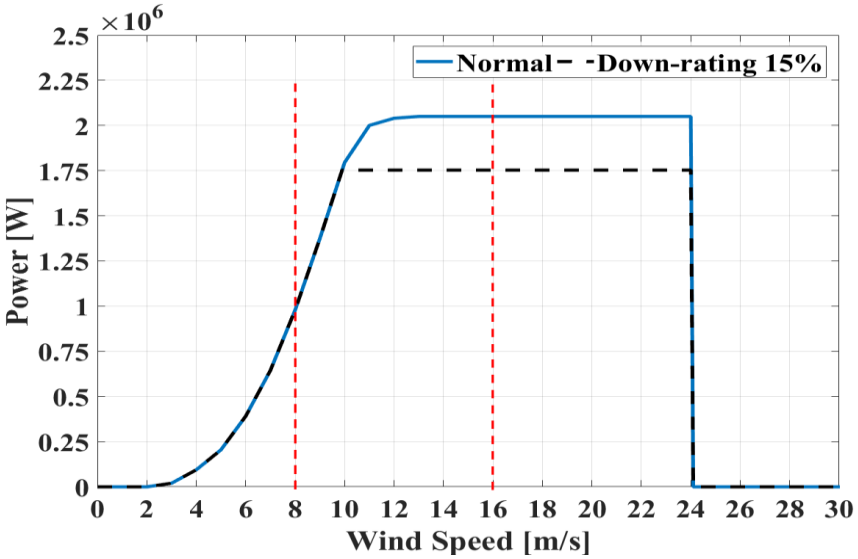

Figure 7.5 a Faulty Power Curves for Down-rating (15%) with red dotted lines identifying region of interest (from 8 m/s to 16 m/s)

It is important to note that the effect of a down-rating of 15% only becomes visible in the high wind speed regions (> 10 m/s) due to the inherent nature of the fault signature. A larger number of high wind speed samples mean that during the fault period (Year 3), the fault signature was excited more frequently for Farm-S as compared to the Farms V, L, D, S. This explains the higher values of detectability indicator PD_{10} for Farm-S. The peculiar fault nature of down-rating (fault excitation for high winds only) and the specific wind distributions (**Fig. 7.5b**) explain the lower detection performance values for wind farms V,L,D and C.

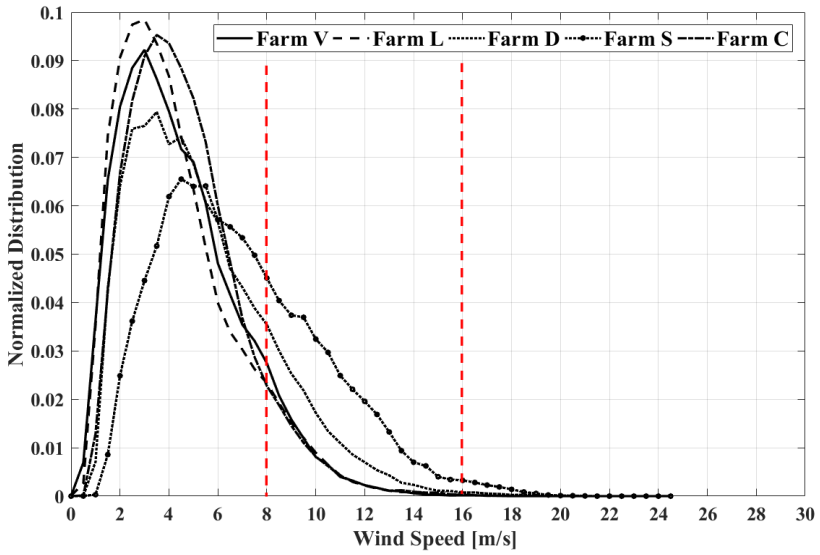

Figure 7.5 b: Wind Distribution of Farms (FarmV,L,D,S,C) with red dotted lines identifying region of interest (from 8 m/s to 16 m/s)

7.2.2 Operational Variation Results

Different turbines from different manufactures can have uniquely characteristic behaviors. The performance evaluation matrix (PEM) provides the opportunity to observe and evaluate the performance variations caused due to variability in these operational profiles. The columns of PEM represent different operational profiles (data dispersion, operational characteristics) from different manufacturers.

The fault type "icing" is a good candidate to evaluate the operational variations. As presented earlier, this fault type impacts the overall behavior of a turbine for all wind speeds. Hence, it is suitable to capture the operational behavior of wind turbines. The performance indicator PD_{10} for fault type icing 5% is calculated and the PEM is populated. The same process is repeated for

all methods of interest and the resulting PEMs are appended vertically. The choice of vertical concatenation is to ensure better visual interpretation.

The fault type of icing with intensity level of 5% is selected to calculate the performance indicators and to perform a meaningful analysis. The 5% fault intensity level for this type of fault presents a fair opportunity for a comparative analysis. As was the case for previous such analysis, the fault intensity level of 5% was chosen through an iterative analysis of different fault intensities. It was determined that 5% intensity for fault type icing, presents a borderline case of sufficiently difficult detection problem. Below this intensity, the fault signature is so low that the detection becomes too difficult and for fault intensities above this value, the fault signatures start becoming relatively easier to detect.

Three wind farms are carefully selected for operational analysis. Since, the wind Farms V & C have wind turbines from the same OEM, they become a natural candidate for control group in such analysis. Wind Farm-D is selected as the third candidate to compare with the control group of similar turbines. **Fig. 7.6** shows the performance indicator PD_{10} calculated for the two methods of fault detection referred to as Method 1 & Method 2.

For an easier visual interpretation, the performance evaluation matrices are shown as an image with scaled colors for two methods of fault detection (Methods 1&2). The color bar on the right hand side shows a color scale associated to the PD_{10} values with higher values depicted as shades of yellow and lower values as blue. The image of the PEMs show globally similar performance (PD_{10}) values for Wind Farms – V& C in contrast to Wind Farm D. This shows that just like the environmental profiles evaluated earlier, data dispersions i.e. operational characteristics also have a direct impact on the fault detection performance.

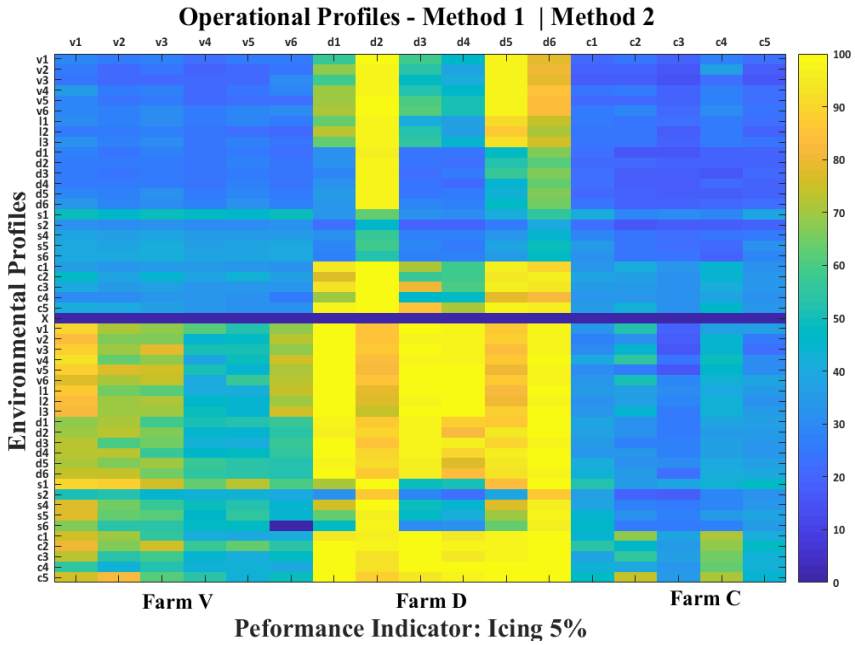

Figure 7.6 a Image of vertically concatenated performance evaluation matrices, Method 1&2 for fault type icing of 5% on Farms V, D and S

To quantify this visual observation further, the mean PD_{10} values for each wind farm (& for each method) is calculated. The results are presented in a tabular form in **Fig. 7.6**b. When comparing the wind farms V & C the mean detection performance remains approx. within 1std of each other. On the contrary, the mean detection values for Farm D for both methods is on average approx. 35% superior for Method 1, 45% superior for Method 2. This makes detection performance for Farm D twice as much as for Farms V & C. The improved performance for Farm D can be associated to the specific operational performance of machines from this OEM. For Farm D, the data dispersion is minimal and the observed power values nicely follow the expected power curve. An example of such phenomenon can be found in **Fig. 4.5.**

As in the case of environmental variation analysis, the mean performance indicator (PD_{10}) values for Method 2, as presented in **Fig. 7.6**b are relatively higher. The same is visually represented in **Fig. 7.6**a through visibly lighter shades for Method 2.This suggests that the Method 2 performs globally better than Methods 1 for this fault type as well. Quantitatively, the gain of Method 2 for the specific fault example here is approx. 20%. This observation of performance gain with Method 2 is in accordance to the conclusions drawn in the fault specific performance evaluation, thoroughly discussed earlier.

	Farm V	Farm D	Farm C
Method 1	31 ± 1.2	62 ± 4.1	25 ± 1.4
Method 2	50 ± 2.2	89 ± 3.1	37 ± 2.0

Figure 7.6 b: Farm Average and 95% confidence interval of Performance Indicator, Method 1&2 for icing of 5%

In this chapter, the novel simulation framework was used to evaluate the performance of three condition monitoring strategies. The extensive results, findings and numerical analysis reported speak to the robustness of the developed framework. It is to be noted here that the results presented thus far were for the methods designed for implementation on a single turbine. The novel simulation framework can also be leveraged to extend the critical analysis to a farm and fleet level as will be presented in the following chapter.

8 Multi turbine Implementation

The improved performance of power based wind turbine fault detection is linked to the dispersion reduction capabilities of the method used to process the condition monitoring information. It has been shown so far and in the literature that various fault detection approaches employ different strategies to address this issue. The strategies seen so far in this research include correction for environmental parameters separate of the model or inclusion of environmental parameters as model input to achieve the same effect. The condition monitoring approaches presented thus-far were turbine centric as the measurements used were sourced from a single turbine.

However, to address the data dispersion issue, another family of condition monitoring solutions can be identified in the literature. Unlike the "single-turbine" methods where the fault indicators are constructed from variables recorded on a single turbine, the so called "multi-turbine" methods are the ones where the indicators are constructed from variables recorded on different turbines in the same wind farm. These methods aim at reducing the variability and dispersion observed in the residuals built for the condition monitoring of individual turbines. This aligns with the global agenda of power based FDI approaches seen so far; i.e. to reduce dispersion in order to increase detection performance.

The basic idea of comparing one turbine to another within the same farm has a very strong empirical foundation. Wind farm operators are interested in comparing the production of each turbine with its neighbors to see how each turbine is faring and if there are any visible production losses/impediments for a particular turbine. The underlying principal for such comparison is to imagine a normal 'farm-inertia' or 'farm reference' in order to contrast the turbine specific production capacity.

This chapter details the objective and rationale for using multi-turbine approach in the overall condition monitoring strategy. A novel modification to the developed simulation framework is presented so that the gains of multi-turbine approach if any, can be evaluated. A benchmark for multi-turbine fault detection approach is presented and use cases are detailed. Finally the realistic experimental set up and implementation results are shared. The findings, conclusions drawn and future perspectives are produced at the end of this chapter.

8.1 Context for the proposed multi-turbine approach

8.1.1 Objective of the approach

As briefly alluded to earlier, one of the key concerns when using power based methods for fault detection is the data dispersion and consequently the variability in built residuals and thus created fault indicators. The proposed methods in power based condition monitoring literature attempt to address these concerns through a variety of ways. (Cambron et al., 2016),(Uluyol et al., 2011), (Bi et al., 2017b), (Park et al., 2014) build residuals through explicit modelling of the power/performance curves and attempt to accommodate and compensate for the dispersion around the power curve separately. This is often done through normalizations and data corrections using environmental parameters.

(Pelletier et al., 2016),(Butler et al., 2013), (Kim et al., 2012), (Kusiak et al., 2009a),however, try to better model the produced power by including potential sources of dispersion and variability as an input to the modelling strategy. On the contrary, to avoid the difficulty caused by residual variability, some methods like (Yang et al., 2013),(de Andrade Vieira & Sanz-Bobi, 2015) and (Jia et al., 2016b) do not use residuals (i.e. difference between and observed value and an expected "normal" value). Instead these methods build models on two sets of data (historic & current or online & offline) and compare the models instead to calculate a comparison constant as fault indicator. This distinction has already been made and detailed in the literature review of this research.

It is of interest to note that all the strategies presented so far have attempted to reduce data dispersion to increase detection capabilities by using indicators built on a single wind turbine. Single turbine methods aim first at generating residuals, but these residuals may still show some dispersion. Different more elaborated single-turbine methods use different means to reduce this

dispersion, but this might not be always sufficient. As referred to earlier, another set of methods may provide a different approach to achieve the same objective. The strategy of using multiple turbine in the same wind farm to build a health indicator has been presented in the literature. Although the idea is fairly generalizable and component temperatures are commonly used, produced power or other measurements may also benefit from this approach.

(Astolfi et al., 2014) present a model comparison method for different models linking the produced power and bearing temperature. (Papatheou et al., 2014) propose to compare the prediction error between models learned on different turbines. The authors in (Lebranchu et al., 2019) propose a hybrid mono- multi-turbine performance indicator using temperature variables. (McLaughlin et al., 2009) provide first ideas of curve comparison involving power curves. However, instead of comparing the power curves of the turbines to each other, the comparison to manufacturer's reference is proposed. (Cambron et al., 2018) similarly use empirical comparison of multiple turbines in a wind farm to build comparison residuals from 'farm inertia'. Hence, a multi-turbine solution could be an alternative or a complementary way to accommodate and compensate for the dispersion around the power curve.

8.1.2 Assumptions and rationale of the approach

In order to benefit from the farm level turbine comparison, certain assumptions need to be made. Although the empirical evidence of comparing the production of one wind turbine to the other is quite intuitive in the industrial context, certain methodological pre-requisites are imperative for the comparison to build its objective foundations. For a "multi-turbine" comparison to be valid, the following assumptions need to hold

- *All wind-turbines in one wind farm are supposed to be homogenous i.e. of the same make and model, installed at the same time.*

This generally holds true as the make and model of wind turbines are selected before installation and most wind farms are constructed in one go. This makes the wind farm operationally homogeneous.

- *All wind-turbines in one wind farm are subject to the same environmental variations (wind speed, wind direction, air density, ambient temperature, etc.).*

This generally holds true as well since all WTs in a wind farm are geographically concentrated and relatively affected by the same environmental variations, since weather conditions are roughly the same over the entire wind farm. This makes a wind farm relatively homogeneous or at least consistent for environmental variations.

Once these assumptions hold true, the principal of 'farm reference' can be leveraged. The principal dictates that despite highly stochastic nature of the wind turbine problem, the overall behavior of all turbines within a wind farm evolves in tandem hence a global farm reference behavior in normal circumstances can be learnt. Any particular deviation of a wind turbine from this 'farm-reference' (the normal evolutionary behavior of the overall farm), can be considered as a fault symptom and can be used for fault detection.

8.2 Presentation of the multi-turbine strategy for fault detection

The same principal of multi-turbine approach can be implemented as an extension to 'mono-turbine' fault detection residuals. The proposed 'hybrid mono-multi-turbine' approach can then resort to a comparison of the single-turbine residuals, assuming that under the fault free situation, the evolution for all the turbine residuals within the same wind farm is the same. If one of the residuals departs from the others, then it is considered as an evidence of a fault on the corresponding turbine. This new strategy is a hybrid multi-level (turbine and farm level) approach to generate a monitoring indicator that will be used for fault detection and performance evolution in this part of the research.

The algorithm for multi-turbine indicator creation for temperature variable is presented in detail by authors in (Lebranchu et al., 2019). The three step hybrid mono-multi health indicator creation strategy for power based approach can be summarized as follows.

$R^{i}_{mono}(\mathrm{k})$ is the value of the residual R_{mono} from turbine I at time k. Let N be the number of turbines in the wind farm. For each turbine i, with i varying from 1 to N , the multi turbine fault indicator $R^{i}_{multi}(\mathrm{k})$ is built at time k, as follows:

i. The **mono turbine residual** for each turbine i in the farm is first calculated depending on the Method chosen but globally as a difference of measured P and modelled/predicted power $\hat{P}$ as eq. 8.1

$$R^i_{mono}(k) = P^i(k) - \hat{P}^i(k) \qquad \text{eq. 8.1}$$

ii. The **farm reference** $R_{farm}(k)$ for turbines *1,.. N* is calculated using the $R^i_{mono}(k)$ at the turbine level, as eq. 8.2 follows:

$$R_{farm}(k) = median_{(l=1,\dots N_L)}(R^l_{mono}(k)) \qquad \text{eq. 8.2}$$

The farm reference is calculated using the median and not the mean, so as to address the abnormal values generated by faulty turbines. For the practical implementation, the farm reference is computed as long as more than half of the turbines used to calculate the reference operate in normal conditions and their data is available. N_L is the lower limit of turbines required for calculation of R_{farm}.

iii. The **multi-turbine residual** fault indicator $R^i_{multi}(k)$ is calculated for each turbine *i* as the distance between the mono Residual R^i_{mono} and Farm Reference R_{farm} .

$$R^i_{multi}(k) = R^i_{mono}(k) - R_{farm}(k) \qquad \text{eq. 8.3}$$

This multi-turbine fault indicator $R^i_{multi}(k)$ is a result of the hybrid mono-multi turbine residual generation and can now be used for fault detection performance analysis. This strategy will be referred to as hybrid mono-multi turbine or for brevity, hybrid multi-turbine approach from here onwards. The same process is repeated to calculate the multi-turbine residuals for all wind turbines in the wind farm. $R^i_{mono}(k)$ residuals are assumed to carry information on the individual turbine deterioration and when used in the multi-turbine configuration as proposed, can provide useful insights to the state of the turbine. The overall principal for the proposed hybrid mono-multi-turbine approach can be summarized as presented in **Fig 8.1.**

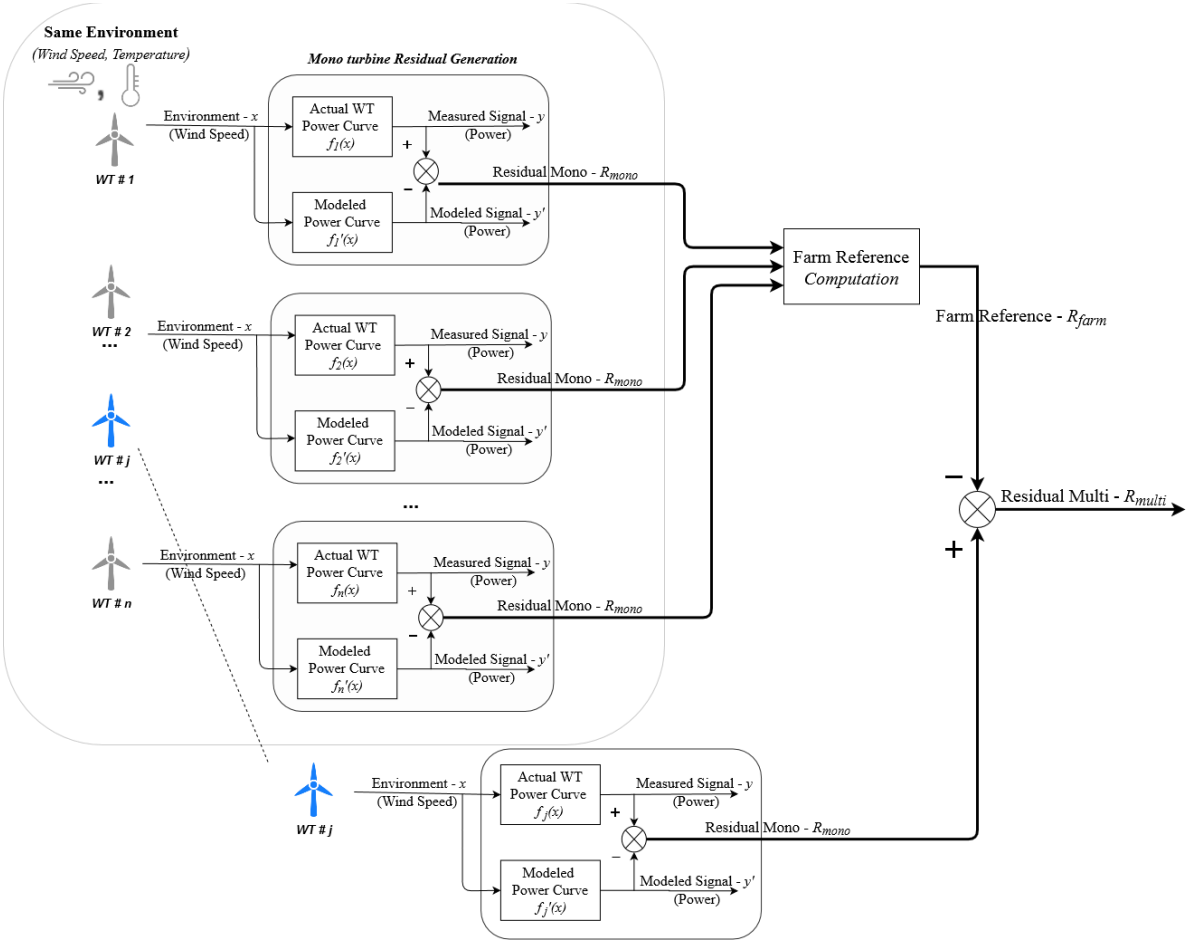

Figure 8.1 Overview of the hybrid mono-multi-turbine approach: generic principle for the synthesis of fault indicator Rmulti for wind turbine i. The mono-turbine residual Rmono is used for calculating farm reference Rfarm & consequently the hybrid mono-multi turbine

The objective of this chapter is to investigate this "multi-turbine" concept in different settings using the rich capabilities of the realistic simulation framework developed by authors in (Aziz et al., 2018) and detailed in one of the previous chapters (Ch. 5: Simulation Framework). In order to achieve that, first, different multi-turbine configurations of the simulation framework are required.

8.3 Multi-turbine simulation framework

The simulation framework developed throughout the course of this research provides a unique opportunity to evaluate the hybrid multi turbine approach. The framework has been

proven so far to be flexible enough so as to include and test for fault, environmental and operational variations. Although the analysis thus far was of turbine level indicators, since the original framework is set up to mimic wind farms as well, it can be extended to multi-turbine simulation and performance evaluation configurations. Such investigation results in a new and original contribution of multi-turbine analysis that leverages the novel framework developed and evaluated thus far.

In order to set up a hybrid multi-level implementation, first a few choices need to be made. Since the turbine level section of the hybrid approach requires a residual generation method as a first step, a fault detection method is required. Different residual generation methods can be chosen for analysis. Moreover, as referred to earlier, for a multi-turbine approach to be valid, the underlying assumption of 'intra-farm' turbine dependence needs to be assured. Due to the high level of flexibility, control and robustness enabled by the realistic simulation process, a number of configurations are possible for this aspect as well. Hence, the multi-turbine setup configurations are proposed and evaluated based on the following two criteria.

i. Choice of a turbine level residual generation method (mono-turbine)
ii. Modelling/representation of the dependence of turbines within the same wind farm

The three unique cases in this research using the combination of above listed criteria are detailed in the following sections.

8.3.1 Case I

A situational inter-dependence of wind turbines within each wind farm is requisite. In case I, the *same power curve reference* is used to generate the simulated data streams (Sec 5.1.1: Reference creation) of each of the wind turbines composing a wind farm. The assumption here is that each turbine of the wind farm produces the same amount of power for a given wind speed, in normal conditions. The realistic variability in this simulation mode comes from the calculation and random selection of the realistic data dispersion residual.

In the original mono-turbine simulation framework, different environmental profiles from turbines within the same wind farm are used as simulation inputs. However, to restrict the scope of this multi-turbine section of this research, we limit the turbine entries with the same

environmental profiles (Wind, Temp) as the candidates to constitute a wind farm. In other words, the same wind/temperature profile is used to generate the power data streams of each turbine of the farm. (This constitutes a row of the performance evaluation matrix – PEM presented in Sec. 6.3 and will be detailed in this context later).

To summarize, Case I of multi-turbine configuration is setup with the following conditions

- A wind farm contains all the turbines with the same input environmental profile and *same reference power curves* for simulation of turbines under normal conditions. This consequently introduces a strong dependence between the turbines within the farm. The introduction of the fault on one turbine is done by changing the power curve from the reference power curve to a faulty power curve for the turbine under study.

8.3.2 Case II

Similar to Case I, in order to meet the dependence criteria for a multi-turbine set-up, a situational inter-dependence of wind turbines within each wind farm is required again. *However,* for Case II, instead of using the same power curve reference for each wind turbine of the farm, a *different power curve reference* is learnt on each data dispersion learning turbine and used to generate the normal conditions simulated data streams (Sec 5.1.1: Reference creation). The assumption here is that there is a variability among the turbines of the same farm. They can produce a slightly different amount of power for the same wind speed. The realistic variability in this simulation mode comes from the variability in learnt reference curves in addition to the learning/calculation and random selection of the realistic data dispersion residuals.

Similar to Case I, the same environmental profile (Wind, Temp) is used to create the power data stream of each turbine of the wind farm. (Row of PEM).

To summarize, Case II is the multi-turbine setup where

- In a wind farm, all the turbines are submitted to the same input environmental profile but they have *different reference power curves* for the simulation of each within the farm. The introduction of the fault on one turbine is done by changing the power curve from the learnt power curve to a faulty power curve for the turbine under study.

8.3.3 Case III

In contrast to Case I and II of the multi-turbine case set up, Case III uses a different approach to generate power data streams.

Similar to Case I, in order to meet the dependence criteria for a multi-turbine set-up, the same power curve reference for each turbine in the wind farm is used to generate the simulated data streams (Sec 5.1.1: Reference creation).

However, for the Case III of multi-turbine setup, a new source of variability in the environmental conditions is introduced in the simulated power data by modeling the wind being laminar and turbulent. The wind is stochastic in nature (laminar or turbulent), moreover the nature of wind can change every 10 minutes sample. This behavior can be modelled by using a Markov Chain made of two states: turbulent and laminar (Ma et al., 2018). The wind nature can change form laminar to turbulent every 10 minutes, depending on the probabilities set in the transition matrix. For our implementation, we can simulate different scenario: The wind is turbulent 10% of the time and the wind is turbulent 90% of the time. The two state Markov chain state diagram along with the transition matrix for 90% turbulent P_{90} wind scenario are presented in **Fig 8.2**.

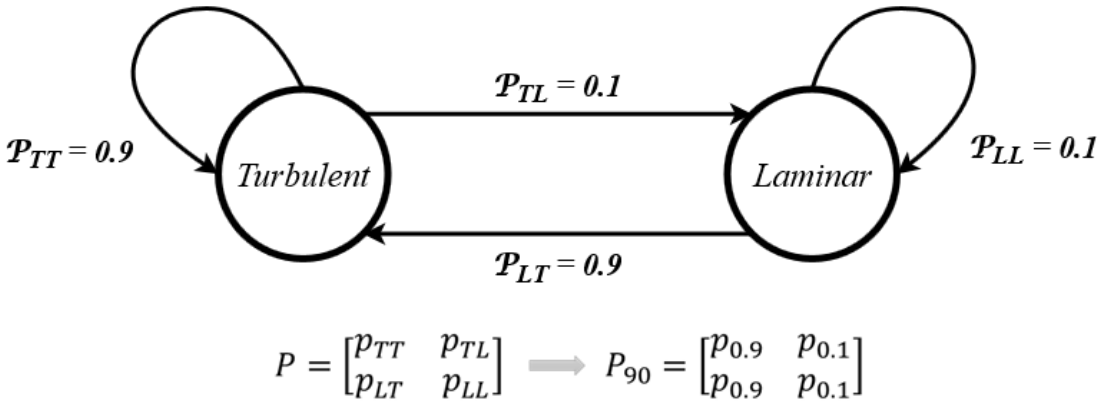

Figure 8.2 2-state Markov chain state diagram with e.g. transition matrix for 90% turbulent case.

The difference between a wind blowing in a laminar or a turbulent way is modelled by using different power curves. When the wind is laminar, the laminar power curve is used and when the wind is turbulent, the turbulent power curve is used. The literature presents various cases where increased turbulence decreases the produced power for higher wind speeds and increases the reference power slightly for lower wind speed durations (Albers et al., n.d.) (Bardal & Sætran, 2017). Since the increased turbulence impacts the power curve negatively, this provides the inspiration for modeling two reference power curves. The relevant transition matrix for required state (turbulent/laminar) determines the percentage of time the relevant reference power curve (laminar/turbulent) is chosen. **Fig 8.3** shows the normal or laminar power curve along with the turbulence reference power curve

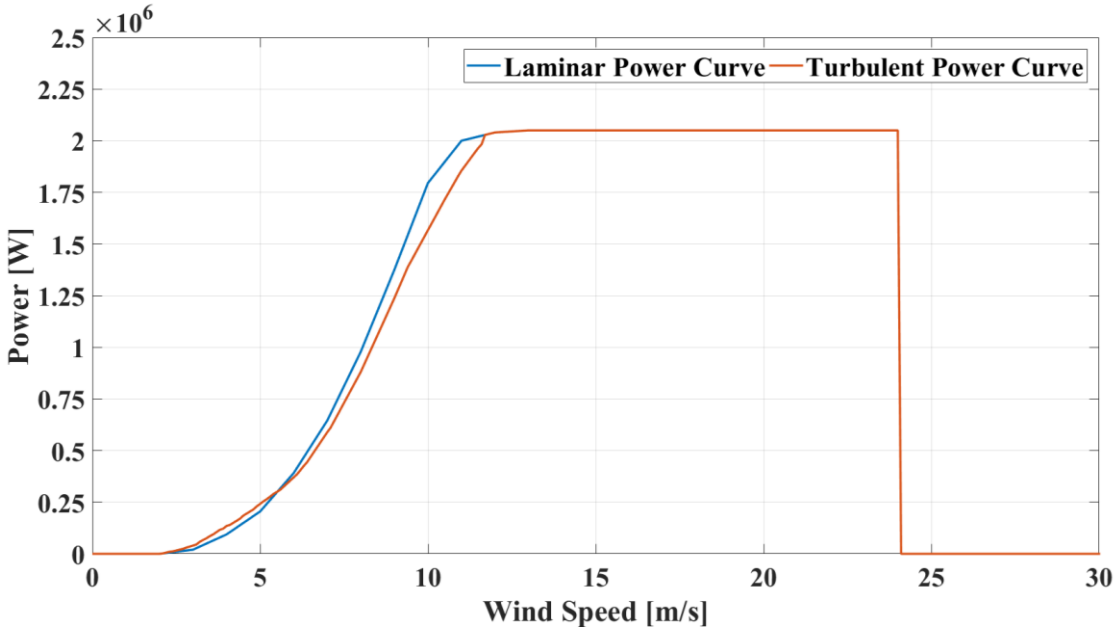

Figure 8.3 Laminar & Turbulent; Reference Power Curves.

Case III is then simulated using 2 different power curves: laminar and turbulent. The "turbulent" or "laminar" state is the same for all the turbines in the park and the switch between turbulent and laminar is done at the same time for all the turbines in normal conditions (modelling of the park effect). When the fault is introduced into a turbine, the power curve of the fault is used. **Fig 8.4** presents the modified simulation process for Case III based on the Markov chain presented above and the distinct reference curves for laminar & turbulent cases. The overall hybrid mono-multi turbine implementation framework is also detailed.

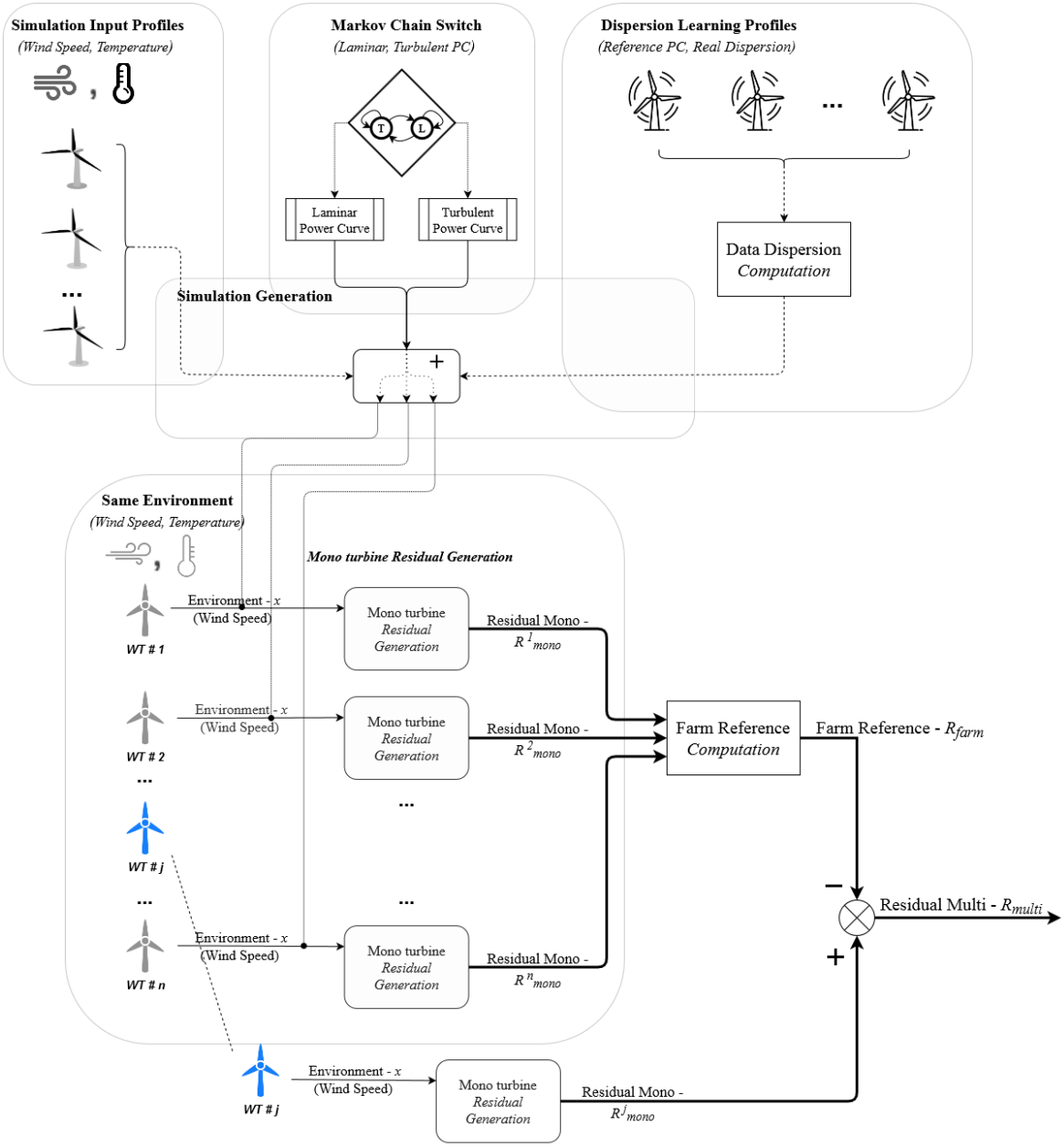

Figure 8.4 Overview of the modified simulation process; Serving as Case III multi-turbine setup

Similar to Cases I,II , the same environmental profile (Wind, Temp) is used to create the power data stream of each turbine of the wind farm. (Row of PEM).

To summarize, the Case III of the multi-turbine setup is where

- A wind farm contains all the turbines with the same input environmental profile and *same reference power curves* for the simulation of each within the farm. A different source of variability in the power curve is added due to the shift from *laminar to turbulent* wind.

The introduction of the fault on one turbine is done by changing the power curve from the reference power curves to a faulty power curve for the turbine under study.

8.3.4 Motivation & Overview of Case setups (I, II & III)

For the sake of this implementation, Case I and Case II will be considered using Method 1 only. Indeed, the abysmal detection performance of this method for mono-turbine implementations presented in earlier chapters could be improved by using a hybrid mono-multi turbine strategy. It is of interest to see if the detection performance of basic strategy of residual generation and fault detection can be improved by using the multi-turbine approach. In addition, the residuals for Method 1 as seen earlier, provide a good candidate and test case for the problems of data variability, dispersion etc. that the multi-turbine strategies claim to resolve. Testing two forms of power curve reference (constant/learnt or same/different) in Cases III provides an additional layer of performance comparison in increased data dispersion scenario.

As seen in the results presented in earlier chapters in the mono turbine setting, Method 2 in a mono-turbine approach performs well. So, the Case III multi-turbine setup uses Method 2 for this analysis to help answer if any performance gain can still be expected. Moreover, the introduction of a new variability in the form of turbulence, will help evaluate if Method 2 still stays performant. It could also be interesting to see the performance capability of Method 2 under two extreme cases of turbulence.

Thus Case I and Case II will be applied on Method 1 only and Case III will be applied on Method 2. An overview of all 3 case setup for multi-turbine configuration are presented in **Fig. 8.5** below.

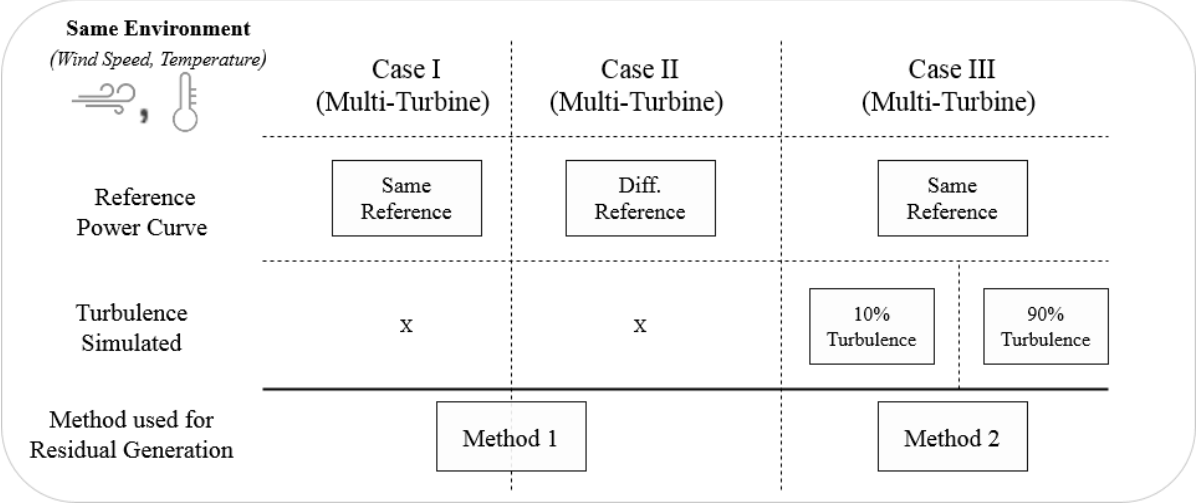

Figure 8.5 Overview of the multi-Turbine configuration settings considered in the study.

Once all three simulation setups have been identified, they can be used to generate the turbine level portion of the hybrid approach. For Case I, II the residual generation approach is Method 1 while for Case 3, Method 2 is used for the mono-turbine indicator creation.

8.4 Performance Evaluation: numerical experiments, results and discussion

This sections explains the experimental protocol for the hybrid mono-multi turbine approach presented thus far. The results and findings are reported in detail as well.

8.4.1 Experimentation protocol

As referred to earlier, each row of the performance evaluation matrix (PEM) corresponds to a simulations carried out with the same environmental (Wind/Temperature) profile.

The performance analysis for this research requires a multi-turbine residual calculation (R_{multi}). This multi-turbine residual, requires the calculation of a mono-turbine residual (R_{mono}) calculated for each of the turbines and thus the generation of power profiles for all turbines of within a park. For each cell of the Performance Evaluation Matrix in the multi-turbine implementation corresponding to the turbine T_{ij} of the wind farm P_j, all turbines of the farm P_j are simulated with the same environmental (wind, temperature) profile. The fault is introduced in the turbine T_{ij} and the multi-turbine residual R_{multi} for turbine i belonging to park

P_j is calculated using all mono-turbine residuals for the turbines in farm P_j. The process is repeated for each turbine in the farm, one by one. Once the multi-turbine residual is calculated, the corresponding performance indicator PD_{10} is calculated for each turbine and each cell of the PEM is populated. The performance evaluation matrix is presented as **Fig. 8.6.**

We recall here the basic principal for performance evaluation used for the calculation of performance indicator PD_{10}. For performance evaluation, Year 1 of the overall 3 year data stream is used to learn the 'normal' reference power curve, used to calculate the residuals for Years 2 & 3. To recall, from earlier chapters (eq. 6.2), PD_{10} is the probability of detection for 10% false alarm rate calculated for R^i_{multi} using the equation

$$PD_{EST} = \frac{No.of\ samples\ below\ threshold\ (Th)}{Total\ No.\ of\ data\ samples\ in\ the\ fault\ period}$$

Where *Th* is set such as PFA_{EST}=0.1 (10% PFA)

It is important to note here that effectively for Case III, since a turbulent/laminar variability is inherent in data, the reference behavior is effectively an average of the two (turbulent and laminar) reference power curves. Since a fault is induced in the Year 3 of the data stream, the performance indicator PD_{10} is calculated on the Year 3 profile.

Fig. 8.6 presents the PEM with different colors representing different wind farms. The multi-turbine residual R^i_{multi} can thus be calculated using the data streams/mono-residuals from the uniquely color coded portions of the PEM for identified rows. This is consistent with the farm labels of V, S, D, S and C for Operational profiles in PEM. The red box in **Fig 8.6** identifies that only the environmental profile of the first turbine i.e. V1,S1,D1,S1 & C1 are taken as representative for the whole wind farm.

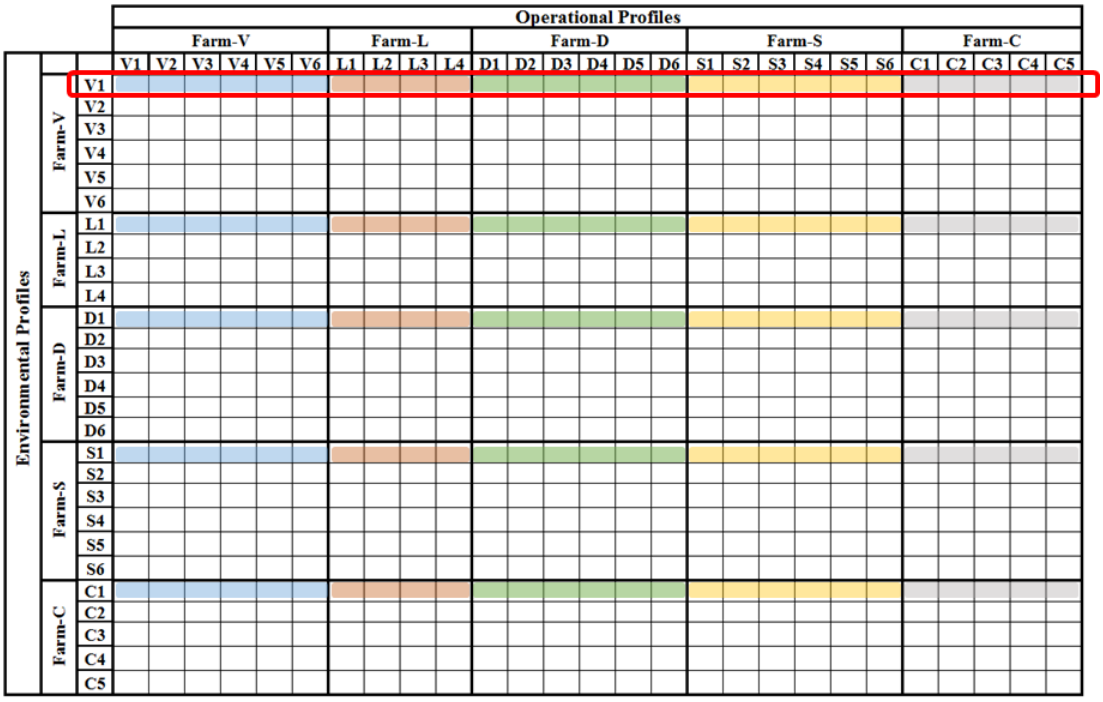

Figure 8.6 Multi-turbine visualization using PEM; with farms highlighted in color. The red box identifies unique environmental (wind, temp.) profile (row)

We note here that for the sake of this research, we consider all turbines T_{ij} of the wind farm P_j to have the *same* environmental (wind, temperature) profiles. This comes from the fact that a wind farm concentrated in a limited geographical location experiences the same environment. In reality, however, although globally consistent and in tandem, there are slight offsets or variations in the environmental measurements of each wind turbine in a wind farm. These variations can be captured by considering the *diagonal* entries instead of the *row* entries of the PEM when constituting a wind farm. To restrict the scope of this work we limit our analysis to the *Row based* implementation for multi-turbine scenario as it is sufficiently representative. The potential color coded representation of *diagonal based* configuration similar to Fig. 8.6 can be found in Annex and can be used in future works

Once the performance evaluation matrix is populated for multi-turbine indicator, a comprehensive performance analysis can be performed. Such visual or statistical performance evaluation is similar to the mono-turbine implementations presented in earlier chapters.

Different intensity levels of these fault signatures presented in previous sections can be generated of which the following fault cases are considered in this analysis.

- Icing 5%: This type of failure appears as a uniform degradation in the operational zone on the power curve. In time series of produced power, the downwards shift is only visible for data corresponding to moderate wind speed values.
- Down-rating 15%: This type of failure appears as a fixed degraded value on the power curve for the higher wind speeds. In time series of produced power, the downward shift is only visible for data corresponding to higher wind speed values.

8.4.2 Results & Findings

We recall the motivation for setting up multi-turbine configuration cases as proposed in this chapter. The aim for case I & II was to evaluate the gain in detection performance for Method 1 when used in the proposed multi-turbine approach. Case II enables an increased variability as compared to the baseline Case I. Additionally, Case III is used to evaluate if an increase in detection performance is possible for Method 2 or if at least, M2 is better suited to account for the adverse environmental turbulence scenarios tested in this work. The results for both scenarios for two faults are presented hereafter.

8.4.2.1 Multi turbine performance evaluation of Method 1 using Case I & Case II

The extended multi turbine simulation framework is used to evaluate the detection performance of simple fault detection method (Method 1). Case 1 & Case II for multi-turbine setup both use Method 1 for turbine level indicator for the overall fleet level multi-turbine residual generation setup. In order to have a realistic quantification of global performance, fault intensities down-rating 15% and icing 5% are considered. The performance indicator is calculated for populating the *row based* performance evaluation matrix presented above. The results are presented and discussed in the following sections.

Since the detection performance of Method 1 for turbine level mono- approach was shown to be low in earlier chapters, the results for two fault cases Down-rating 15% and Icing 5% for the same *rows* for both mono-turbine Method 1 and our proposed hybrid mono-multi approach using Method 1 are reported for a one-on-one comparison. The visual comparison is *only* presented for Case I to avoid recurrence but the results for both Case I & Case II will be reported with the absolute detection values for mono & hybrid multi approaches, the percentage point

gains (abbreviated *pp.)* and their 95% confidence intervals. Recall here that for brevity, the proposed hybrid mono-multi approach can alternatively be referred as hybrid multi or multi hereon in contrast to mono.

8.4.2.1.1 Fault type -Down-rating 15%

As referred to earlier, for a first visual representation, the *row based* PEM for fault type down-rating in both scenarios (mono & hybrid multi) can be useful. **Fig 8.7 a** shows the PD_{10} indicators calculated for Down-rating 15% fault case using the Method 1 in 'mono-Turbine' implementation. The 3 level color scale goes from red to green for 0-100 absolute values. It can be seen from the shades that globally the detection performance of Method 1 is low for all Farms tested, except for Farm S. This exception has to do with the specific fault signature and the wind distribution for Farm S as explained in Sec **7.2.1**.

Fig 8.7 b shows the PD_{10} indicators calculated for Down-rating 15% fault case using the Method 1 in the hybrid mono-multi-turbine' implementation on the same 3 level Red-Yellow-Green color scale. At a first glance, it is clearly visible from the much lighter shades that as compared to **Fig 8.7a**, globally the detection performance of 'Method 1-multi' is significantly higher for all Farms tested. This gain is quantified at around 16 *pp*. for down-rating 15% and will be reported later along with the absolute detection values for mono & hybrid multi approaches and their 95% confidence intervals.

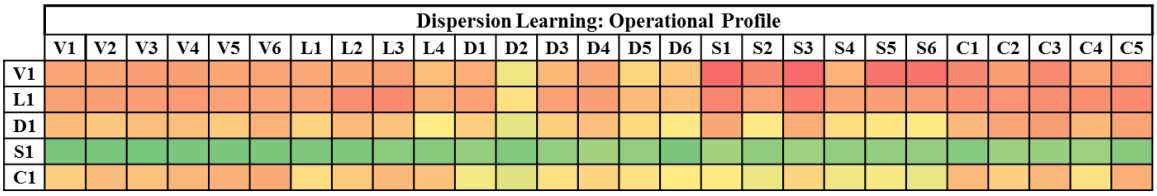

Figure 8.7 a Performance evaluation matrix, Method 1- 'mono' for down-rating of 15% (0-100 on Red-Yellow-Green Scale)

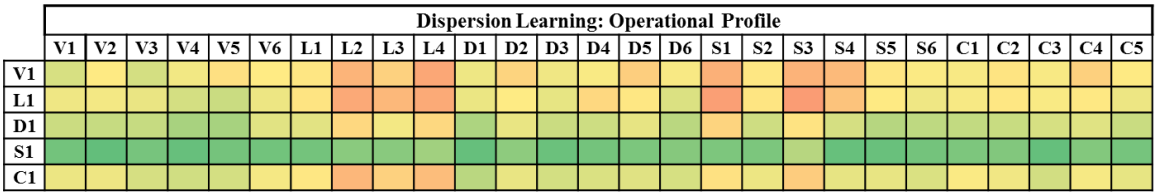

Figure 8.7 b: Performance evaluation matrix, Method 1- 'multi' for down-rating of 15% (0-100 on Red-Yellow-Green Scale)

8.4.2.1.2 Fault type -Icing 5%

Similarly, for better visual representation, the *row based* PEM for fault type icing in both scenarios (mono & hybrid mono-multi) can be useful as well. The PD_{10} indicators calculated for Icing 5% fault case using the Method 1 in 'mono-turbine' implementation is shown in **Fig 8.8a**. The 3 level color scale goes from red to green for 0-100 absolute values and is consistent with previous implementation. It can be seen from the reddish shades, that globally the detection performance of Method 1 is low for all Farms tested with a few exceptions.

Fig 8.8 b shows the PD_{10} indicators calculated for Icing 5% fault case using the Method 1 in the hybrid 'mono-multi-Turbine' implementation. The over-whelming shade of green is clearly visible in **Fig 8.6b**. Even a first glance, it is clearly visible that globally the detection performance of 'Method 1-hybrid multi' is significantly higher for Icing 5% and for all Farms tested. As visible, the detection performance gain of this fault family is higher than the gain observed for down-rating. 45 percentage points (*pp*.) increase in detection performance is reported when using the hybrid mono-multi Turbine approach as compared to simple mono Turbine strategy for Icing 5%. These quantified results are reported in **Table 8.1**.

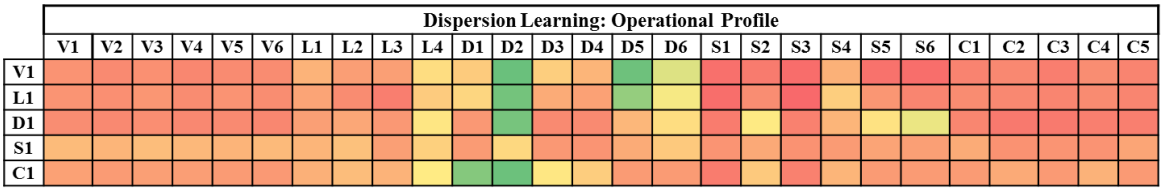

Figure 8.8 a Performance evaluation matrix, Method 1- 'mono' for icing of 5% (0-100 on Red-Yellow-Green Scale)

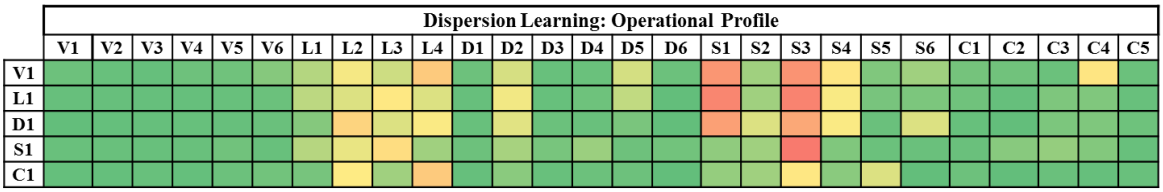

Figure 8.8 b: Performance evaluation matrix, Method 1- 'hybrid multi' for icing of 5% (0-100 on Red-Yellow-Green Scale)

8.4.2.1.3 Overview of Method 1 Analysis

The visual representation for Case I in row based PEM for fault type down-rating 15% and icing 5% have been presented so far. Intuitively and visually, the performance gain for using hybrid mono-multi turbine approach are clear. The same results can be quantified by taking a mean of the PEM matrix and calculating the 95% confidence interval for these values. This will help evaluate the quantifiable gain in terms of mean performance indicator (PD_{10}). We recall here that the visual representation of PEM for Case II are not reported earlier to avoid repetition but the calculated results are reported in Table 8 as sec 8.1b.

Table 8.1 reports the mean detection performance indicator for mono and hybrid mono-multi turbine approaches. As the *row based* hybrid multi-turbine configuration requires selected rows of data, for consistency, the mean detection indicators reported for mono-turbine implementations are from the same row entries as well. Moreover, we recall that Case II uses Method 1 with learnt power curve reference instead of the same reference power curve, this is expected to increase the data dispersion. Since, increased dispersion means increased difficulty of detection and hence a decreased detection performance is expected. The detection comparison of Case I vs. Case II makes it evident that that the detection performance is slightly worse in Case II than Case I (about 2.5 *pp*. less). This is due to the greater variability introduced between turbines in the same fleet. All results in Table 8.1 are reported for fault types down-rating 15% and icing 5%.

TABLE 8.1A CASE I – SAME POWER CURVE – METHOD 1

	Down-rating 15%			Icing 5%		
Detection Strategy	**Mono**	**Multi**	**Performance Gain (*pp.*)**	**Mono**	**Multi**	**Performance Gain (*pp.*)**
Performance Indicator	43.22 ± 3.92	59.72 ± 3.20	16.5	42.95 ± 4.08	88.05 ± 3.45	45.1

TABLE 8.1B CASE II – LEARNT POWER CURVE – METHOD 1

	Down-rating 15%			Icing 5%		
Detection Strategy	**Mono**	**Multi**	**Performance Gain (*pp.*)**	**Mono**	**Multi**	**Performance Gain (*pp.*)**
Performance Indicator	40.60 ± 3.89	56.99 ± 3.41	16.39	40.08 ± 3.91	85.94 ± 3.75	45.86

It is visible from Table 8.1a & Table 8.1b that for both Case I and Case II, Method1 greatly benefits from the proposed hybrid multi turbine approach. For down-rating 15% a clear gain of ~16 *pp.* is reported. We recall here that down-rating 15% is a sufficiently difficult fault case for detection hence it was chosen for mono-turbine analysis in earlier chapters as well. Although relatively easier to detect, the downward shifting fault signature for icing is of interest in the industrial context. A significant gain of ~45*pp.* is reported for hybrid multi-turbine approach in both configurations of hybrid multi implementation using Method 1. The reported 95% confidence intervals reassure of the gains for both fault cases tested.

As briefly explained earlier, Case II adds complexity to Case I by adding data dispersion to the mix. The expected decrease in performance for Case II is observed as the detection loss of around ~2-3*pp.* for all fault scenarios caused by increased data dispersion in Case II. Hence we draw a conclusion from our findings that for both Case I & II, the detection performance of Method 1 can be increased using hybrid multi-turbine approach. The performance using Learnt Reference PCs (Case II) is slightly lower than with fixed reference PC but the mono-turbine vs. hybrid mono-multi Gain is consistent in both cases.

8.4.2.2 Multi turbine performance evaluation of Method 2 using Case III

The extended hybrid multi turbine simulation framework is set up in Case III to evaluate the detection performance of the second fault detection method (Method 2). The interest for Case III is to evaluate the detection performance in hybrid multi-turbine configuration and to subject

Method 2 to turbulent wind conditions of different intensities (e.g. 10% & 90%). This additional variation is introduced as explained in the earlier sections.

Table 8.2 reports the mean detection performance indicator for mono and hybrid multi turbine approach for both 10% turbulence and 90% turbulence intensities. Similar to earlier investigation, to perform a consistent analysis, the row data selected for hybrid multi-turbine configuration is the same used for mono-turbine implementations. This is due to the fact that *row based* configuration for the multi-turbine scenario of this part of the research only uses the first rows to model a park. Moreover, we recall that Case III uses Method 2 with same power curve reference instead of the learnt reference power curve. The increased variability is introduced by the turbulent behavior simulated. All results in Table 8.2 are reported for fault types down-rating 15% and icing 5%.

TABLE 8.2 CASE III – SAME POWER CURVE – METHOD 2

		Down-rating 15%			**Icing 5%**		
		Mono	**Multi**	**Gain (*pp.*)**	**Mono**	**Multi**	**Gain (*pp.*)**
Method 2	Turbulence 10%	50.33 ± 3.82	57.67 ± 3.33	7.34	63.34 ± 4.42	90.53 ± 2.73	27.19
	Turbulence 90%	46.47 ± 3.88	54.12 ± 3.37	7.65	60.43 ± 4.43	90.44 ± 2.74	30.01
Turbulence Loss	**10% vs 90%**	**3.86**	**3.55**		**2.91**	**0.09**	

It is visible from the Table 8.2 that for both 10% and 90% turbulence, Method 2 benefits from the proposed hybrid mono-multi turbine approach. For down-rating 15% a gain of ~7.5*pp.* is reported for both turbulence intensity ranges. We recall here that down-rating 15% is a sufficiently difficult fault case for detection and has an upper limit of detection cases linked to the actual number of sample that observe a fault signature in the total fault period. For the fault type Icing 5%, similar to earlier findings, a significant average gain of ~28.5 *pp.* is reported for hybrid multi-turbine approach in both turbulence configurations of hybrid multi implementation using Method 2. The reported 95% confidence intervals reassure of the gains for both fault cases tested.

We recall that another interest of testing two turbulence intensities was to quantify the otherwise intuitive impact of increased turbulence on detection performance. Table 8.2 reports

a mean detection loss of 3.86 *pp.* & 3.55 *pp.* for both mono and hybrid multi approaches respectively when the turbulence increases from 10% to 90% in the down-rating 15% fault scenario. For icing 5% fault case, in the mono turbine approach increase in turbulence translates to ~3 *pp.* decrease in the detection performance. The impact of turbulence if negligible <1 *pp.* for hybrid multi-turbine approach as the fault is easily detectable with the detection performance of ~90 *pp.* in both turbulence cases.

Although the Case III requires only the evaluation of the impact of turbulence on Method 2 for our implementation, the impact of turbulence on Method 1 if of interest, in the tabular form similar to Table 8.2 can be found in Annex. The results for Method 1 can however be viewed in Table 8.3 for comparison. It can be reported that the Method 1 is impacted more by turbulence as compared to Method 2 at least for fault type down-rating 15%. Table 8.3 presents a global overview and summary of all evaluated cases by reporting mean detection indicator.

TABLE 8.3 GLOBAL ANALYSIS OVERVIEW

	Simple Wind (Non Turbulent)				Turbulent Wind (10% Turbulence)				Turbulent Wind (90% Turbulence)			
	Drawn PC				Drawn PC				Drawn PC			
	Method 1		Method 1		Method 1		Method 2		Method 1		Method 2	
	Mono	Multi	Mono	Multi	Mono	Multi	Mono	Multi	Mono	Multi	Mono	Multi
Brid 15%	43.22	59.69	40.60	56.99	41.88	57.68	50.32	57.67	36.20	52.03	46.47	54.12
Ice 5%	42.95	88.09	40.08	85.94	43.01	87.92	63.35	90.61	40.83	87.09	60.43	90.44

It is of interest to summarize the results presented so far. Based on the analysis performed in this chapter, following unique and useful conclusions can be drawn through each of the cases evaluated.

Case I:

- The detection performance of Method 1 can be increased using proposed multi-turbine approach. A mono vs multi gain of ~16.5 *pp.* for down-rating 15% and a gain of ~45.5 *pp.* for fault type icing 5% has been reported.

Case II:

- The detection performance using Learnt Reference PCs is slightly lower than with fixed reference PC in Case I due do added data dispersion. The mean detection loss of ~2.5 *pp.* has been reported for both fault cases tested.

Case III:

- Method 2 gains from the multi-turbine approach as well. An average mono vs multi gain of ~7 *pp.* for down-rating (15%) and ~29 *pp.* for icing (5%) under both turbulence cases has been seen.

- The detection performance of Method 2 (Case III) is better than Method 1 under both 10% and 90% Turbulence. This gain of M2 vs M1 is significant (10 *pp.* in down-rating & 20 *pp.* for icing) in mono turbine cases.

- However, since the multi-turbine approach provides for the best case dispersion reduction scenario for both methods (M1 & M2), so the gain of M2 vs M1 is negligible. (~2 *pp.*). This is due to the fact that the multi-turbine approach inherently takes environmental variability into account, without the need to add an additional variable (i.e. temperature as in M2).

- Moreover Method 2 is less sensitive to turbulence. For example, the turbulence loss for 10% - 90% turbulence is reported to be ~5.5 *pp.* for Method 1 and ~3.5 *pp.* for Method 2 under 15% down-rating.

Case I vs Case II vs Case III:

- The variation of detection performance amongst all three cases (I,II & III) could also be of interest. Intuitively each case adds slight dispersion or variation to the overall residual so the detection performance is expected to suffer.

- Method 1 detection performance for down-rating 15% shows a decrease in detection performance from 43.22 to 40.6 from drawn to learnt Power Curve. This reduction is from 43.22 for drawn Power Curve to 41.88 and 36.2 in case of 10 & 90% turbulence respectively.

- This variation is less visible for fault type icing 5%. This could be due to the peculiar fault signature, the fault intensity under analysis or the number of data samples and could be analyzed further.

Globally, we could observe in comparison of Method 1 and Method 2 for mono and multi turbine simulation cases that the core cause of data dispersion and seasonal variability are already taken into account by Method 2. When comparing the multi-turbine performance M2 in multi-turbine implementation does not outperform M1 in multi-turbine implementation by a significant margin. The hybrid multi-turbine implementations allows to reduce all the variability due to the environment (temperature, type of wind). Using multi-turbine approach a simple method such as Method 1 gains significantly and becomes as efficient as a more elaborate Method 2.

8.5 Multi-turbine conclusion

In this chapter, we make three distinct contributions listed below.

- Proposal of a hybrid mono-multi-turbine implementation of fault detection methods based on the power curve

- Extension and adaptation of the simulation framework to hybrid mono-multi-turbine configuration

- Numerical and experimental analysis of the performance of this hybrid mono-multi-turbine implementation.

Additionally, to account for more realistic environmental variations, changes in the nature of the wind (from laminar to turbulent) have also been included in the analysis. Two familiar fault detection approaches, Method 1 and Method 2 have been tested in a multi turbine approach. Through the extensive framework and results presented in this chapter, it has been shown that the hybrid mono-multi-turbine detection strategy has the potential to significantly improve the overall fault detection capability for produced power based methods.

It has also been established that under all (Normal or Turbulent) circumstances hybrid-mono-multi-turbine approach performs better than mono-Turbine. Moreover, the detection

performance gain for Method 1 using multi turbine approach is significant while Method 2 enjoys improved performance as well. The strength of Method 2 however comes from its slightly better handling of high turbulence cases. The increase in Turbulence has been shown to have a link with decrease in performance. Although currently, the tested turbulence cases are of two extremes i.e. 10% turbulence means the learnt reference is mostly laminar power curve and 90% turbulence translates to mostly turbulent reference power curve. It could be of interest to evaluate the detection performance under 50/50, 60/40 or 30/70 scenarios in the future to better conclude on this aspect.

These results for gain in detection performance of power based methods are coherent with the findings of hybrid mono-multi solution, implemented for temperature based fault detection methods (Lebranchu et al., 2019). Both these contributions have profound implications in industrial context as any improvement in detection performance is highly desirable. Similar to the mono-turbine simulation framework presented in earlier chapters, the hybrid mono-multi framework is highly robust as well. The future work may include the *diagonal based* setup for added variation and even more realistic farm condition modelling as identified earlier. Other possibilities may include additional fault detection methods, other fault and turbulence intensity cases as well.

9 General Conclusions & Future work

Wind turbines being power generators make the power produced by a machine a variable of interest for monitoring and detection of a possible fault. In this thesis, a thorough literature review focusing on methods to detect faults in wind turbines using the power produced was first done. It showed that, though many methods were proposed in the literature, it was very difficult to compare their performances in an objective way because of a lack of a data benchmark, enabling all these methods to be implemented and evaluated on the same data.

This created the motivation to establish a comparison framework for existing solutions that can help quantify the performance capabilities of existing fault detection solutions and establish their limitations.

To address these concerns, an approach with a twofold contribution was proposed in this thesis. First, a novel and realistic simulation framework was presented. It made use of real data recorded on several French wind farms, located at different geographical sites. Secondly, a framework for performance assessment of various methods proposed in the literature was presented. The benchmark enabled a rigorous comparison of the performances of power based fault detection solutions. The key assets of the proposed benchmark are:

- Any fault for which the signature is a modification of the power curve can be implemented in the framework.
- The data dispersion around the power curve, which is the main difficulty that fault detection methods have to overcome, to detect faults efficiently, is not modelled by Gaussian white noise but by using the dispersion measured on real data. This makes the benchmark a powerful tool to evaluate fault detection methods performances in a realistic way.
- The framework enables the generation of data streams, using data from different wind farms and different wind turbines, in an infinite way. This makes it possible to evaluate

the impact of environmental conditions and operation conditions on the fault detection method performances.

The benchmark was implemented and validated with 4 power based faults and under-performance scenarios of various intensities using data from 5 geographically distant wind farms and on multiple SCADA variables. A total of 1875 years of simulated, 10 minutes SCADA data was used to compare the fault detection performances of 3 fault detection methods.

The results clearly identify the impact of environmental and operational variations on fault detection performances. Some fault types were shown to be easier to detect as compared to others proving the influence of fault signature on detection performance, hence urging fine tuning of specific techniques for specific fault types. Conclusions were also drawn on the choice of method showing that the approach that performs best is the one that best caters for these operational and environmental variations of WT data.

In the second part of the research, an extension of the existing simulation framework to account for a multi-turbine configuration was proposed. Indeed, several multi turbine strategies were published in the literature as a means to overcome the impact of environmental conditions on fault detection methods using temperature. To evaluate the gain in performance a multi turbine strategy could bring, a hybrid mono-multi-turbine implementation of fault detection methods based on the power curve was proposed at first. Then the simulation framework proposed to evaluate mono turbine methods was extended to multi turbines approaches and numerical experimental analysis of the performance of this hybrid mono-multi-turbine implementation was done.

- The results showed that the multi-turbine strategy significantly increased the detection performance of existing solutions. Even the simplest method using only the wind speed and power produced as inputs were significantly improved when a hybrid mono-multi-turbine approach was used.

The controlled simulation framework proposed in this research has been proven to be a robust and powerful tool for wind turbine condition monitoring research. Several expansions based on the existing platform can be achieved in the future.

One of the easily upgradable expansion of the proposed framework can be the implementation of more fault detection techniques and fault scenarios. The duration and location of fault induction can also be explored. Since a seasonality can be observed for basic fault

indicators, it could be interesting to see if detection performance varies for faults observed in winter as opposed to summer. Combined use of power and temperature based indicators could also be a move towards a merged and global solution for condition monitoring on a fleet level.

Due to the scope of this work, a relatively basic performance indicator for analysis was chosen in consultation with the industrial partners. Other, more intelligent performance indicators could also be of interest. The examples may include using (maximum probability of detection, minimum false alarm) pair, advanced detection, number of unnecessary interventions etc.

An additional consideration for the real life implementation of this research is a potential inclusion of different levels of wind variation to the research. As shown in the multi-turbine implementation of this work, the inherent, alternatively turbulent and laminar nature of the wind adds significant value to the overall analysis. The IEC standard (IEC 61400-12-1, 2005) talks about the production loss due to wind turbulence within the 10 min SCADA data sampling duration. To cater for the wind variation within the 10 minutes window, a normalization for turbulence is proposed. It can thus be concluded that further analysis of the impact of turbulence on detection performance is also of interest. The simulated data for desired turbulence intensity values, can help quantify their impact on detection performance. Preliminary results conclude that increased turbulence decreases the detection performance.

This thesis presents a key platform which is intended to standardize and advance the use of SCADA data for CM in wind turbines; through the use of power based fault detection techniques. The goal is to answer pertinent questions of wind turbine operations and maintenance teams that arise concerning the real life implementation of solutions proposed in the literature. In this respect, the thesis has achieved these broad goals.

However, it represents a foundation and basic step towards implementation of proposed solutions in field-ready scenarios. In this respect, it is hoped that future researchers in the space can use the work in this thesis, and the resulting publications, as a platform to build upon with the ultimate goal of expanding the scope of CM using existing SCADA data. Building a comprehensive and field-deployable fault prognostic or diagnostic system will require further research and a coordinated effort from stakeholders including operators and OEMs.

Chapter 9- Conclusion

Bibliography

Albers, A., Jakobi, T., Rohden, R., & Stoltenjohannes, J. (n.d.). *Influence of Meteorological Variables on Measured Wind Turbine Power Curves*. 8.

Astolfi, D., Castellani, F., & Terzi, L. (2014). Fault prevention and diagnosis through scada temperature data analysis of an onshore wind farm. *Diagnostyka*, *15*. https://yadda.icm.edu.pl/baztech/element/bwmeta1.element.baztech-39f61d71-3121-4734-af0c-014388452c51

Axel Albers, T. J. (n.d.). *Influence of meteorological variables on measured wind turbine power curves*.

Aziz, U., Charbonnier, S., Bérenguer, C., Lebranchu, A., & Prevost, F. (2018). *Simulation of wind turbine faulty production profiles and performance assessment of fault monitoring methods*. 8.

Aziz, U., Charbonnier, S., Berenguer, C., Lebranchu, A., & Prevost, F. (2019). SCADA data based realistic simulation framework to evaluate environmental impact on performance of wind turbine condition monitoring systems. *2019 4th Conference on Control and Fault Tolerant Systems (SysTol)*, 360–365. https://doi.org/10.1109/SYSTOL.2019.8864769

Bardal, L. M., & Sætran, L. R. (2017). Influence of turbulence intensity on wind turbine power curves. *Energy Procedia*, *137*, 553–558. https://doi.org/10.1016/j.egypro.2017.10.384

Bi, R., Zhou, C., & Hepburn, D. M. (2017a). Detection and classification of faults in pitch-regulated wind turbine generators using normal behaviour models based on

performance curves. *Renewable Energy*, *105*, 674–688. https://doi.org/10.1016/j.renene.2016.12.075

Bi, R., Zhou, C., & Hepburn, D. M. (2017b). Detection and classification of faults in pitch-regulated wind turbine generators using normal behaviour models based on performance curves. *Renewable Energy*, *105*, 674–688. https://doi.org/10.1016/j.renene.2016.12.075

BS EN 13306:2010. (2010). *Maintenance—Maintenance terminology*. BSI Standards Publication.

Burton, T., Jenkins, N., Sharpe, D., & Bossanyi, E. (2011). *Wind Energy Handbook* (Second Edition). Wiley.

Butler, S., Ringwood, J., & O'Connor, F. (2013). Exploiting SCADA system data for wind turbine performance monitoring. *Control and Fault-Tolerant Systems (Systol), 2013 Conference On*, 389–394. http://ieeexplore.ieee.org/abstract/document/6693951/

Cambron, P., Lepvrier, R., Masson, C., Tahan, A., & Pelletier, F. (2016). Power curve monitoring using weighted moving average control charts. *Renewable Energy*, *94*, 126–135. https://doi.org/10.1016/j.renene.2016.03.031

Cambron, P., Masson, C., Tahan, A., & Pelletier, F. (2018). Control chart monitoring of wind turbine generators using the statistical inertia of a wind farm average. *Renewable Energy*, *116*, 88–98. https://doi.org/10.1016/j.renene.2016.09.029

de Andrade Vieira, R. J., & Sanz-Bobi, M. A. (2015). Power curve modelling of a wind turbine for monitoring its behaviour. *Renewable Energy Research and Applications (ICRERA), 2015 International Conference On*, 1052–1057. http://ieeexplore.ieee.org/abstract/document/7418571/

Farkas, Z. (2011). Considering air density in wind power production. *ArXiv Preprint ArXiv:1103.2198*. https://arxiv.org/abs/1103.2198

IEC 61400-12-1. (2005). *Power Performance Measurements of Electricity Producing Wind Turbines*.

Isermann, R. (2006). *Fault-diagnosis systems: An introduction from fault detection to fault tolerance*. Springer.

Jia, X., Jin, C., Buzza, M., Wang, W., & Lee, J. (2016a). Wind turbine performance degradation assessment based on a novel similarity metric for machine performance curves. *Renewable Energy*, *99*, 1191–1201. https://doi.org/10.1016/j.renene.2016.08.018

Jia, X., Jin, C., Buzza, M., Wang, W., & Lee, J. (2016b). Wind turbine performance degradation assessment based on a novel similarity metric for machine performance curves. *Renewable Energy*, *99*, 1191–1201. https://doi.org/10.1016/j.renene.2016.08.018

Kim, S.-Y., Ra, I.-H., & Kim, S.-H. (2012). Design of wind turbine fault detection system based on performance curve. *Soft Computing and Intelligent Systems (SCIS) and 13th International Symposium on Advanced Intelligent Systems (ISIS), 2012 Joint 6th International Conference On*, 2033–2036. http://ieeexplore.ieee.org/abstract/document/6505401/

Koebrich, S., Tian, T., & Chen, E. (n.d.). *2017 Renewable Energy Data Book: Including Data and Trends for Energy Storage and Electric Vehicles*. 142.

Kusiak, A., Zheng, H., & Song, Z. (2009a). Models for monitoring wind farm power. *Renewable Energy*, *34*(3), 583–590. https://doi.org/10.1016/j.renene.2008.05.032

Kusiak, A., Zheng, H., & Song, Z. (2009b). On-line monitoring of power curves. *Renewable Energy*, *34*(6), 1487–1493. https://doi.org/10.1016/j.renene.2008.10.022

Lapira, E., Brisset, D., Davari Ardakani, H., Siegel, D., & Lee, J. (2012). Wind turbine performance assessment using multi-regime modeling approach. *Renewable Energy*, *45*, 86–95. https://doi.org/10.1016/j.renene.2012.02.018

Lebranchu, A., Charbonnier, S., Bérenguer, C., & Prévost, F. (2019). A combined mono- and multi-turbine approach for fault indicator synthesis and wind turbine monitoring using SCADA data. *ISA Transactions*, *87*, 272–281. https://doi.org/10.1016/j.isatra.2018.11.041

Lydia, M., Kumar, S. S., Selvakumar, A. I., & Prem Kumar, G. E. (2014). A comprehensive review on wind turbine power curve modeling techniques. *Renewable and Sustainable Energy Reviews*, *30*, 452–460. https://doi.org/10.1016/j.rser.2013.10.030

Ma, J., Fouladirad, M., & Grall, A. (2018). Flexible wind speed generation model: Markov chain with an embedded diffusion process. *Energy*, *164*, 316–328. https://doi.org/10.1016/j.energy.2018.08.212

Masson-Delmotte, V., Zhai, P., Pörtner, H.-O., Roberts, D., Skea, J., & Shukla, P. R. (2018). *Global warming of 1.5°C*.

McLaughlin, D., J. M Clive, P., & McKenzie, J. H. (2009). *Wind farm performance assessment in the real world.pdf*. European Wind Energy Conference (EWEC), Marseille, France.

Morice, C. P., Kennedy, J. J., Rayner, N. A., & Jones, P. D. (2012). Quantifying uncertainties in global and regional temperature change using an ensemble of observational estimates: The HadCRUT4 data set: THE HADCRUT4 DATASET. *Journal of*

Geophysical Research: Atmospheres, *117*(D8), n/a-n/a. https://doi.org/10.1029/2011JD017187

Odgaard, P. F., Stoustrup, J., & Kinnaert, M. (2013). Fault-Tolerant Control of Wind Turbines: A Benchmark Model. *IEEE Transactions on Control Systems Technology*, *21*(4), 1168–1182. https://doi.org/10.1109/TCST.2013.2259235

Odgaard, P. F., Stoustrup, J., Nielsen, R., & Damgaard, C. (2009). *Observer Based Detection of Sensor Faults In Wind Turbines*. 11.

Papatheou, E., Dervilis, N., Maguire, E., & Worden, K. (2014). Wind turbine structural health monitoring: A short investigation based on SCADA data. *EWSHM-7th European Workshop on Structural Health Monitoring*. https://hal.inria.fr/hal-01020389/

Park, J.-Y., Lee, J.-K., Oh, K.-Y., & Lee, J.-S. (2014). Development of a Novel Power Curve Monitoring Method for Wind Turbines and Its Field Tests. *IEEE Transactions on Energy Conversion*, *29*(1), 119–128. https://doi.org/10.1109/TEC.2013.2294893

Pelletier, F., Masson, C., & Tahan, A. (2016). Wind turbine power curve modelling using artificial neural network. *Renewable Energy*, *89*, 207–214. https://doi.org/10.1016/j.renene.2015.11.065

Picard, A., Davis, R. S., Gläser, M., & Fujii, K. (2008). Revised formula for the density of moist air (CIPM-2007). *Metrologia*, *45*(2), 149–155. https://doi.org/10.1088/0026-1394/45/2/004

Projected Costs of Generating Electricity. (2005). *OECD, IAE*, 233.

Schmidt, G. A., Ruedy, R. A., Miller, R. L., & Lacis, A. A. (2010). Attribution of the present-day total greenhouse effect. *Journal of Geophysical Research*, *115*(D20), D20106. https://doi.org/10.1029/2010JD014287

Tavner, P. J. (2012). *Offshore wind turbines: Reliability, availability and maintenance*. Institution of Engineering and Technology.

Uluyol, O., Parthasarathy, G., Foslien, W., & Kim, K. (2011). Power curve analytic for wind turbine performance monitoring and prognostics. *Annual Conference of the Prognostics and Health Management Society*, *2*, 1–8. http://72.27.231.73/sites/phmsociety.org/files/phm_submission/2011/phmc_11_049.pdf

Walford, C. A. (2006). *Wind Turbine Reliability: Understanding and Minimizing Wind Turbine Operation and Maintenance Costs* (No. SAND2006-1100; p. 27). Sandia Labs.

Yang, W., Court, R., & Jiang, J. (2013). Wind turbine condition monitoring by the approach of SCADA data analysis. *Renewable Energy*, *53*, 365–376. https://doi.org/10.1016/j.renene.2012.11.030

Annex

TABLE: Impact of Turbulence on Method 1

		Bridage 15%		Icing 5%	
		Mono	**Multi**	**Mono**	**Multi**
Method 1	Turbulence 10%	41,88	57,68	43,01	87,92
	Turbulence 90%	36,20	52,03	40,83	87,09
Turbulence Loss	**10% vs 90%**	**5,68**	**5,65**	**2,18**	**0,83**
Method 2	Turbulence 10%	50,32	57,67	63,34	90,53
	Turbulence 90%	46,47	54,12	60,43	90,44
Turbulence Loss	**10% vs 90%**	**3,86**	**3,55**	**2,91**	**0,09**
Average Gain	**M1 vs M2**	9,35	1,04	19,97	2,98

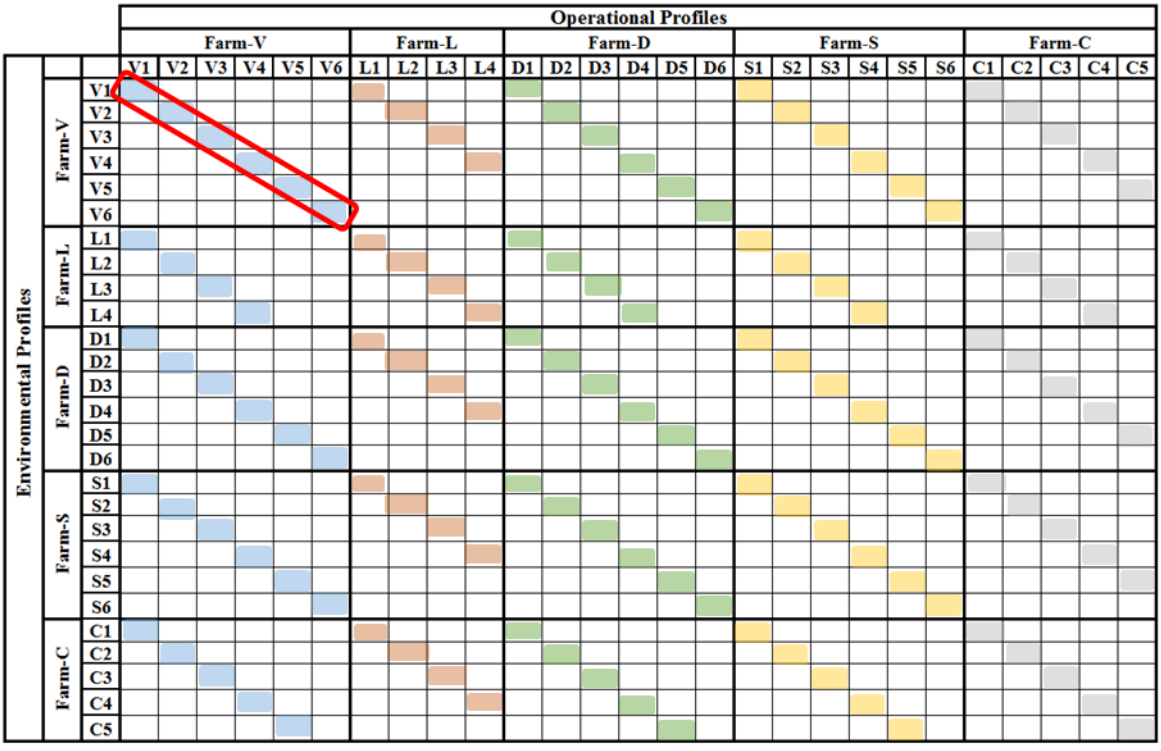

Figure: Multi-turbine visualization using PEM; with farms highlighted in color. The red box identifies unique environmental (wind, temp.) diagonal based approach

Annex

Détection des défauts des éoliennes basée sur la courbe de puissance : Comparaison critique des performances et proposition d'une approche multi-turbines

Les éoliennes étant des générateurs d'électricité, la puissance électrique produite par une machine est une variable pertinente pour la surveillance et la détection d'éventuels défauts. Dans le cadre de cette thèse, une analyse bibliographique approfondie a d'abord été réalisée sur les méthodes de détection des défauts des éoliennes utilisant la puissance électrique produite. Elle a montré que, bien que de nombreuses méthodes aient été proposées dans la littérature, il est très difficile de comparer leurs performances de manière objective en raison de l'absence de données de référence, permettant de mettre en œuvre et d'évaluer toutes ces méthodes sur la base des mêmes données.

Pour répondre à ce problème, dans un premier temps, une nouvelle approche de simulation réaliste a été proposée dans cette thèse. Elle permet de créer des flots de données simulées, couplant la puissante produite, la vitesse du vent et la température, dans des conditions normales et dans des situations défauts, de manière infinie. Les défauts qui peuvent être simulés sont ceux qui impactent la forme de la courbe de puissance. Les données simulées sont générées à partir de données réelles enregistrées sur plusieurs parcs éoliens français, situés sur des sites géographiques différents. Dans un deuxième temps, une méthode permettant l'évaluation des performances des méthodes de détection des défauts utilisant la puissance produite a été proposé.

Cette nouvelle méthode de simulation a été mise en œuvre sur 4 situations de défauts affectant la courbe de puissance différents, à l'aide de données provenant de 5 parcs éoliens géographiquement éloignés. Un total de 1875 années de données SCADA 10 minutes a été généré et utilisé pour comparer les performances en détection de 3 méthodes de détection de défauts proposées dans la littérature. Ceci a permis une comparaison rigoureuse de leurs performances.

Dans la deuxième partie de cette recherche, la méthode de simulation proposée a été étendue à une configuration multi-turbines. En effet, plusieurs stratégies multi-turbines ont été publiées dans la littérature, avec comme objectif de réduire l'impact des conditions environnementales

sur les performances des méthodes de détection de défauts utilisant comme variable la température. Pour évaluer le gain de performance qu'une stratégie multi-turbines pourrait apporter, une implémentation hybride mono-multi-turbines des méthodes de détection de défauts basées sur la courbe de puissance a été proposée dans un premier temps. Ensuite, le cadre de simulation proposé pour évaluer les méthodes mono-turbines a été étendu aux approches multi-turbines et une analyse expérimentale numérique des performances de cette implémentation hybride mono-turbines-multi-turbines a été réalisée.

Mots clés : cadre de simulation, analyse des données, monitoring & diagnoses, comparaison critique, prédictive maintenance, évaluation de performance, Wind Turbine

Abstract

Power curve based wind turbine fault detection:
A critical performance comparison and proposition of a multi-turbine approach

Since wind turbines are electricity generators, the electrical power produced by a machine is a relevant variable for monitoring and detecting possible faults. In the framework of this thesis, an in-depth literature review was first performed on fault detection methods for wind turbines using the electrical power produced. It showed that, although many methods have been proposed in the literature, it is very difficult to compare their performance in an objective way due to the lack of reference data, allowing to implement and evaluate all these methods on the basis of the same data.

To address this problem, as a first step, a new realistic simulation approach has been proposed in this thesis. It allows to create simulated data streams, coupling the power output, wind speed and temperature, in normal conditions and in fault situations, in an infinite way. The defects that can be simulated are those that impact the shape of the power curve. The simulated data are generated from real data recorded on several French wind farms, located on different geographical sites. In a second step, a method for evaluating the performance of fault detection methods using the power produced has been proposed.

This new simulation method was implemented on 4 different fault situations affecting the power curve, using data from 5 geographically remote wind farms. A total of 1875 years of 10-minute SCADA data was generated and used to compare the detection performance of 3 fault detection methods proposed in the literature. This allowed a rigorous comparison of their performance.

In the second part of this research, the proposed simulation method was extended to a multi-turbine configuration. Indeed, several multi-turbine strategies have been published in the literature, with the objective of reducing the impact of environmental conditions on the performance of fault detection methods using temperature as a variable. In order to evaluate the performance gain that a multi-turbine strategy could bring, a hybrid mono-multi-turbine implementation of fault detection methods based on the power curve was first proposed. Then, the simulation framework proposed to evaluate mono-turbine methods was extended to multi-

turbine approaches and a numerical experimental analysis of the performance of this hybrid mono-multi-turbine implementation was performed.

Keywords: simulation framework, critical comparison, monitoring & diagnosis, predictive maintenance, performance evaluation, multi-turbine approach, wind turbine